Exponential asymptotics of localised patterns and snaking bifurcation diagrams.

S.J. Chapman* G. Kozyreff†

October 8, 2008

Abstract

Localised patterns emerging from a subcritical modulation instability are analysed by carrying the multiple-scales analysis beyond all orders. The model studied is the Swift-Hohenberg equation of nonlinear optics, which is equivalent to the classical Swift-Hohenberg equation with a quadratic and a cubic nonlinearity. Applying the asymptotic technique away from the Maxwell point first, it is shown how exponentially small terms determine the phase of the fast spatial oscillation with respect to their slow sech-type amplitude. In the vicinity of the Maxwell point, the beyond-all-orders calculation yields the "pinning range" of parameters where stable stationary fronts connect the homogeneous and periodic states. The full bifurcation diagram for localised patterns is then computed analytically, including snake and ladder bifurcation curves. This last step requires the matching of the periodic oscillation in the middle of a localised pattern both with an up- and a down-front. To this end, a third, super-slow spatial scale needs to be introduced, in which fronts appear as boundary layers. In addition, the location of the Maxwell point and the oscillation wave number of localised patterns are required to fourth-order accuracy in the oscillation amplitude.

1 Introduction

An important problem in the study of spatially extended dynamical systems is to determine when periodic patterns and homogeneous base states can be separated by stationary fronts. This allows localised patterns and structures to exist, which can be combined as building blocks for more complicated inhomogeneous solutions, such as those depicted in Fig. 1.

A typical bifurcation diagram associated with localised patterns is shown in Fig. 2, where the L^2 norm of the oscillations is plotted against a control parameter. The diagram mainly consists of two interweaved "snaking" curves, one corresponding to localised patterns with

*OCIAM, Mathematical Institute, 24-29 St Giles', Oxford OX13LB (UK).

†Optique Nonlinéaire Théorique, Université libre de Bruxelles (U.L.B.), C.P. 231, Campus Plaine, B-1050 Bruxelles (Belgium)

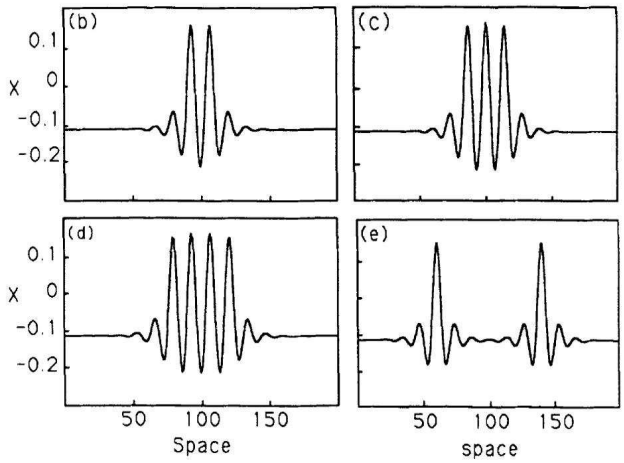

Figure 1: Example of localised patterns resulting from the existence of stationary fronts between the homogeneous and periodic solutions of (1). Reproduced from [69] with permission.

odd numbers of peaks, the latter associated to even numbers of peaks. Each cycle in the snakes signals the appearance of a new pair of peaks in the localised pattern. Hence, these two curves delimit a finite "pinning range" of parameters where stable localised patterns of arbitrary extent can exist [39, 40, 56, 16]. Additionally, a set of branches of asymmetric solutions, the "ladder", was found to connect the two snakes [73, 17]. Along each rung of the ladder, the phase of the oscillations varies in such a way that the localised pattern progressively acquires or loses one peak. These asymmetric solutions are reputedly unstable and, in systems with reflectional symmetry in the space variable, they are expected to be stationary only if the underlying system is variational [18]. Moreover, as recently discussed in [8], the snaking curves can also break up into a set of isolas. Finally, in the presence of a non-local coupling, the snaking curves can become slanted [34, 33, 29], thus enlarging the domain of existence of localised patterns but reducing the multistability between localised states.

If the system is variational, it tends to minimise a Lyapunov functional as time progresses. Identifying this functional with an energy, there generally exists a parameter value where both the homogeneous solution and the periodic pattern have the same energy. Such a point is called a Maxwell point, by analogy with phase transitions in thermodynamics [61]. Note that in the limit of small amplitude oscillations, the leading-order description of the system is a Ginzburg-Landau equation, which is variational, and therefore a Maxwell point can always be defined. The pinning range is understood to be intimately related to the Maxwell point and indeed it always includes it.

In two spatial dimensions, the situation naturally becomes more complicated [41, 69, 38], but the snaking bifurcation structure persists [53, 52]. As described in that paper, when the localised pattern has an hexagonal structure, the direction along which the pattern grows strongly influences the shape of the snakes in the bifurcation diagram. Even for two-

dimensional patterns that are localised in only one direction, the discussion of the stability becomes significantly more involved [37, 18].

While plenty of numerical evidence [9, 65, 66, 56, 71, 6, 7, 10] and experimental confirmations [59, 70, 51, 68, 50, 62, 31, 4, 58, 67] of the existence of localised patterns have been gathered over the years, their theoretical description has remained extremely difficult (see [63] for a review). Some important results have been obtained in one spatial dimension, where geometrical arguments in the phase-space establish the existence and robustness of localised patterns [39, 24, 36]. In this regard, Lin's method is proving useful to find one's way in the multi-dimensional phase spaces where these homoclinic orbits sit [44, 49]. For further analytical understanding, multiple-scales analysis seems the obvious way forward. Indeed, near the bifurcation point where the oscillations are born, there is a natural separation of spatial scales: one is associated to the progressive onset of oscillations, another corresponds to the oscillation period. A standard multiple-scales analysis, however, leads to the incorrect conclusion that fronts are only stationary at the Maxwell point. Such an analysis misses the exponentially small terms that couple the slow and fast scales. As a result, it cannot explain the fact that the slowly varying front can be pinned to the underlying periodic structure over a finite parameter range. This question was posed in [61] and has stimulated much research towards improving the multiple-scales approach. However, it was solved only recently [45] by a study beyond all orders of the multiple-scales analysis and the purpose of this paper is to explain in detail how.

Most of previous works on the problem follow more or less explicitly the strategy set out in [9]. In this paper, it is argued that the solvability condition leading to an equation for the slowly-varying amplitude of the pattern should contain some fast oscillating terms that were previously overlooked (see, for instance Eq. (6) of [9]). Upon integration, these fast oscillations do not quite integrate to zero, but rather yield corrections that are exponentially small in the ratio of the fast and slow scales. Taking as a small parameter ϵ the maximum amplitude of the periodic solution at the Maxwell point, the slow spatial scale is $X = \epsilon^2 x$ [26] and the pinning is thus found to scale as

$$\epsilon^{\eta} e^{-\pi/\epsilon^2},$$

where η is some exponent. The exponential factor was confirmed in [25] but, as noted in [63], the value of η in the pre-factor remained unclear. Nevertheless, this was significant progress which has inspired similar results on fronts between one-dimensional patterns and homogeneous states [2] and, in two-dimensions, between hexagonal patterns and rolls [54] and hexagonal patterns of different orientations [13, 14]. However encouraging these results may be, one must bear in mind that the approach in [9] is clearly inconsistent. Indeed, at the heart of multiple-scales analysis lies the assumption that the front is independent of the fast scale, which gives rise to solvability conditions such as the Ginzburg-Landau (GL) equation. Re-introducing fast oscillating driving terms in the GL equation violates that assumption. Actually, these fast oscillating terms, being non-resonant, produce no secular divergence in the higher corrections of the solution. Hence including non-resonant terms in the GL equation, while tempting, is both unjustified and arbitrary. In particular, this leads to an incorrect exponent η in the pinning range. For a discussion on this issue, see [22, 46].

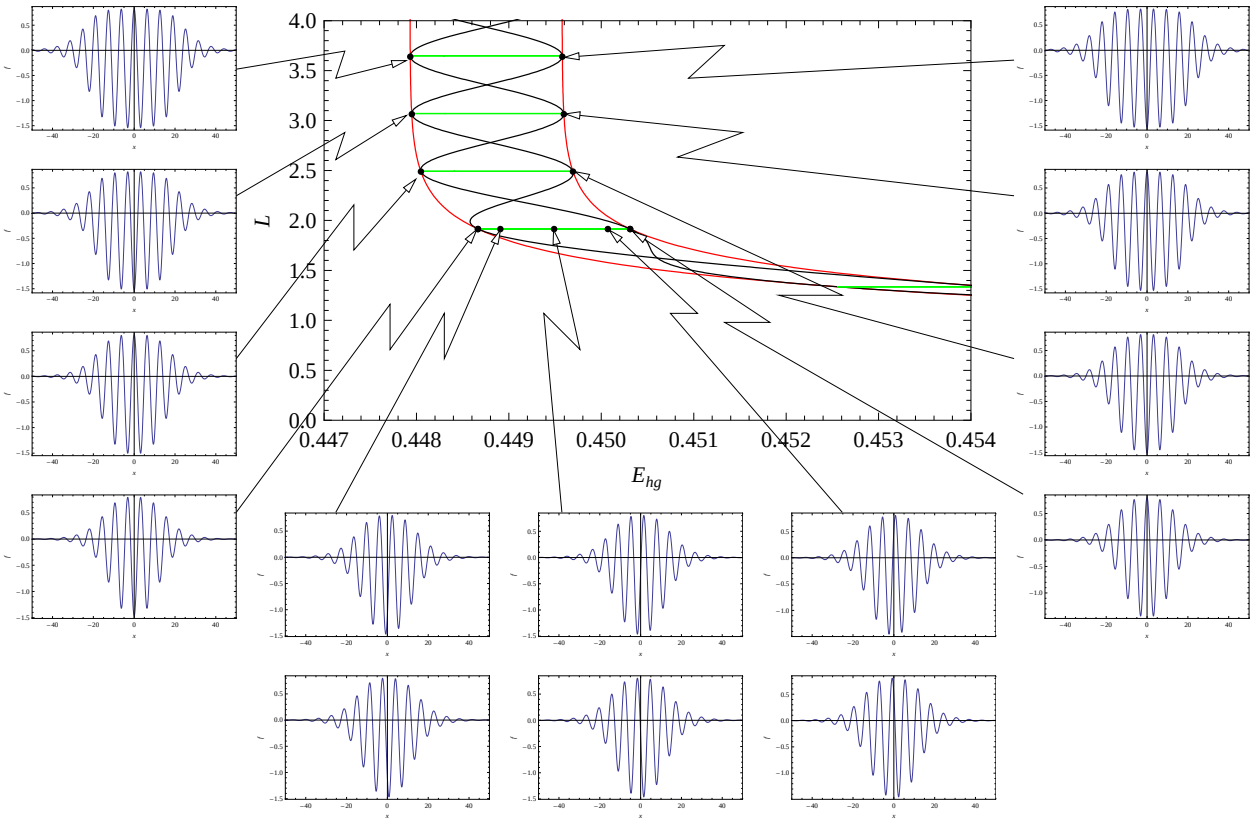

Figure 2: The bifurcation diagram of (3) with $\epsilon = 0.55$, determined through the asymptotic analysis of §5. The horizontal lines are the "rungs" of the ladders. Each point on the ladder represents two asymmetric localised solutions, which are the image of one other by the transformation $x \to -x$. The rungs do not start at the folds of the snakes, even though they approach them exponentially as the size of the localised solution increases.

To conclude this overview, let us mention that snaking bifurcation diagrams of the type analysed here are being found in an increasing number of models: integro-differentials models for firing neurons [23], delay-differential models for electronic transmission lines [5], spatially discrete models for coupled optical cavities [60, 76], and models displaying Saddle-node Hopf [48] or T-point-Hopf bifurcations [32]. In all these cases, localised structures can be envisaged as sets of fronts that are pinned to an underlying periodic structure. The latter can be either in the solution itself (dynamical oscillations) or imprinted in space (spatial discreteness). This similarity strongly suggests to us that the technique presented here can be adapted to these situations. Finally a series of open questions on the subject of localized structures were recently formulated in [43].

One physical setting that is especially suited to the study of dynamical patterns is an optical cavity containing a nonlinear medium and in which a coherent beam is injected. When the nonlinear medium is assumed to be a collection of two-level atoms, then the simplest model for that system is given by the following non-dimensional equation [11, 55]

$$\frac{\partial E}{\partial t} = \mathcal{Y} + \mathcal{C}E - E^3 - \left(1 + \frac{\partial^2}{\partial x^2}\right)^2 E. \tag{1}$$

In this equation, E is the amplitude of the optical electric field inside the cavity, $\mathcal{Y}$ is the injection field, and $\mathcal{C}$ is the cooperativity parameter. We will be concerned with steady perturbations to the homogeneous steady state E_{hg}, which satisfies $\mathcal{Y} = E_{hg}^3 - \mathcal{C}E_{hg} + E_{hg}$. There is a modulation instability, or Turing bifurcation, with unit wave number when $3E_{hg}^2 = \mathcal{C}$ [69].

In the immediate vicinity of this bifurcation, we parametrise the homogeneous solution by E_{hg} and set

$$\mathcal{C} = 3E_{hg}^2 - \epsilon^2, \quad E(x,t) = E_{hg} + \epsilon f(x),$$

where $0 < \epsilon \ll 1$, to give

$$\left(1 + \frac{d^2}{dx^2}\right)^2 f + \epsilon^2 f + 3\epsilon E_{hg} f^2 + \epsilon^2 f^3 = 0. \tag{2}$$

This is appropriate to describe localised solutions away from the snaking region, and in §2, we perform the multiple-scales analysis of this equation. This procedure allows us to construct solutions containing fast oscillations modulated by a pulsed envelope. However the phase of the oscillations relative to their envelope remains arbitrary until we go beyond all orders of the multiple scale analysis. We will see that exponentially small terms are turned on across Stokes lines. These terms, although exponentially small when they appear, are exponentially growing in space, so that for the solution to be valid at infinity the coefficient of the growing exponential must be zero. This is the solvability condition which selects the phase of the fast oscillation. In fact, [72, 73] effectively performed a beyond-all-orders analysis of (2), but with a slightly different technique than ours, borrowed from [74, 75]. We, on the other hand, follow the technique in [1]; as well as motivating the rescalings which follow, §2 serves as an introduction to the beyond-all-orders technique, before we move on to consider the more complicated analysis in the vicinity of the Maxwell point in §3.

The amplitude of the solutions identified in §2 is monotonic in the bifurcation parameter E_{hg}, tending to infinity as the Maxwell point is approached. This calls for a different scaling [15] so that near the Maxwell point we need to set

$$\mathcal{C} = 3E_{hg}^2 - \epsilon^4, \quad E(x,t) = E_{hg} + \epsilon f(x),$$

to give[1]

$$\left(1 + \frac{d^2}{dx^2}\right)^2 f + \epsilon^4 f + 3\epsilon E_{hg} f^2 + \epsilon^2 f^3 = 0. \tag{3}$$

In §3 we perform a new beyond-all-orders multiple-scales analysis of (3) with front solutions connecting the uniform state to a uniformly oscillating state. The algebra is considerably more complicated but the methodology is the same. Again we find that there is a Stokes line across which exponentially-small but exponentially-growing terms are turned on. However, this time we also have another exponentially-growing term generated by the deviation of E_{hg} from the Maxwell point. The solvability condition that the coefficient of the growing exponential vanish gives a loop of solutions, with two stationary front solutions existing for an (exponentially-small) range of values of E_{hg}.

In §4 we construct solutions comprising an up-front and a down-front separated by an extended period of uniform oscillation. By matching the growing and decaying exponentials from each front solution we obtain a solvability condition which describes the snaking bifurcation diagram near the Maxwell point. The matching procedure will require us to introduce a new, super slow, scale on which the distance between fronts is $O(1)$. On that scale, fronts become boundary layers. The three situations above are depicted schematically in Fig. 3.

In §5 we analyse the solutions to this equation, and find that the bifurcation diagram comprises two interleaving snakes joined by pairs of rungs. The width of the snakes is found to be proportional to

$$\epsilon^{-4} e^{-\pi/\epsilon^2}$$

and the constant of proportionality is given explicitly in (163). In the course of constructing the localized solution, we also obtain the location of the Maxwell point to fourth order accuracy in ϵ,

$$E_{hg} \sim \sqrt{3/38} + \epsilon^2 \frac{4}{19}\sqrt{\frac{367}{57}} + \epsilon^4 \frac{63711\sqrt{3/38}}{264974} + \ldots,$$

as well as the frequency of the oscillations for the front solution

$$1 - \epsilon^2 \frac{1}{2\sqrt{734}} + \epsilon^4 \frac{43163}{4310048} + \ldots.$$

The latter is necessary to establish the far field behaviour of the front solution and arises as a solvability condition at sixth order in ϵ, after the introduction of the super-slow scale $\xi = \epsilon^4 x$, see Appendix A. Finally, in §6, we summarise our results and present our conclusions.

[1] To make contact with earlier work, Eq. (3) can be transformed into $0 = ru + su^2 - u^3 - \left(1 + d^2/dx^2\right)^2 u$, via the transformation $u = -\epsilon f$, $r = -\epsilon^4$ and $s = 3E_{hg}$

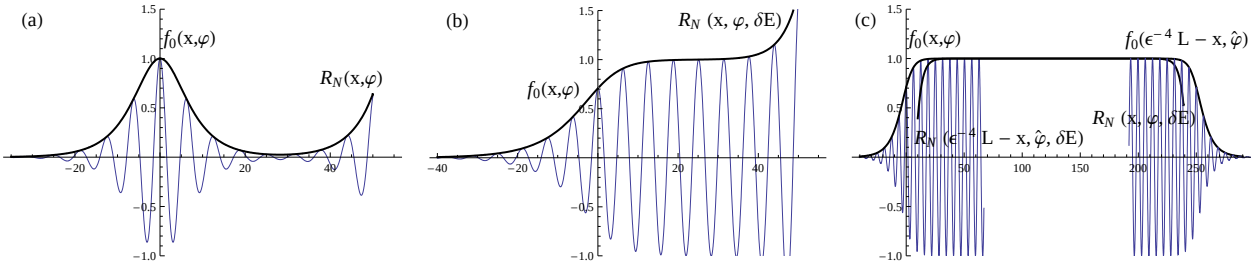

Figure 3: Leading order solution f_0 and exponentially small terms R_N away (a) and near (b,c) the Maxwell point. In (a) R_N must vanish to avoid blow up, which determines the phase φ of the oscillations. In (b), the vanishing of R_N relates φ to the deviation δE from the Maxwell point and yields the pinning range. In (c), two front solutions, one at $x = 0$, the other at $x = \epsilon^{-4}L$ are combined to construct a localized state. The exponentially small terms are necessary to ensure matching. The matching conditions determine the bifurcation diagram.

2 Multiple scale analysis far from the Maxwell point

2.1 Summary of this section

We will see in §3 that in order to describe fully the bifurcation diagram we need to perform a detailed beyond-all-orders multiple-scales analysis close to the Maxwell point, which will involve a further rescaling of (2). However, before presenting such an analysis we first demonstrate the beyond-all-orders technique on the simpler problem away from the Maxwell point. We emphasise that the analysis in the present section is equivalent to the previous work by Wadee et al. [73]. However the method used here is different, and the present section will be useful both to introduce our methodology and illustrate why a rescaling is necessary.

The translational invariance of equation (2) gives one degree of freedom, so that any solution represents a one-parameter family of solutions. However, when the method of multiple scales is used, the spatial variable is split into two spatial variables, and there are therefore two degrees of freedom associated with translational invariance. More specifically, we will find that

$$f \sim A_0(X)\, e^{ix-i\varphi} + \text{c.c.} + O(\epsilon),$$

where A_0 is a pulse-like amplitude, $X = \epsilon x$ is a slow spatial scale and the extra degree of freedom comes from the "phase difference" φ between the fast and slow scales. Such a phase difference is not normally considered in multiple-scales problems (for initial value problems it can be determined by the initial conditions), but for the present problem it is crucial. As we will see, it is not determined at any order of ϵ but is selected by exponentially-small terms beyond all orders.

We will identify these terms by optimally truncating the divergent multiple-scales expan-

sion and examining the behaviour of the remainder, i.e. we will set

$$f \sim \sum_{n=0}^{N-1} \epsilon^n f_n + R_N(x-\varphi, X).$$

The reason the series above diverges and has to be truncated will be understood by examining the solution near the singularities of $A_0(X)$ in the complex plane. An inner expansion in this region will show that $\epsilon^n f_n$ grows as $\epsilon^n \Gamma(n+\alpha)$ for some α for large n. Optimal truncation, corresponding to the smallest possible remainder, is therefore expected to take place at some order $N \sim \epsilon^{-1}$ and R_N will then be exponentially small in ϵ.

Away from the singularities of $A_0(X)$ but across the Stokes line that joins the singularities nearest to the real axis, exponentially-small terms in R_N are turned on. Indeed, by performing a multiple-scales matched-asymptotic analysis in the vicinity of the Stokes line we will find that, after the Stokes line is crossed,

$$R_N(x, X) \sim a_0(X) e^{ix} + \text{c.c.}$$

to leading order, where

$$a_0(X) = \tilde{\Lambda} \epsilon^{-4} e^{-\pi/\epsilon} \cos(\varphi + \phi) e^{X/2}$$

and $\tilde{\Lambda}$ and ϕ are constants explicitly given in (61), see Fig. 3. Since a_0 diverges exponentially as $X \to \infty$, there is a formal homoclinic solution to 0 only if

$$\varphi = -\phi + \frac{\pi}{2} + n\pi, \qquad n \in \mathbb{Z}.$$

This is the solvability condition which selects the phase shift, and it reduces the one-parameter family of solutions to just two.

The remainder of this section is organised as follows. In §2.2 the multiple scales expansion of f is developed to determine A_0. In §2.3 the equations for the late terms in this expansion are formulated, which are necessary to determine the optimal truncation point and equation for the remainder. These equations are first solved in the vicinity of the complex singularity of A_0 in §2.4, where the factorial/power divergence of f_n is demonstrated. In §2.5 the equations for the late terms are solved away from the singularity of A_0, making use of a factorial/power ansatz as $n \to \infty$. Having found the form of f_n for large n, the multiple scales expansion is optimally truncated in §2.6. The equation for the remainder R_N is formulated, and a multiple-scales boundary layer analysis in the vicinity of the Stokes line is used to demonstrate the rapid switching on of an exponentially small remainder term. In §2.7 the equation for R_N is solved away from the Stokes line. The results of §2.6 provide a jump condition as the Stokes line is crossed, which is determined in §2.8. Finally, in §2.9, the remainder term is evaluated as $X \to \infty$, and the solvability condition for the existence of a formal homoclinic solution is determined.

2.2 Multiple scale analysis: leading orders

We begin by developing the first few orders of the multiple scales expansion of f. We let $X = \epsilon x$ and treat x and X as independent variables to give

$$\begin{aligned}\frac{\partial^4 f}{\partial x^4} + 4\epsilon\frac{\partial^4 f}{\partial x^3 \partial X} + 6\epsilon^2\frac{\partial^4 f}{\partial x^2 \partial X^2} + 4\epsilon^3\frac{\partial^4 f}{\partial x \partial X^3} + \epsilon^4\frac{\partial^4 f}{\partial X^4} \\ +2\frac{\partial^2 f}{\partial x^2} + 4\epsilon\frac{\partial^2 f}{\partial x \partial X} + 2\epsilon^2\frac{\partial^2 f}{\partial X^2} + f &= -\epsilon^2 f - 3\epsilon E_{hg} f^2 - \epsilon^2 f^3. \end{aligned} \tag{4}$$

We expand f in powers of ϵ as

$$f = f_0(x, X) + \epsilon f_1(x, X) + \cdots . \tag{5}$$

Substituting the expansion (5) into (4) we find that at $O(\epsilon^0)$,

$$\mathcal{L} f_0 \equiv \frac{\partial^4 f_0}{\partial x^4} + 2\frac{\partial^2 f_0}{\partial x^2} + f_0 = 0$$

so that

$$f_0 = A_0(X)e^{i\tilde{x}} + \bar{A}_0(X)e^{-i\tilde{x}}, \tag{6}$$

where $\tilde{x} = x - \varphi$, with $0 \le \varphi < 2\pi$. Here φ is an (as yet) arbitrary constant which determines the relative phase between the fast oscillation and the slow amplitude modulation. This arbitrary phase difference is always present in multiple-scales calculations, but in initial value problems it can be determined from the initial conditions. Here we are on an infinite domain, and, as we will see, the determination of the phase difference occurs beyond-all-orders of the expansion (5). That there must be some condition determining φ is clear, since equation (2) exhibits translational invariance in x, but equation (4) exhibits translational invariance in both x and X. This extra degree of freedom corresponds to φ. Equating coefficients of ϵ in (4) gives

$$\mathcal{L} f_1 = -3E_{hg} f_0^2,$$

so that

$$f_1 = -\frac{E_{hg} A_0^2 e^{2i\tilde{x}}}{3} - \frac{E_{hg}\bar{A}_0^2 e^{-2i\tilde{x}}}{3} - 6E_{hg}|A_0|^2. \tag{7}$$

Equating coefficients of ϵ^2 in (4) gives

$$\mathcal{L} f_2 = 4\frac{\partial^2 f_0}{\partial X^2} - f_0^3 - f_0 - 6E_{hg} f_0 f_1.$$

To avoid secular terms the coefficients of $e^{\pm i\tilde{x}}$ on the right-hand side must be zero, giving the solvability condition

$$4A_0'' + (38E_{hg}^2 - 3)|A_0|^2 A_0 - A_0 = 0, \tag{8}$$

with solution

$$A_0 = \frac{4e^{X/2}e^{i\phi}}{1 + (76E_{hg}^2 - 6)e^X}, \tag{9}$$

where ϕ is an arbitrary real constant. Without loss of generality we may take $\phi = 0$, since ϕ can be absorbed into φ. The leading-order amplitude A_0 has singularities at the points

$$X = \pm ik\pi - \log(76E_{hg}^2 - 6),$$

for $k \in \mathbb{Z}$. If $E_{hg} > \sqrt{\frac{3}{38}}$ then there are two complex singularities nearest to the real X axis, and the imaginary part of these singularities is $\pm\pi$.

Now, in terms of X, equation (4) is a singular perturbation (ϵ multiplies the highest derivative in X). Whenever the leading-order amplitude A_0 has singularities (possibly complex) this singular perturbation will generate a divergent asymptotic expansion in the form factorial/power, since to compute the next term one has to differentiate the previous term [21]. Thus we expect that the expansion (5) will be divergent. Such divergent expansions are intimately related to the presence of exponentially small terms "beyond-all-orders". In [21] a technique was developed for examining the appearance of such terms as they are switched on across Stokes lines in the complex plane. This technique involves optimally truncating the series (5) and examining the behaviour of the remainder, which allows the exponentially small terms to be observed explicitly through a boundary-layer analysis near the Stokes line [27, 12]. This technique was extended to the case of multiple scales asymptotic expansions in [1] and we follow their methodology here.

The first step is to determine the behaviour of the late terms in the expansion (5).

2.3 Late term expansion

For n large the equation for the n th term in the expansion of f is

$$\begin{aligned}\frac{\partial^4 f_n}{\partial x^4} + 2\frac{\partial^2 f_n}{\partial x^2} + f_n = &-4\frac{\partial^4 f_{n-1}}{\partial x^3 \partial X} - 6\frac{\partial^4 f_{n-2}}{\partial x^2 \partial X^2} - 4\frac{\partial^4 f_{n-3}}{\partial x \partial X^3} - \frac{\partial^4 f_{n-4}}{\partial X^4} \\ &- 4\frac{\partial^2 f_{n-1}}{\partial x \partial X} - 2\frac{\partial^2 f_{n-2}}{\partial X^2} - \sum_{j=0}^{n-2}\sum_{m=0}^{n-2-j} f_j f_m f_{n-2-j-m} - f_{n-2} - 3E_{hg}\sum_{j=0}^{n-1} f_j f_{n-1-j}. \quad (10)\end{aligned}$$

For each n the solution will be a sum of harmonics of $e^{i\tilde{x}}$ in the form

$$f_n(x, X) = \sum_{k=-n-1}^{n+1} A_{n,k}(X) e^{ik\tilde{x}}. \quad (11)$$

In fact, it is easy to infer from the first few orders that odd harmonics only appear at even order and *vice versa*. Hence, in (11) $A_{n,k}$ is nonzero only when $n+k$ is odd. Let us also note that at each order the coefficients of the terms with $k = \pm 1$ are arbitrary, being solutions of the homogeneous equation. They are determined by the elimination of secular terms in the equation for f_{n+2}, in the same way that A_0 was determined by eliminating the secular terms

in the equation for f_2. Substituting (11) into (10) and equating coefficients of $e^{ik\tilde{x}}$ gives

$$(1-k^2)^2 A_{n,k} = 4ik^3 \frac{\partial A_{n-1,k}}{\partial X} + 6k^2 \frac{\partial^2 A_{n-2,k}}{\partial X^2} - 4ik \frac{\partial^3 A_{n-3,k}}{\partial X^3} - \frac{\partial^4 A_{n-4,k}}{\partial X^4}$$
$$- 4ik \frac{\partial A_{n-1,k}}{\partial X} - 2\frac{\partial^2 A_{n-2,k}}{\partial X^2} - \sum_p \sum_q \sum_{j=0}^{n-2} \sum_{m=0}^{n-2-j} A_{j,p} A_{m,q} A_{n-2-j-m,k-p-q}$$
$$- A_{n-2,k} - 3E_{hg} \sum_p \sum_{j=0}^{n-1} A_{j,p} A_{n-1-j,k-p}. \tag{12}$$

To determine the optimal truncation point and the equation for the remainder we need to solve for $A_{n,k}$ as $n \to \infty$. We begin in §2.4 by examining the behaviour of $A_{n,k}$ close to the singularity at $X = X_0 = i\pi - \log(76E_{hg}^2 - 6)$. Then, in §2.5, we solve for $A_{n,k}$ away from $X = X_0$.

2.4 Inner expansion near $X = X_0$

We will show in this section that as $X \to X_0$ and $n \to \infty$,

$$f_n(x, X) \sim \frac{\lambda \Gamma(n+4)(-i)^n}{(X - X_0)^{n+1}} \left(1 - (-1)^n + e^{2i\tilde{x}} - (-1)^n e^{-2i\tilde{x}}\right),$$

for some constant λ.

Near $X = X_0$ the leading-order solution $A_{0,0}$ has a simple pole. Since each new term in the expansion involves differentiating the previous term we expect the singularity in $A_{n,k}$ to be of the form $(X - X_0)^{-n-1}$. We therefore write

$$A_{n,k} \sim \frac{B_{n,k}}{(X - X_0)^{n+1}} \qquad \text{as} \quad X \to X_0. \tag{13}$$

Then the leading order solution (6), (7), (9) gives $B_{0,0} = B_{1,1} = B_{1,-1} = 0$ and

$$B_{0,1} = B_{0,-1} = \frac{-4i}{\sqrt{76E_{hg}^2 - 6}}, \quad B_{1,2} = B_{1,-2} = \frac{8E_{hg}}{114E_{hg}^2 - 9}, \quad B_{1,0} = \frac{48E_{hg}}{38E_{hg}^2 - 3}.$$

Substituting (13) into (12) gives

$$\begin{aligned}(k^2-1)^2 B_{n,k} \;=\; & -4nik^3 B_{n-1,k} + 6n(n-1)k^2 B_{n-2,k} + 4n(n-1)(n-2)ikB_{n-3,k} \\ & - n(n-1)(n-2)(n-3)B_{n-4,k} + 4nikB_{n-1,k} - 2n(n-1)B_{n-2,k} \\ & - \sum_{j=0}^{n-2} \sum_{m=0}^{n-2-j} \sum_p \sum_q B_{j,p} B_{m,q} B_{n-2-j-m,k-p-q} \\ & - 3E_{hg} \sum_{j=0}^{n-1} \sum_p B_{j,p} B_{n-1-j,k-p} \end{aligned} \tag{14}$$

When $k \neq \pm 1$ this equation gives $B_{n,k}$. The pair of equations with $k = \pm 1$ form a coupled set of equations for $B_{n-2,\pm 1}$, and are analogous to the secularity conditions which determine the coefficients of $e^{\pm i\tilde{x}}$ in the multiple scales expansion at each order.

From the right hand side of (14), $B_{n,k}$ is a combination of $nB_{n-1,k}$, $n\,(n-1)\,B_{n-2,k}$, etc. This motivates the ansatz

$$B_{n,k} \quad \sim \quad \Gamma(n+\alpha_k) b_{n,k}, \qquad \text{as } n \to \infty,$$

where the offsets α_k are to be determined. We will find that $B_{n,k}$ with $k = 0, \pm 2$ will dominate, followed by $k = \pm 1, \pm 3$, then ± 4 etc. Thus, for the $b_{n,k}$ to be of the same order for each k as $n \to \infty$, we set $\alpha_0 = \alpha_{\pm 2} = \alpha$, $\alpha_{\pm 1} = \alpha_{\pm 3} = \alpha - 1$, etc. This gives the system of equations

$$\vdots$$

$$\begin{aligned}
64 b_{n,-3} \sim\ & 96i\,(1+\cdots)\,b_{n-1,-3} + 52\,(1+\cdots)\,b_{n-2,-3} - 12i\,(1+\cdots)\,b_{n-3,-3} \\
& - (1+\cdots)\,b_{n-4,-3} + \cdots - 6E_{hg} B_{0,-1}\,(1+\cdots)\,b_{n-1,-2}, \\
9 b_{n,-2} \sim\ & 24i \left(1 + \frac{(1-\alpha)}{n} + \frac{(1-\alpha)^2}{n^2} + \cdots\right) b_{n-1,-2} \\
& + 22 \left(1 + \frac{2(1-\alpha)}{n} + \frac{(1-\alpha)(4-3\alpha)}{n^2} + \cdots\right) b_{n-2,-2} \\
& - 8i \left(1 + \frac{3(1-\alpha)}{n} + \frac{3(1-\alpha)(3-2\alpha)}{n^2} + \cdots\right) b_{n-3,-2} \\
& - \left(1 + \frac{4(1-\alpha)}{n} + \frac{2(1-\alpha)(8-5\alpha)}{n^2} + \cdots\right) b_{n-4,-2} \\
& - \frac{3}{n^2}\left(B_{0,-1}^2 b_{n-2,0} + 2B_{0,1}B_{0,-1} b_{n-2,-2}\right) \\
& - \frac{6E_{hg}}{n^2}\left(B_{0,-1} b_{n-1,-1} + B_{0,1} b_{n-1,-3} + B_{1,0} b_{n-2,-2} + B_{1,-2} b_{n-2,0}\right) + \cdots \\
0 \sim\ & 4 \left(1 + \frac{2(2-\alpha)}{n} + \cdots\right) b_{n-2,-1} - 4 \left(1 + \frac{3(2-\alpha)}{n} + \cdots\right) i b_{n-3,-1} \\
& - \left(1 + \frac{4(2-\alpha)}{n} + \cdots\right) b_{n-4,-1} - 6E_{hg}\left(B_{0,1} b_{n-1,-2} + B_{0,-1} b_{n-1,0}\right), \\
b_{n,0} \sim\ & - \left(1 + \frac{4(1-\alpha)}{n} + \frac{2(1-\alpha)(8-5\alpha)}{n^2} + \cdots\right) b_{n-4,0} \\
& - 2 \left(1 + \frac{2(1-\alpha)}{n} + \frac{(1-\alpha)(4-3\alpha)}{n^2} + \cdots\right) b_{n-2,0} \\
& - \frac{3}{n^2}\left(B_{0,1}^2 b_{n-2,-2} + 2B_{0,1}B_{0,-1} b_{n-2,0} + B_{0,-1}^2 b_{n-2,2}\right) \\
& - \frac{6E_{hg}}{n^2}\left(B_{0,1} b_{n-1,-1} + B_{0,-1} b_{n-1,1} + B_{1,0} b_{n-2,0} + B_{1,2} b_{n-2,-2} + B_{1,-2} b_{n-2,2}\right) + \cdots,
\end{aligned}$$

$$
\begin{aligned}
0 \sim\; & 4\left(1+\frac{2(2-\alpha)}{n}+\cdots\right)b_{n-2,1}+4i\left(1+\frac{3(2-\alpha)}{n}+\cdots\right)b_{n-3,1}\\
& -\left(1+\frac{4(2-\alpha)}{n}+\cdots\right)b_{n-4,1}-6E_{hg}\left(B_{0,-1}b_{n-1,2}+B_{0,1}b_{n-1,0}\right),\\
9b_{n,2} \sim\; & -24i\left(1+\frac{(1-\alpha)}{n}+\frac{(1-\alpha)^2}{n^2}+\cdots\right)b_{n-1,2}\\
& +22\left(1+\frac{2(1-\alpha)}{n}+\frac{(1-\alpha)(4-3\alpha)}{n^2}+\cdots\right)b_{n-2,2}\\
& +8i\left(1+\frac{3(1-\alpha)}{n}+\frac{3(1-\alpha)(3-2\alpha)}{n^2}+\cdots\right)b_{n-3,2}\\
& -\left(1+\frac{4(1-\alpha)}{n}+\frac{2(1-\alpha)(8-5\alpha)}{n^2}+\cdots\right)b_{n-4,2}\\
& -\frac{3}{n^2}\left(B_{0,1}^2b_{n-2,0}+2B_{0,1}B_{0,-1}b_{n-2,2}\right)\\
& -\frac{6E_{hg}}{n^2}\left(B_{0,1}b_{n-1,1}+B_{0,-1}b_{n-1,3}+B_{1,0}b_{n-2,2}+B_{1,2}b_{n-2,0}\right)+\cdots\\
64b_{n,3} \sim\; & -96i\left(1+\cdots\right)b_{n-1,3}+52\left(1+\cdots\right)b_{n-2,3}+12i\left(1+\cdots\right)b_{n-3,3}\\
& -\left(1+\cdots\right)b_{n-4,3}-6E_{hg}B_{0,1}\left(1+\cdots\right)b_{n-1,2}+\cdots,
\end{aligned}
$$

$$\vdots$$

To exploit the limit $n\to\infty$ we let $b_{n,k}\sim b_{n,k}^{(0)}+\frac{1}{n}\,b_{n,k}^{(1)}+\cdots$. At leading order, we have

$$
\begin{aligned}
64b_{n,-3}^{(0)} &\sim 96ib_{n-1,-3}^{(0)}+52b_{n-2,-3}^{(0)}-12ib_{n-3,-3}^{(0)}-b_{n-4,-3}^{(0)}-6E_{hg}B_{0,-1}b_{n-1,-2}^{(0)},\\
9b_{n,-2}^{(0)} &\sim 24ib_{n-1,-2}^{(0)}+22b_{n-2,-2}^{(0)}-8ib_{n-3,-2}^{(0)}-b_{n-4,-2}^{(0)},\\
0 &\sim 4b_{n-2,-1}^{(0)}-4ib_{n-3,-1}^{(0)}-b_{n-4,-1}^{(0)}-6E_{hg}\left(B_{0,1}b_{n-1,-2}^{(0)}+B_{0,-1}b_{n-1,0}^{(0)}\right),\\
b_{n,0}^{(0)} &\sim -b_{n-4,0}^{(0)}-2b_{n-2,0}^{(0)},\\
0 &\sim 4b_{n-2,1}^{(0)}+4ib_{n-3,1}^{(0)}-b_{n-4,1}^{(0)}-6E_{hg}\left(B_{0,-1}b_{n-1,2}^{(0)}+B_{0,1}b_{n-1,0}^{(0)}\right),\\
9b_{n,2}^{(0)} &\sim -24ib_{n-1,2}^{(0)}+22b_{n-2,2}^{(0)}+8ib_{n-3,2}^{(0)}-b_{n-4,2}^{(0)},\\
64b_{n,3}^{(0)} &\sim -96ib_{n-1,3}^{(0)}+52b_{n-2,3}^{(0)}+12ib_{n-3,3}^{(0)}-b_{n-4,3}^{(0)}-6E_{hg}B_{0,1}b_{n-1,2}^{(0)},
\end{aligned}
$$

Seeking a solution in the form $b_{n,k}^{(0)}=\kappa^n b_k^{(0)}$ gives

$$
\begin{aligned}
0 &\sim (-64\kappa^4+96i\kappa^3+52\kappa^2-12i\kappa-1)b_{-3}^{(0)}-6\kappa^3E_{hg}B_{0,-1}b_{-2}^{(0)}, &(15)\\
0 &\sim (-9\kappa^4+24i\kappa^3+22\kappa^2-8i\kappa-1)b_{-2}^{(0)}, &(16)\\
0 &\sim (4\kappa^2-4i\kappa-1)b_{-1}^{(0)}-6E_{hg}\kappa^3\left(B_{0,1}b_{-2}^{(0)}+B_{0,-1}b_0^{(0)}\right), &(17)
\end{aligned}
$$

$$
\begin{aligned}
0 &\sim (-\kappa^4 - 2\kappa^2 - 1)b_0^{(0)}, && (18)\\
0 &\sim (4\kappa^2 + 4i\kappa - 1)b_1^{(0)} - 6E_{hg}\kappa^3\left(B_{0,-1}b_2^{(0)} + B_{0,1}b_0^{(0)}\right), && (19)\\
0 &\sim (-9\kappa^4 - 24i\kappa^3 + 22\kappa^2 + 8i\kappa - 1)b_2^{(0)}, && (20)\\
0 &\sim (-64\kappa^4 - 96i\kappa^3 + 52\kappa^2 + 12i\kappa - 1)b_3^{(0)} - 6E_{hg}\kappa^3 B_{0,1}b_2^{(0)}. && (21)
\end{aligned}
$$

This is an eigenvalue problem for κ. Note that each of the equations for $b_2^{(0)}$, $b_0^{(0)}$ and $b_{-2}^{(0)}$ decouples. The roots of (16) are $\kappa = i$ and $\kappa = i/3$, those of (18) are $\kappa = \pm i$, and those of (20) are $\kappa = -i$, $\kappa = -i/3$. Since the late terms behave as κ^n, the eigenmodes involving $\kappa = \pm i/3$ are exponentially subdominant to those involving $\kappa = \pm i$, and we do not need to consider them further. Let us examine the eigenmodes with $\kappa = \pm i$ in more detail.

Case $\kappa = -i$ In this case, proceeding to next order in (18) and (20), the full set of leading-order equations is

$$
\begin{aligned}
0 &\sim -225b_{-3}^{(0)} - 6E_{hg}B_{0,-1}ib_{-2}^{(0)}, && (22)\\
0 &\sim -64b_{-2}^{(0)}, && (23)\\
0 &\sim -9b_{-1}^{(0)} - 6E_{hg}i\left(B_{0,1}b_{-2}^{(0)} + B_{0,-1}b_0^{(0)}\right), && (24)\\
0 &\sim -4(1-\alpha)(2-\alpha)b_0^{(0)} + 3\left(B_{0,1}^2 b_{-2}^{(0)} + 2B_{0,1}B_{0,-1}b_0^{(0)} + B_{0,-1}^2 b_2^{(0)}\right)\\
&\quad - 6E_{hg}\left(B_{0,1}ib_{-1}^{(0)} + B_{0,-1}ib_1^{(0)} - B_{1,0}b_0^{(0)} - B_{1,2}b_{-2}^{(0)} - B_{1,-2}b_2^{(0)}\right), && (25)\\
0 &\sim -b_1^{(0)} - 6E_{hg}i\left(B_{0,-1}b_2^{(0)} + B_{0,1}b_0^{(0)}\right), && (26)\\
0 &\sim -4(1-\alpha)(2-\alpha)b_2^{(0)} + 3\left(B_{0,1}^2 b_0^{(0)} + 2B_{0,1}B_{0,-1}b_2^{(0)}\right)\\
&\quad - 6E_{hg}\left(B_{0,1}ib_1^{(0)} + B_{0,-1}ib_3^{(0)} - B_{1,0}b_2^{(0)} - B_{1,2}b_0^{(0)}\right) && (27)\\
0 &\sim -9b_3^{(0)} - 6E_{hg}B_{0,1}ib_2^{(0)}. && (28)
\end{aligned}
$$

We see immediately that $b_{-3}^{(0)} = b_{-2}^{(0)} = 0$. Eliminating $b_{\pm 1}^{(0)}$ and $b_3^{(0)}$ and using the expressions for $B_{0,\pm 1}$, $B_{1,0}$ and $B_{1,\pm 2}$, leaves the following system for $b_0^{(0)}$ and $b_2^{(0)}$:

$$
\begin{aligned}
(2 + 3\alpha - \alpha^2)b_0^{(0)} + 2b_2^{(0)} &= 0, && (29)\\
2b_0^{(0)} + (2 + 3\alpha - \alpha^2)b_2^{(0)} &= 0. && (30)
\end{aligned}
$$

The condition for a non-zero solution is

$$(2 + 3\alpha - \alpha^2)^2 = 4 \qquad (31)$$

giving the roots

$$\alpha = -1,\ 0,\ 3,\ 4.$$

The solutions with $\alpha = 0$ and $\alpha = 3$ satisfy $b_0^{(0)} = -b_2^{(0)}$, while those with $\alpha = -1$ and $\alpha = 4$ satisfy $b_0^{(0)} = b_2^{(0)}$. The large n behaviour is dominated by the largest value of α.

Case $\kappa = i$ In this case $b_3^{(0)} = b_2^{(0)} = 0$. Solving (15), (17), and (19), and eliminating $b_{\pm 1}^{(0)}$ and $b_{-3}^{(0)}$ in (16) and (18), we now find:

$$\begin{aligned} (2 + 3\alpha - \alpha^2) b_0^{(0)} + 2 b_{-2}^{(0)} &= 0, \qquad (32) \\ 2 b_0^{(0)} + (2 + 3\alpha - \alpha^2) b_{-2}^{(0)} &- 0. \qquad (33) \end{aligned}$$

Again, the condition for a non-zero solution is

$$(2 + 3\alpha - \alpha^2)^2 = 4 \qquad (34)$$

with roots

$$\alpha = -1,\ 0,\ 3,\ 4.$$

The solutions with $\alpha = 0$ and $\alpha = 3$ satisfy $b_0^{(0)} = -b_{-2}^{(0)}$, while those with $\alpha = -1$ and $\alpha = 4$ satisfy $b_0^{(0)} = b_{-2}^{(0)}$.

Combining the two eigenvectors associated to $\alpha = 4$ we see that

$$\begin{aligned} f_n(x, X) &= \sum_{k=-n-1}^{n+1} A_{n,k} e^{ik\tilde{x}} \sim \sum_{k=-n-1}^{n+1} \frac{B_{n,k}\, e^{ik\tilde{x}}}{(X - X_0)^{n+1}} \\ &\sim \frac{\Gamma(n+4)}{(X - X_0)^{n+1}} \left((-i)^n \lambda (1 + e^{2i\tilde{x}}) + i^n \mu (1 + e^{-2i\tilde{x}}) + O(n^{-1}) \right) \\ &= \frac{\Gamma(n+4)(-i)^n}{(X - X_0)^{n+1}} \left(\lambda + (-1)^n \mu + \lambda e^{2i\tilde{x}} + e^{-2i\tilde{x}} \mu + O(n^{-1}) \right), \end{aligned}$$

where for $\kappa = -i$ we have set $b_0^{(0)} = b_2^{(0)} = \lambda$, and for $\kappa = i$ we have set $b_0^{(0)} = b_{-2}^{(0)} = \mu$. From the form of the equation (14) we find that f_n has no term constant in $\tilde{x}$ when n is even, so that we must have $\mu = -\lambda$, giving finally

$$f_n(x, X) \sim \frac{\lambda \Gamma(n+4)(-i)^n}{(X - X_0)^{n+1}} \left(1 - (-1)^n + e^{2i\tilde{x}} - (-1)^n e^{-2i\tilde{x}} \right). \qquad (35)$$

Note that $B_{1,0}$ and $B_{1,2}$ are real and the equations for $B_{n,0}$ and $B_{n,2}$ are also real. Hence, considering (35) with n odd, we see that λ is purely imaginary.

2.5 Outer expansion away from $X = X_0$

We now turn to the behaviour of f_n as $n \to \infty$ for values of X not close to the singularity $X = X_0$. We will show that

$$\begin{aligned} f_n(x, X) \sim\ & \frac{\Gamma(n+4)(-i)^n}{(X - X_0)^{n+4}} \left(F_0^{(0)}(X) + F_2^{(0)}(X) e^{2i\tilde{x}} \right) \\ & + \frac{\Gamma(n+4) i^n}{(X - X_0)^{n+4}} \left(G_0^{(0)}(X) + G_{-2}^{(0)}(X) e^{-2i\tilde{x}} \right) + \text{c.c.}, \end{aligned}$$

where $F_0^{(0)}$ and $F_2^{(0)}$ are given by (40) and $G_0^{(0)}$ and $G_{-2}^{(0)}$ are given by (41), with K_0 and K_1 given by (42).

Motivated by the inner expansion in the vicinity of the singularity we write

$$f_n(x,X) \;\sim\; \sum_k \frac{\Gamma(n+\alpha_k)(-i)^n}{(X-X_0)^{n+\alpha_k}} f_{n,k}(X) e^{ik\tilde{x}}$$

with

$$f_{n,k}(X) \sim F_k^{(0)}(X) + (-1)^n G_k^{(0)}(X) + \frac{1}{n}\left(F_k^{(1)}(X) + (-1)^n G_k^{(1)}(X)\right) + \cdots,$$

and $\alpha_0 = \alpha_{\pm 2} = \alpha$, $\alpha_{\pm 1} = \alpha_{\pm 3} = \alpha - 1, \cdots$ as before. Then at order $\Gamma(n+\alpha)$ we find

$$F_{-2}^{(0)} = G_2^{(0)} = 0.$$

Next, at order $\Gamma(n+\alpha-1)$ we find

$$\begin{aligned}
F_{-3}^{(0)} = F_{-2}^{(1)} &= 0, \\
3iF_{-1}^{(0)} &= 2E_{hg}\bar{A}_0 F_0^{(0)}, \\
iF_1^{(0)} &= 6E_{hg}A_0 F_0^{(0)} + 6E_{hg}\bar{A}_0 F_2^{(0)}, \\
3iF_3^{(0)} &= 2E_{hg}A_0 F_2^{(0)}, \\
G_3^{(0)} = G_2^{(1)} &= 0, \\
-3iG_{-3}^{(0)} &= 2E_{hg}\bar{A}_0 G_{-2}^{(0)}, \\
-iG_{-1}^{(0)} &= 6E_{hg}A_0 G_{-2}^{(0)} + 6E_{hg}\bar{A}_0 G_0^{(0)}, \\
-3iG_1^{(0)} &= 2E_{hg}A_0 G_0^{(0)}.
\end{aligned}$$

Finally, at order $\Gamma(n+\alpha-2)$ we obtain a set of differential equations for the remaining leading-order terms

$$4F_{2_{XX}}^{(0)} - F_2^{(0)} + (38E_{hg}^2 - 3)A_0^2 F_0^{(0)} + 2(38E_{hg}^2 - 3)|A_0|^2 F_2^{(0)} = 0, \tag{36}$$

$$4F_{0_{XX}}^{(0)} - F_0^{(0)} + (38E_{hg}^2 - 3)\bar{A}_0^2 F_2^{(0)} + 2(38E_{hg}^2 - 3)|A_0|^2 F_0^{(0)} = 0, \tag{37}$$

$$4G_{0_{XX}}^{(0)} - G_0^{(0)} + (38E_{hg}^2 - 3)A_0^2 G_{-2}^{(0)} + 2(38E_{hg}^2 - 3)|A_0|^2 G_0^{(0)} = 0, \tag{38}$$

$$4G_{-2_{XX}}^{(0)} - G_{-2}^{(0)} + (38E_{hg}^2 - 3)\bar{A}_0^2 G_0^{(0)} + 2(38E_{hg}^2 - 3)|A_0|^2 G_{-2}^{(0)} = 0. \tag{39}$$

Recall that A_0 is real and satisfies

$$4A_0'' - A_0 + (38E_{hg}^2 - 3)A_0^3 = 0.$$

Thus we can immediately spot two solutions of (36)-(37) as

$$\begin{aligned}
F_0^{(0)} = -F_2^{(0)} &= A_0, \\
F_0^{(0)} = F_2^{(0)} &= A_{0_X}.
\end{aligned}$$

(These correspond to differentiating f_0 with respect to x and X respectively.) Using variation of parameters on these solutions gives the other two solutions as

$$\begin{aligned} F_0^{(0)} = -F_2^{(0)} &= A_0 \int_{X_0}^{X} \frac{1}{A_0^2}\, dX, \\ F_0^{(0)} = F_2^{(0)} &= A_{0_X} \int_{X_0}^{X} \frac{1}{A_{0_X}^2}\, dX. \end{aligned}$$

Similarly the four independent solutions for $G_0^{(0)}$ and $G_{-2}^{(0)}$ are

$$\begin{aligned} G_0^{(0)} = G_{-2}^{(0)} &= A_{0_X}, \\ G_0^{(0)} = G_{-2}^{(0)} &= A_{0_X} \int_{X_0}^{X} \frac{1}{A_{0_X}^2}\, dX, \\ G_0^{(0)} = -G_{-2}^{(0)} &= A_0, \\ G_0^{(0)} = -G_{-2}^{(0)} &= A_0 \int_{X_0}^{X} \frac{1}{A_0^2}\, dX, \end{aligned}$$

Now, as $X \to X_0$,

$$\begin{aligned} A_0 &\sim -\frac{2\sqrt{2}i}{\sqrt{38E_{hg}^2 - 3}\,(X - X_0)}, \\ A_{0_X} &\sim \frac{2\sqrt{2}i}{\sqrt{38E_{hg}^2 - 3}\,(X - X_0)^2}, \\ A_0 \int_{X_0}^{X} \frac{1}{A_0^2}\, dX &\sim \frac{\sqrt{38E_{hg}^2 - 3}\, i(X - X_0)^2}{6\sqrt{2}}, \\ A_{0_X} \int_{X_0}^{X} \frac{1}{A_{0_X}^2}\, dX &\sim -\frac{\sqrt{38E_{hg}^2 - 3}\, i(X - X_0)^3}{10\sqrt{2}}, \end{aligned}$$

Since $f_{n,2} = O((X - X_0)^{\alpha - 1})$ to match with the inner region in the vicinity of the singularity, these four solutions give α values of 0, -1, 3 and 4 respectively, corresponding to the four different behaviours we found in the inner region. The large n behaviour will be dominated by the $\alpha = 4$ term. The others will also be present, but are lower order in n. Thus the dominant behaviour as $n \to \infty$ is given by

$$F_0^{(0)} = F_2^{(0)} = K_0 A_{0_X} \int_{X_0}^{X} \frac{1}{A_{0_X}^2}\, dX, \tag{40}$$

$$G_0^{(0)} = G_{-2}^{(0)} = K_1 A_{0_X} \int_{X_0}^{X} \frac{1}{A_{0_X}^2}\, dX, \tag{41}$$

for some constants K_0, K_1. Then, as $X \to X_0$,

$$\begin{aligned} F_0^{(0)} &\sim F_2^{(0)} \sim -\frac{K_0\sqrt{38E_{hg}^2-3}\,i(X-X_0)^3}{10\sqrt{2}}, \\ G_0^{(0)} &\sim G_{-2}^{(0)} \sim -\frac{K_1\sqrt{38E_{hg}^2-3}\,i(X-X_0)^3}{10\sqrt{2}}. \end{aligned}$$

Matching with (35) gives

$$K_0 = -K_1 = \lambda\frac{10\sqrt{2}\,i}{\sqrt{38E_{hg}^2-3}}, \tag{42}$$

and since λ is imaginary, K_0 is real. Thus the leading-order behaviour as $n \to \infty$ is given by

$$\begin{aligned} f_n(x,X) \sim\ & \frac{\Gamma(n+4)(-i)^n}{(X-X_0)^{n+4}}\left(F_0^{(0)}(X) + F_2^{(0)}(X)e^{2i\tilde{x}}\right) \\ & + \frac{\Gamma(n+4)i^n}{(X-X_0)^{n+4}}\left(G_0^{(0)}(X) + G_{-2}^{(0)}(X)e^{-2i\tilde{x}}\right), \end{aligned} \tag{43}$$

where $F_0^{(0)}$ and $F_2^{(0)}$ are given by (40) and $G_0^{(0)}$ and $G_{-2}^{(0)}$ are given by (41), with K_0 and K_1 given by (42). So far we have been concerned with the contribution to the late terms from the singularity at $X = X_0$. We can determine the contribution from the conjugate singularity at $X = \bar{X}_0$ by symmetry, since the sum of both combinations must be real when X is real. Thus this second contribution is

$$\begin{aligned} f_n(x,X) \sim\ & \frac{\Gamma(n+4)i^n}{(X-\bar{X}_0)^{n+4}}\left(\bar{F}_0^{(0)}(X) + \bar{F}_2^{(0)}(X)e^{-2i\tilde{x}}\right) \\ & + \frac{\Gamma(n+4)(-i)^n}{(X-\bar{X}_0)^{n+4}}\left(\bar{G}_0^{(0)}(X) + \bar{G}_{-2}^{(0)}(X)e^{2i\tilde{x}}\right). \end{aligned} \tag{44}$$

2.6 Optimal truncation

We have now found the behaviour of the late terms in the expansion (5). From (43) we can see that, as expected, terms initially get smaller as n increases (by a factor of ϵ each time) but eventually increase with n due to the presence of the factorial; the expansion diverges as $n \to \infty$ for any fixed x, X, ϵ. The next step in the procedure developed in [21] is to truncate the expansion, at $n = N-1$ say, and study the remainder. If we truncate at any fixed order N then the remainder will be of $O(\epsilon^N)$. However, if we truncate optimally, that is, we truncate the expansion at it smallest term, then the remainder will be exponentially small in ϵ. Truncating after N terms we write

$$f = \sum_{n=0}^{N-1}\epsilon^n f_n(\tilde{x},X) + R_N(\tilde{x},X).$$

We will show that R_N exhibits a boundary layer behaviour, undergoing a rapid transition in the vicinity of the Stokes line (which we will identify shortly). We will show that the jump in R_N as X crosses the Stokes line is

$$2\pi i\, e^{i\alpha\pi/2}\epsilon^{-\alpha}e^{iX_0/\epsilon}e^{-i\varphi}\left(F_0^{(0)}e^{-i\tilde{x}}+F_2^{(0)}e^{i\tilde{x}}\right)+\text{c.c.}$$

The equation for the remainder R_N is

$$\begin{aligned}
&R_{N_{\tilde{x}\tilde{x}\tilde{x}\tilde{x}}}+2R_{N_{\tilde{x}\tilde{x}}}+R_N\\
&\quad+4\epsilon R_{N_{\tilde{x}\tilde{x}\tilde{x}X}}+6\epsilon^2R_{N_{\tilde{x}\tilde{x}XX}}+4\epsilon^3R_{N_{\tilde{x}XXX}}+\epsilon^4R_{N_{XXXX}}+4\epsilon R_{N_{\tilde{x}X}}+2\epsilon^2R_{N_{XX}}\\
&\quad+\epsilon^2(3f_0^2R_N+\cdots)+\epsilon^2R_N+6E_{hg}\epsilon f_0R_N+6E_{hg}\epsilon^2f_1R_N\\
&\sim\ \epsilon^N\left(f_{N_{\tilde{x}\tilde{x}\tilde{x}\tilde{x}}}+2f_{N_{\tilde{x}\tilde{x}}}+f_N\right)\\
&\quad+\epsilon^{N+1}\left(-6f_{N-1_{\tilde{x}\tilde{x}XX}}-4f_{N-2_{\tilde{x}XXX}}-f_{N-3_{XXXX}}-2f_{N-1_{XX}}\right)\\
&\quad+\epsilon^{N+2}\left(-4f_{N-1_{\tilde{x}XXX}}-f_{N-2_{XXXX}}\right)\\
&\quad+\epsilon^{N+3}\left(-f_{N-1_{XXXX}}\right)+\cdots,
\end{aligned}\tag{45}$$

where we have used the equation for f_N to simplify the right-hand side. The omitted terms, represented by $\cdots$, are all lower order as $N\to\infty$, $\epsilon\to 0$. When we approximate the terms on the right-hand side of (45) as $N\to\infty$ and $\epsilon\to 0$ we will obtain terms from the singularity at $X=X_0$ through (43) and terms from the singularity at $X=\bar{X}_0$ through (44); we denote the former by rhs^+ and the latter by rhs^-. Each of these will be composed of two parts—one for the terms in F and one for the terms in G; we denote these with the subscripts F and G respectively. Now, as $\epsilon\to 0$, $N\to\infty$,

$$\text{rhs}_F^+\ \sim\ e^{i\tilde{x}}\epsilon^N(-i)^N\frac{\Gamma(N+\alpha)}{(X-X_0)^{N+\alpha}}\sum_{k=0,2}e^{i(k-1)\tilde{x}}C_{N,k}\tag{46}$$

where

$$\begin{aligned}
C_{N,k}\ =\ F_k^{(0)}\Bigg(&(k^2-1)^2-(6k^2-4k-1)\epsilon(-i)\frac{(N+\alpha)}{(X-X_0)}\\
&-(-4k+1)\epsilon^2(-i)^2\frac{(N+\alpha+1)(N+\alpha)}{(X-X_0)^2}\\
&-\epsilon^3(-i)^3\frac{(N+\alpha+2)(N+\alpha+1)(N+\alpha)}{(X-X_0)^3}\Bigg),
\end{aligned}$$

and we have brought out one factor of $e^{i\tilde{x}}$, which we will see shortly will combine with the factorial/power as in [21]. We can see from (43) that the ratio of successive terms is approximately $-in\epsilon/(X-X_0)$. Following Dingle [30], we expect there to be Stokes lines where successive terms have the same phase, that is, where $-i/(X-X_0)$ is real and positive. By optimally truncating the expansion and observing the behaviour of the remainder as in [21], we will explicitly see the switching on of exponentially small terms as the Stokes lines are crossed.

The optimal truncation point, corresponding to the smallest term, is approximately $N = |X - X_0|/\epsilon$. Since N depends on $|X - X_0|$ only we write $X - X_0 = re^{i\theta}$ giving $N = r/\epsilon + \nu$, where ν is required to ensure that N is an integer, but is bounded as $\epsilon \to 0$. We first approximate the premultiplier of the sum in (46) at optimal truncation, following [21]. Writing

$$e^{i\tilde{x}} = e^{ix}e^{-i\varphi} = e^{i(X-X_0)/\epsilon}e^{iX_0/\epsilon}e^{-i\varphi}, \tag{47}$$

and using Stirling's formula, we find

$$\begin{aligned}
&e^{i(X-X_0)/\epsilon}\epsilon^{N+\alpha}(-i)^{N+\alpha}\frac{\Gamma(N+\alpha)}{(X-X_0)^{N+\alpha}} \\
&\quad\sim \frac{\sqrt{2\pi}\, e^{ire^{i\theta}/\epsilon}\epsilon^{r/\epsilon+\nu+\alpha}e^{-i\pi/2(r/\epsilon+\nu+\alpha)}(r/\epsilon+\alpha+\nu)^{r/\epsilon+\alpha+\nu-1/2}e^{-r/\epsilon-\alpha-\nu}}{r^{r/\epsilon+\nu+\alpha}e^{i\theta(r/\epsilon+\nu+\alpha)}} \\
&\quad\sim \frac{\sqrt{2\pi}\,\epsilon^{1/2}e^{-i\pi/2(r/\epsilon+\nu+\alpha)}(1+\epsilon(\alpha+\nu)/r)^{r/\epsilon+\alpha+\nu-1/2}e^{-r/\epsilon-\alpha-\nu}e^{ire^{i\theta}/\epsilon}}{r^{1/2}e^{i\theta(r/\epsilon+\nu+\alpha)}} \\
&\quad\sim \frac{\sqrt{2\pi}\,\epsilon^{1/2}e^{-i\pi/2(r/\epsilon+\nu+\alpha)}e^{\alpha+\nu}e^{-r/\epsilon-\alpha-\nu}e^{ire^{i\theta}/\epsilon}}{r^{1/2}e^{i\theta(r/\epsilon+\nu+\alpha)}} \\
&\quad\sim \frac{\sqrt{2\pi}\,\epsilon^{1/2}e^{-i\pi/2(r/\epsilon+\nu+\alpha)}e^{-r/\epsilon}e^{ire^{i\theta}/\epsilon}}{r^{1/2}e^{i\theta(r/\epsilon+\nu+\alpha)}}.
\end{aligned}$$

This expression is exponentially small except in the vicinity of the Stokes line $\theta = -\pi/2$. Writing $\theta = -\pi/2 + \epsilon^{1/2}\bar{\theta}$ gives

$$\begin{aligned}
e^{i(X-X_0)/\epsilon}\epsilon^{N+\alpha}(-i)^{N+\alpha}\frac{\Gamma(N+\alpha)}{(X-X_0)^{N+\alpha}} &\sim \frac{\sqrt{2\pi}\,\epsilon^{1/2}e^{-i\pi/2(r/\epsilon+\nu+\alpha)}e^{-r/\epsilon}e^{r(1+i\epsilon^{1/2}\bar{\theta}-\epsilon\bar{\theta}^2/2)/\epsilon}}{r^{1/2}e^{i(-\pi/2+\epsilon^{1/2}\bar{\theta})(r/\epsilon+\nu+\alpha)}} \\
&\sim \frac{\sqrt{2\pi}\,\epsilon^{1/2}e^{-r\bar{\theta}^2/2}}{r^{1/2}}.
\end{aligned} \tag{48}$$

Hence, combining (46), (47) and (48) we have, in the vicinity of the Stokes line,

$$\mathrm{rhs}_F^+ \sim e^{i\alpha\pi/2}\epsilon^{-\alpha}e^{iX_0/\epsilon}e^{-i\varphi}\frac{\sqrt{2\pi}\,\epsilon^{1/2}e^{-r\bar{\theta}^2/2}}{r^{1/2}}\sum_{k=0,2}C_{N,k}e^{i(k-1)\tilde{x}}. \tag{49}$$

It remains to approximate $C_{N,k}$ near the Stokes line. Using (47) we find

$$\begin{aligned}
C_{N,k} &\sim F_k^{(0)}\left((k^2-1)^2 - (6k^2-4k-1)e^{-i\epsilon^{1/2}\bar{\theta}} - (-4k+1)e^{-2i\epsilon^{1/2}\bar{\theta}} - e^{-3i\epsilon^{1/2}\bar{\theta}}\right) \\
&\sim F_k^{(0)}\left(k(k^3-8k+8) + 2i\sqrt{\epsilon}\bar{\theta}(3k^2-6k+2) + \cdots\right),
\end{aligned}$$

where $F_k^{(0)}$ is evaluated on the Stokes line and so is a function of r but not of $\bar{\theta}$. Hence

$$\begin{aligned}
C_{N,0} &\sim 4i\sqrt{\epsilon}\bar{\theta}F_0^{(0)} + \cdots, \\
C_{N,2} &\sim 4i\sqrt{\epsilon}\bar{\theta}F_2^{(0)} + \cdots.
\end{aligned}$$

With $X = X_0 + re^{i\theta}$ we have

$$\frac{\partial}{\partial X} = -\frac{ie^{-i\theta}}{r}\frac{\partial}{\partial \theta},$$

so that in the vicinity of the Stokes line, with $\theta = -\pi/2 + \epsilon^{1/2}\bar{\theta}$, we have

$$\frac{\partial}{\partial X} = \frac{e^{-i\epsilon^{1/2}\bar{\theta}}}{r\epsilon^{1/2}}\frac{\partial}{\partial \bar{\theta}}.$$

Thus equation (45) for the remainder due to the singularity at X_0 (which we write as R_N^+) becomes

$$\begin{aligned}
&R^+_{N_{\tilde{x}\tilde{x}\tilde{x}\tilde{x}}} + 2R^+_{N_{\tilde{x}\tilde{x}}} + R^+_N \\
&\quad + 4\epsilon^{1/2}\frac{(1-i\epsilon^{1/2}\bar{\theta})}{r}R^+_{N_{\tilde{x}\tilde{x}\tilde{x}\bar{\theta}}} + \frac{6\epsilon}{r^2}R^+_{N_{\tilde{x}\tilde{x}\bar{\theta}\bar{\theta}}} + 4\epsilon^{1/2}\frac{(1-i\epsilon^{1/2}\bar{\theta})}{r}R^+_{N_{\tilde{x}\bar{\theta}}} + \frac{2\epsilon}{r^2}R^+_{N_{\bar{\theta}\bar{\theta}}} \\
&\quad + 6E_{hg}\epsilon f_0 R^+_N + o(\epsilon R^+_N) \\
&\sim\ e^{i\alpha\pi/2}\epsilon^{-\alpha+1/2}e^{iX_0/\epsilon}e^{-i\varphi}\frac{\sqrt{2\pi}\,e^{-r\bar{\theta}^2/2}}{r^{1/2}}\left(4i\sqrt{\epsilon}\bar{\theta}F_0^{(0)}e^{-i\tilde{x}} + 4i\sqrt{\epsilon}\bar{\theta}F_2^{(0)}e^{i\tilde{x}}\right) \\
&= \epsilon^{-\alpha+1/2}e^{iX_0/\epsilon}\left(\epsilon^{1/2}c_{-1}(\bar{\theta})e^{-i\tilde{x}} + \epsilon^{1/2}c_1(\bar{\theta})e^{i\tilde{x}}\right), \qquad (50)
\end{aligned}$$

say. Now, equation (50) must again be solved via a multiple scales expansion, since the rescaled X coordinate $\bar{\theta}$ is still much longer than the fast scale. The forcing term in (50) is a resonant term, so that the solution will be an order of magnitude larger: $R_N^+ = O(\epsilon^{-\alpha}e^{iX_0/\epsilon})$. We seek an expansion of the form

$$R_N^+ \sim \epsilon^{-\alpha}e^{iX_0/\epsilon}\left(R_0^+ + \epsilon^{1/2}R_1^+ + \epsilon R_2^+ + \cdots\right).$$

Then, at leading order,

$$R^+_{0_{\tilde{x}\tilde{x}\tilde{x}\tilde{x}}} + 2R^+_{0_{\tilde{x}\tilde{x}}} + R_0^+ = 0,$$

so that

$$R_0^+ = S_{-1}(\bar{\theta})e^{-i\tilde{x}} + S_1(\bar{\theta})e^{i\tilde{x}}.$$

Equating coefficients at $O(e^{iX_0/\epsilon}\epsilon^{-\alpha+1/2})$ gives

$$R^+_{1_{\tilde{x}\tilde{x}\tilde{x}\tilde{x}}} + 2R^+_{1_{\tilde{x}\tilde{x}}} + R_1^+ = 0,$$

with solution

$$R_1^+ = 0.$$

Finally, equating coefficients at $O(e^{iX_0/\epsilon}\epsilon^{-\alpha+1})$ gives

$$\begin{aligned}
&R^+_{2_{\tilde{x}\tilde{x}\tilde{x}\tilde{x}}} + 2R^+_{2_{\tilde{x}\tilde{x}}} + R_2^+ - \frac{4}{r^2}\left(S''_{-1}(\bar{\theta})e^{-i\tilde{x}} + S''_1(\bar{\theta})e^{i\tilde{x}}\right) \\
&+ 6E_{hg}\left(A(X)e^{i\tilde{x}} + \bar{A}(X)e^{-i\tilde{x}}\right)\left(S_{-1}(\bar{\theta})e^{-i\tilde{x}} + S_1(\bar{\theta})e^{i\tilde{x}}\right) \\
&\qquad\qquad \sim\ c_{-1}(\bar{\theta})e^{-i\tilde{x}} + c_1(\bar{\theta})e^{i\tilde{x}}.
\end{aligned}$$

The solvability condition that there are no inhomogeneous terms of the form $e^{\pm i\tilde{x}}$ then gives

$$-\frac{4}{r^2}S''_{-1}(\bar{\theta}) = c_{-1}(\bar{\theta}) = e^{i\alpha\pi/2}e^{-i\varphi}\frac{\sqrt{2\pi}\,e^{-r\bar{\theta}^2/2}}{r^{1/2}}4i\bar{\theta}F_0^{(0)},$$
$$-\frac{4}{r^2}S''_{1}(\bar{\theta}) = c_{1}(\bar{\theta}) = e^{i\alpha\pi/2}e^{-i\varphi}\frac{\sqrt{2\pi}\,e^{-r\bar{\theta}^2/2}}{r^{1/2}}4i\bar{\theta}F_2^{(0)},.$$

Hence

$$S_{-1} \sim i\sqrt{\pi}\,e^{i\alpha\pi/2}\epsilon^{-\alpha}e^{iX_0/\epsilon}e^{-i\varphi}F_0^{(0)}\int_{-\infty}^{\frac{\sqrt{r}\bar{\theta}}{\sqrt{2}}} e^{-v^2}\,dv,$$
$$S_{1} \sim i\sqrt{\pi}\,e^{i\alpha\pi/2}\epsilon^{-\alpha}e^{iX_0/\epsilon}e^{-i\varphi}F_2^{(0)}\int_{-\infty}^{\frac{\sqrt{r}\bar{\theta}}{\sqrt{2}}} e^{-v^2}\,dv,$$

where we have imposed the matching condition that S_{-1} and $S_1 \to 0$, as $\bar{\theta} \to -\infty$. Thus, across the Stokes line as $\bar{\theta}$ goes from $-\infty$ to ∞,

$$2\pi i\,e^{i\alpha\pi/2}\epsilon^{-\alpha}e^{iX_0/\epsilon}e^{-i\varphi}\left(F_0^{(0)}e^{-i\tilde{x}} + F_2^{(0)}e^{i\tilde{x}}\right) \tag{51}$$

is switched on by the upper singularity. Since the solution is real on the real axis we know that

$$-2\pi i\,e^{-i\alpha\pi/2}\epsilon^{-\alpha}e^{-i\bar{X}_0/\epsilon}e^{i\varphi}\left(\bar{F}_0^{(0)}e^{i\tilde{x}} + \bar{F}_2^{(0)}e^{-i\tilde{x}}\right) \tag{52}$$

is switched on by the lower singularity due to rhs_F^-.

2.6.1 $\mathbf{rhs}_G^+$ and $\mathbf{rhs}_G^-$

Stokes lines occur when successive terms in the expansion have the same phase [30]. For rhs_F^+ this occurs when $-i/(X - X_0)$ is real and positive, corresponding to $\theta = -\pi/2$ and a Stokes line down from the singularity in the upper half-plane parallel to the imaginary axis.

Successive terms in rhs_G^+ have the same phase when $i/(X - X_0)$ is real and positive, corresponding to $\theta = \pi/2$. Thus the Stokes line associated with these terms is up parallel to the imaginary axis, and therefore that generated by the singularity in the upper half-plane does not intersect the real axis. Thus, on the real line, there are no additional exponentially small terms switched on by rhs_G^+.

Similarly the Stokes line associated with rhs_G^- lies on $-i/(X - \bar{X}_0)$ real and positive, corresponding to $X = \bar{X}_0 + re^{i\theta}$ with $\theta = -\pi/2$. Thus this Stokes line goes down parallel to the imaginary axis from a singularity in the lower half-plane and so it too does not intersect the real axis.

2.7 Solution away from the Stokes line

Since the remainder R_N is exponentially small in ϵ, away from the Stokes line the equation for R_N valid to all orders in ϵ is simply the linearisation of (4), namely

$$\begin{aligned} & R_{N_{\tilde{x}\tilde{x}\tilde{x}\tilde{x}}} + 2R_{N_{\tilde{x}\tilde{x}}} + R_N \\ & \quad + 4\epsilon R_{N_{\tilde{x}\tilde{x}\tilde{x}X}} + 6\epsilon^2 R_{N_{\tilde{x}\tilde{x}XX}} + 4\epsilon^3 R_{N_{\tilde{x}XXX}} + \epsilon^4 R_{N_{XXXX}} + 4\epsilon R_{N_{\tilde{x}X}} + 2\epsilon^2 R_{N_{XX}} \\ = & \quad - 3\epsilon^2(f_0 + \epsilon f_1 + \cdots)^2 R_N - \epsilon^2 R_N - 6E_{hg}\epsilon(f_0 + \epsilon f_1 + \cdots)R_N. \end{aligned} \tag{53}$$

We expand R_N in ϵ by setting $R_N \sim R_N^{(0)}(\tilde{x}, X) + \epsilon R_N^{(1)}(\tilde{x}, X) + \cdots$. Then at $O(\epsilon^0)$ in (53)

$$R^{(0)}_{N_{\tilde{x}\tilde{x}\tilde{x}\tilde{x}}} + 2R^{(0)}_{N_{\tilde{x}\tilde{x}}} + R_N^{(0)} = 0$$

so that

$$R_N^{(0)} = a_0(X)e^{i\tilde{x}} + \bar{a}_0(X)e^{-i\tilde{x}}, \tag{54}$$

where $a_0(X)$ is unknown at this stage. At $O(\epsilon)$ in (53)

$$\begin{aligned} R^{(1)}_{N_{\tilde{x}\tilde{x}\tilde{x}\tilde{x}}} + 2R^{(1)}_{N_{\tilde{x}\tilde{x}}} + R_N^{(1)} &= -6E_{hg}(A_0e^{i\tilde{x}} + \bar{A}_0e^{-i\tilde{x}})(a_0(X)e^{i\tilde{x}} + \bar{a}_0(X)e^{-i\tilde{x}}) \\ &= -6E_{hg}\left(A_0a_0e^{2i\tilde{x}} + A_0\bar{a}_0 + \bar{A}_0a_0 + \bar{A}_0\bar{a}_0e^{-2i\tilde{x}}\right). \end{aligned}$$

Hence

$$R^{(1)} = -6E_{hg}(A_0\bar{a}_0 + \bar{A}_0a_0) - \frac{2E_{hg}}{3}A_0a_0e^{2i\tilde{x}} - \frac{2E_{hg}}{3}\bar{A}_0\bar{a}_0e^{-2i\tilde{x}}. \tag{55}$$

Finally, at $O(\epsilon^2)$ in (53)

$$\begin{aligned} & R^{(2)}_{N_{\tilde{x}\tilde{x}\tilde{x}\tilde{x}}} + 2R^{(2)}_{N_{\tilde{x}\tilde{x}}} + R_N^{(2)} \\ = & \quad - 6R^{(0)}_{N_{\tilde{x}\tilde{x}XX}} - 2R^{(0)}_{N_{XX}} - 3(f_0)^2R_N^{(0)} - R_N^{(0)} - 6E_{hg}f_0R_N^{(1)} - 6E_{hg}f_1R_N^{(0)} \\ = & \quad 4(a_{0_{XX}}e^{i\tilde{x}} + \bar{a}_{0_{XX}}e^{-i\tilde{x}}) - 3(A_0e^{i\tilde{x}} + \bar{A}_0e^{-i\tilde{x}})^2(a_0e^{i\tilde{x}} + \bar{a}_0e^{-i\tilde{x}}) \\ & \quad - a_0e^{i\tilde{x}} - \bar{a}_0e^{-i\tilde{x}} \\ & \quad - 6E_{hg}(A_0e^{i\tilde{x}} + \bar{A}_0e^{-i\tilde{x}})(-6E_{hg}(A_0\bar{a}_0 + \bar{A}_0a_0) - \frac{2E_{hg}}{3}A_0a_0e^{2i\tilde{x}} - \frac{2E_{hg}}{3}\bar{A}_0\bar{a}_0e^{-2i\tilde{x}}) \\ & \quad - 6E_{hg}(-\frac{E_{hg}A_0^2e^{2i\tilde{x}}}{3} - \frac{E_{hg}\bar{A}_0^2e^{-2i\tilde{x}}}{3} - 6E_{hg}|A_0|^2)(a_0e^{i\tilde{x}} + \bar{a}_0e^{-i\tilde{x}}) \end{aligned}$$

Eliminating the secular terms on the right-hand side gives the solvability condition

$$0 = 4a_{0_{XX}} - 3A_0^2\bar{a}_0 - 6|A_0|^2a_0 - a_0 + 38E_{hg}^2A_0^2\bar{a}_0 + 76E_{hg}^2|A_0|^2a_0$$

Writing $a_0 = u_0 + iv_0$ with u_0 and v_0 real, and recalling that A_0 is real, we have

$$0 = 4u_{0_{XX}} - u_0 + 3(38E_{hg}^2 - 3)A_0^2u_0, \tag{56}$$

$$0 = 4v_{0_{XX}} - v_0 + (38E_{hg}^2 - 3)A_0^2v_0. \tag{57}$$

Recalling that A_0 satisfies (8) we see that one solution of (57) is simply A_0, and one solution of (56) is simply A_{0_X}. These correspond to translating the original solution in x and X respectively. As in §2.5 the other solutions can be found by variation of parameters, giving

$$a_0(X) = B_1 A_{0_X} + B_2 A_{0_X} \int_{X_0}^{X} \frac{1}{A_{0_X}^2}\, dX + i\left(B_3 A_0 + B_4 A_0 \int_{X_0}^{X} \frac{1}{A_0^2}\, dX \right) \tag{58}$$

where B_1, B_2, B_3 and B_4 are real constants. The important contribution here is that due to B_2, since it is the one which is switched on across the Stokes line. That multiplying B_1 corresponds to translation in X, while that multiplying B_3 corresponds to translation in x.

2.8 Matching with the solution in the vicinity of the Stokes line

Focusing on the solution which is switched on across the Stokes line let us write

$$\begin{aligned} a_0(X) &\sim B_2^+ A_{0_X} \int_{X_0}^{X} \frac{1}{A_{0_X}^2}\, dX + B_2^- A_{0_X} \int_{\bar{X}_0}^{X} \frac{1}{A_{0_X}^2}\, dX & (59)\\ &= \frac{B_2^+}{K_0} F_2^{(0)} + \frac{B_2^-}{\bar{K}_0} \bar{F}_0^{(0)}. & (60) \end{aligned}$$

Then, by matching (60) with (51) and (52) we find that, for $X > \mathrm{Re}(X_0)$,

$$\begin{aligned} B_2^+ &= 2\pi i K_0 e^{i\alpha\pi/2} \epsilon^{-\alpha} e^{iX_0/\epsilon} e^{i\varphi},\\ B_2^- &= -2\pi i \bar{K}_0 e^{-i\alpha\pi/2} \epsilon^{-\alpha} e^{-iX_0/\epsilon} e^{-i\varphi}. \end{aligned}$$

2.9 Solutions of the equation

As $X \to \infty$

$$A_{0_X} \int^{X} \frac{dX}{A_{0_X}^2} \sim (3 - 38E_{hg}^2) e^{X/2},$$

so that

$$\begin{aligned} a_0(X) &\sim (B_2^+ + B_2^-)(3 - 38E_{hg}^2) e^{X/2}\\ &= 4\pi\Lambda (3 - 38E_{hg}^2) \epsilon^{-4} e^{-\pi/\epsilon} \cos\left(\frac{\pi}{2} - \frac{\log(76E_{hg}^2 - 6)}{\epsilon} + \varphi + \chi \right) e^{X/2}, \end{aligned} \tag{61}$$

where $K_0 = \Lambda e^{i\chi}$ with Λ and χ real. Although this term is exponentially small when it is turned on across the Stokes line, it is exponentially growing in X. For the multiple-scales solution we have constructed to hold the coefficient of $e^{X/2}$ must vanish, giving the solvability condition

$$\frac{\pi}{2} - \frac{\log(76E_{hg}^2 - 6)}{\epsilon} + \varphi + \chi = (2n+1)\frac{\pi}{2},$$

for some $n \in \mathbb{Z}$. This, finally, is the condition which determines the phase shift φ between the fast and slow scales. Recalling that K_0 is real, $\chi = 0$ and we see that there are two solutions for φ in $[0, 2\pi)$, corresponding to the centre of the bump being a local maximum and a local minimum.

3 Study near the Maxwell point

3.1 Summary of this section

We are now poised to study the conditions of existence of localised patterns near the Maxwell point, given in first approximation by $E_{hg} = \sqrt{3/38}$. As discussed in §1, the vicinity of the Maxwell point requires a different scaling of the parameters in (1), which now becomes

$$\left(1 + \frac{d^2}{dx^2}\right)^2 f + \epsilon^4 f + 3\epsilon E_{hg} f^2 + \epsilon^2 f^3 = 0, \tag{62}$$

where $0 < \epsilon \ll 1$. This time the slow scale is $X = \epsilon^2 x$. We develop a multiple scales solution

$$f \sim \sum_{n=0}^{N-1} \epsilon^n f_n(x, X) + R_N(x - \varphi, X). \tag{63}$$

We also expand

$$E_{hg} \sim E_0 + \epsilon E_1 + \epsilon^2 E_2 + \cdots + \delta E;$$

we will see that δE is exponentially small in ϵ. The program is the same as in the previous section, but is algebraically more complicated. In §3.2, the leading orders of the analysis will give us a front solution $f_0 + \epsilon f_1 + \ldots$ for well defined values of E_0, E_1,.... In §3.3, we set up the problem for the late terms of (63) and in §3.4, we examine them in the vicinity of the singular point $X = i\pi$. This inner limit allows us to establish the factorial/power divergence of f_n for large n and then to deduce asymptotically f_n away from this singularity (§3.5). The finite sum $\sum_{n=0}^{N-1} \epsilon^n f_n$ can then be evaluated and we find that it leaves a non-vanishing, exponentially small, right hand side in (62). This yields the equation for R_N (§3.6). The problem for R_N requires separate consideration near the Stokes line (§3.7) and away from it (§3.8). At the end of the day, two exponentially-small-but-growing terms are found, one proportional to δE, the other switched on at the Stoke line, and the two must cancel for large X. This eventually yields the pinning range for the front solution.

3.2 Leading orders of the multiple scale analysis

As before, substituting (63) into (62) we have, at $O(\epsilon^0)$,

$$\mathcal{L} f_0 \equiv \frac{\partial^4 f_0}{\partial x^4} + 2\frac{\partial^2 f_0}{\partial x^2} + f_0 = 0$$

so that

$$f_0 = A_0(X) e^{i\tilde{x}} + \bar{A}_0(X) e^{-i\tilde{x}}, \tag{64}$$

where $\tilde{x} = x - \varphi$, with $0 \le \varphi < 2\pi$. At $O(\epsilon)$

$$\mathcal{L} f_1 = -3E_0 f_0^2,$$

so that

$$f_1 = -\frac{E_0 A_0^2 e^{2i\tilde{x}}}{3} - \frac{E_0 \bar{A}_0^2 e^{-2i\tilde{x}}}{3} - 6E_0|A_0|^2. \tag{65}$$

In all generality, we should add $A_1(X)e^{i\tilde{x}} + \bar{A}_1(X)e^{-i\tilde{x}}$ to f_1. However, a solvability condition at $O(\epsilon^5)$ would lead to $A_1 = 0$. We thus omit this term here. At $O(\epsilon^2)$

$$\begin{aligned}
\mathcal{L}f_2 &= -f_0^3 - 6E_0 f_0 f_1 - 3E_1 f_0^2 \\
&= (2E_0^2 - 1)A_0^3 e^{3i\tilde{x}} + (38E_0^2 - 3)A_0|A_0|^2 e^{i\tilde{x}} - 3E_1 A_0^2 e^{2i\tilde{x}} - 3E_1|A_0|^2 + \text{c.c.}
\end{aligned}$$

In order to remove the secular terms so that f_2 has a bounded solution we require

$$E_0 = \sqrt{3/38}. \tag{66}$$

In this case

$$f_2 = -\frac{A_0^3 e^{3i\tilde{x}}}{76} - \frac{E_1}{3}A_0^2 e^{2i\tilde{x}} + A_2 e^{i\tilde{x}} - 3E_1|A_0|^2 + \text{c.c.} \tag{67}$$

At $O(\epsilon^3)$

$$\begin{aligned}
\mathcal{L}f_3 &= -4\frac{\partial^2 f_1}{\partial X \partial x} - 4\frac{\partial^4 f_1}{\partial X \partial x^3} - 3f_0^2 f_1 - 6E_0 f_0 f_2 - 3E_0 f_1^2 - 6E_1 f_0 f_1 - 3E_2 f_0^2 \\
&= -3E_2|A_0|^2 - \frac{E_0}{3}\left(163E_0^2 - 57\right)|A_0|^4 - 6E_0\bar{A}_0 A_2 + 76E_0E_1|A_0|^2 A_0 e^{i\tilde{x}} \\
&\quad - \left(3E_2 A_0^2 + 16iE_0 A_0 A_0' + \frac{390E_0^3 - 643E_0}{32}|A_0|^2 A_0^2 + 6E_0 A_0 A_2\right)e^{2i\tilde{x}} \\
&\quad + 4E_0 E_1 A_0^3 e^{3i\tilde{x}} + \frac{5E_0}{96}\left(21 - 10E_0^2\right)A_0^4 e^{4i\tilde{x}} + c.c.
\end{aligned}$$

This time, we have the solvability condition

$$E_1 = 0, \tag{68}$$

and the solution at this order is

$$\begin{aligned}
f_3 &= -3E_2|A_0|^2 - \frac{E_0}{3}\left(163E_0^2 - 57\right)|A_0|^4 - 6E_0\bar{A}_0 A_2 \\
&\quad - \left(\frac{E_2}{3}A_0^2 + \frac{16}{9}iE_0 A_0 A_0' + \frac{390E_0^3 - 643E_0}{288}|A_0|^2 A_0^2 + \frac{2}{3}E_0 A_0 A_2\right)e^{2i\tilde{x}} \\
&\quad + \frac{E_0}{4320}\left(21 - 10E_0^2\right)A_0^4 e^{4i\tilde{x}} + c.c.
\end{aligned} \tag{69}$$

Finally, at $O(\epsilon^4)$ we must again eliminate secular terms on the right-hand side of the equation, which gives the following solvability condition on A_0:

$$4A_0'' + \frac{16iA_0'|A_0|^2}{19} - \frac{8820|A_0|^4 A_0}{361} + 2\sqrt{114}E_2|A_0|^2 A_0 - A_0 = 0. \tag{70}$$

Writing $A_0 = \mathcal{R}_0 e^{i\phi_0}$ we find

$$\phi_0' = -\frac{\mathcal{R}_0^2}{19} \tag{71}$$

and

$$4\mathcal{R}_0'' - \mathcal{R}_0 + 2\sqrt{114}E_2\mathcal{R}_0^3 - \frac{8808}{361}\mathcal{R}_0^5 = 0. \tag{72}$$

Integrating once, using the fact that $\mathcal{R}_0 \to 0$ as $X \to -\infty$, gives

$$4(\mathcal{R}_0')^2 = \mathcal{R}_0^2 + \sqrt{114}E_2\mathcal{R}_0^4 - \frac{2936}{361}\mathcal{R}_0^6.$$

Separating the variables and integrating again gives

$$\mathcal{R}_0^2 = \frac{76e^X}{1 + 38\sqrt{114}E_2e^X + 2(20577E_2^2 - 5872)e^{2X}}. \tag{73}$$

For $E_2 > \frac{4}{19}\sqrt{\frac{367}{57}}$, $\mathcal{R}_0$ decays to zero as $X \to \pm\infty$, corresponding to an extended "bump" solution. There are singularities at

$$e^X = \frac{-19\sqrt{114}E_2 \pm 4\sqrt{734}}{(41154E_2^2 - 11744)}$$

Each of these singularities generates Stokes lines, and a similar analysis to that seen previously can be performed, with similar results. The exponentially small terms determine the phase difference between the fast and slow scales, but no snaking bifurcation diagram is revealed.

As E_2 approaches the critical value $\frac{4}{19}\sqrt{\frac{367}{57}}$ the bump becomes more and more extended. At the critical value (after a change of origin) the solutions are

$$\mathcal{R}_0 = \sqrt{\frac{19\beta}{2}}\left(\frac{1}{1+e^{-X}}\right)^{1/2}, \tag{74}$$

corresponding to an up-front between the zero solution and a periodic solution, and

$$\mathcal{R}_0 = \sqrt{\frac{19\beta}{2}}\left(\frac{1}{1+e^{X}}\right)^{1/2}, \tag{75}$$

corresponding to a down-front from the periodic solution to the zero solution, where

$$\beta = \frac{1}{\sqrt{734}}. \tag{76}$$

These solutions have inverse square root singularities at $X = i(2n+1)\pi$.

We will see that the snaking bifurcation diagram corresponds to an extended region of oscillation in the solution. This is formed by an up-front followed by a long (of $O(\epsilon^{-2})$)

region of uniform oscillations, and then a down front. A beyond-all-orders analysis of the up-front will identify an exponentially small term turned on across a Stokes line. This term slowly grows during the extended oscillating region, until it finally becomes large enough to cause the down-front.

We focus first on the up-front solution. From (71) we find that

$$\phi_0 = -\frac{\beta}{2}\ln\left(1+e^X\right). \tag{77}$$

and thus

$$A_0 = \sqrt{\frac{19\beta}{2}}\frac{e^{X/2}}{(1+e^X)^{1/2+i\beta/2}}, \qquad \beta = \frac{1}{\sqrt{734}}. \tag{78}$$

We follow the same methodology as in §2. The first step is to identify the form of the late terms in the multiple-scales expansion.

3.3 Late term expansion

For n sufficiently large the equation for the n th term in the expansion of f is

$$\begin{aligned}\frac{\partial^4 f_n}{\partial x^4} + 2\frac{\partial^2 f_n}{\partial x^2} + f_n = &-4\frac{\partial^4 f_{n-2}}{\partial x^3\partial X} - 6\frac{\partial^4 f_{n-4}}{\partial x^2\partial X^2} - 4\frac{\partial^4 f_{n-6}}{\partial x\partial X^3} - \frac{\partial^4 f_{n-8}}{\partial X^4}\\ &- 4\frac{\partial^2 f_{n-2}}{\partial x\partial X} - 2\frac{\partial^2 f_{n-4}}{\partial X^2} - f_{n-4} - \sum_{j=0}^{n-2}\sum_{m=0}^{n-2-j} f_j f_m f_{n-2-j-m}\\ &- 3E_0\sum_{j=0}^{n-1} f_j f_{n-1-j} - 3E_2\sum_{j=0}^{n-3} f_j f_{n-3-j}.\end{aligned} \tag{79}$$

As before, for each n the solution will be a sum of multiples of $e^{i\tilde{x}}$ in the form

$$f_n(x,X) = \sum_{k=-n-1}^{n+1} A_{n,k}(X)e^{ik\tilde{x}}. \tag{80}$$

At each order the coefficients of the terms with $k=\pm 1$ are arbitrary (being solutions of the homogeneous equation), and are determined by the elimination of secular terms in the equation for f_{n+4}, in the same way that A_0 was determined by eliminating the secular terms in the equation for f_4. Substituting (80) into (79) and equating coefficients of $e^{ik\tilde{x}}$ gives

$$\begin{aligned}(1-k^2)^2 A_{n,k} = &\,4ik^3\frac{\partial A_{n-2,k}}{\partial X} + 6k^2\frac{\partial^2 A_{n-4,k}}{\partial X^2} - 4ik\frac{\partial^3 A_{n-6,k}}{\partial X^3} - \frac{\partial^4 A_{n-8,k}}{\partial X^4}\\ &- 4ik\frac{\partial A_{n-2,k}}{\partial X} - 2\frac{\partial^2 A_{n-4,k}}{\partial X^2} - \sum_p\sum_q\sum_{j=0}^{n-2}\sum_{m=0}^{n-2-j} A_{j,p}A_{m,q}A_{n-2-j-m,k-p-q}\\ &- A_{n-4,k} - 3E_0\sum_p\sum_{j=0}^{n-1} A_{j,p}A_{n-1-j,k-p} - 3E_2\sum_p\sum_{j=0}^{n-3} A_{j,p}A_{n-3-j,k-p}.\end{aligned} \tag{81}$$

As in §2, to determine the optimal truncation point and the equation for the remainder we need to solve for $A_{n,k}$ as $n \to \infty$. We begin in §3.4 by examining the behaviour of $A_{n,k}$ close to the singularity at $X = i\pi$. Then, in §3.5, we solve for $A_{n,k}$ away from $X = i\pi$.

3.4 Inner expansion near $X = i\pi$

We will show in this section that as $X \to i\pi$ and $n \to \infty$,

$$\begin{aligned} f_n(x,X) \;\sim\; & \lambda_1 \frac{e^{in\pi/4}\Gamma(n/2+\alpha)}{(i\pi - X)^{\frac{n+1}{2}}}\left(1-(-1)^n\right)\left(1+\frac{e^{-i\psi}e^{2i\tilde{x}}}{(i\pi-X)^{i\beta}}\right) \\ & + \lambda_3 \frac{e^{-in\pi/4}\Gamma(n/2+\bar{\alpha})}{(i\pi - X)^{\frac{n+1}{2}}}\left(1-(-1)^n\right)\left(1+\frac{e^{i\psi}e^{-2i\tilde{x}}}{(i\pi-X)^{-i\beta}}\right), \end{aligned}$$

for some constants λ_1, λ_3, where $\alpha = 3 + i\beta/2$ and $e^{i\psi} = (3i-\beta)/(3i+\beta)$.

From (78) we see that as $X \to i\pi$,

$$A_0(X) \sim i\sqrt{\frac{19\beta}{2}}\frac{1}{(i\pi - X)^{\frac{1}{2}+\frac{i\beta}{2}}}.$$

This suggests the ansatz

$$A_{n,k} \sim \frac{B_{n,k}}{(i\pi - X)^{\frac{n+1}{2}+\frac{ik\beta}{2}}} \quad \text{as } X \to i\pi. \tag{82}$$

Substituting (82) into (81), gives, in the limit $X \to i\pi$, the nonlinear recurrent set of algebraic equations

$$\begin{aligned} \left(1-k^2\right)^2 B_{n,k} \;\sim\; & -4ik\left(1-k^2\right)\left(\frac{n}{2}-\frac{1}{2}+\frac{ik\beta}{2}\right)B_{n-2,k} \\ & -\left(2-6k^2\right)\left(\frac{n}{2}-\frac{1}{2}+\frac{ik\beta}{2}\right)\left(\frac{n}{2}-\frac{3}{2}+\frac{ik\beta}{2}\right)B_{n-4,k} \\ & -4ik\left(\frac{n}{2}-\frac{1}{2}+\frac{ik\beta}{2}\right)\left(\frac{n}{2}-\frac{3}{2}+\frac{ik\beta}{2}\right)\left(\frac{n}{2}-\frac{5}{2}+\frac{ik\beta}{2}\right)B_{n-6,k} \\ & -\left(\frac{n}{2}-\frac{1}{2}+\frac{ik\beta}{2}\right)\left(\frac{n}{2}-\frac{3}{2}+\frac{ik\beta}{2}\right)\left(\frac{n}{2}-\frac{5}{2}+\frac{ik\beta}{2}\right)\left(\frac{n}{2}-\frac{7}{2}+\frac{ik\beta}{2}\right)B_{n-8,k} \\ & -3E_0\sum_p\sum_{j=0}^{n-1} B_{j,p}B_{n-1-j,k-p} \\ & -\sum_p\sum_q\sum_{j=0}^{n-2}\sum_{m=0}^{n-2-j} B_{j,p}B_{m,q}B_{n-2-j-m,k-p-q} \end{aligned} \tag{83}$$

In the limit as $n \to \infty$ we use the ansatz

$$B_{n,k} \;\sim\; \Gamma\left(\frac{n}{2}+\alpha_k\right)b_{n,k},$$

where the offsets α_k are to be determined. We will again find that $B_{n,k}$ with $k = 0, \pm 2$ will dominate, followed by $k = \pm 1, \pm 3$, then ± 4 etc. For the $b_{n,k}$ to be of the same order for each k as $n \to \infty$, we require

$$\alpha_0 = \alpha_{\pm 2} = \alpha, \qquad \alpha_{\pm 1} = \alpha_{\pm 3} = \alpha - \frac{1}{2}, \qquad \alpha_{\pm 4} = \alpha - 1, \qquad \dots$$

where α is to be determined. Expanding

$$b_{n,k} \sim b^{(0)}_{n,k} + \frac{1}{n} b^{(1)}_{n,k} + \cdots,$$

gives, at leading order as $n \to \infty$, the linear system of equations

$$\vdots$$

$$\begin{aligned} 225 b^{(0)}_{n,-4} + 240 i b^{(0)}_{n-2,-4} - 94 b^{(0)}_{n-4,-4} & \\ -16 i b^{(0)}_{n-6,-4} + b^{(0)}_{n-8,-4} \quad &\sim \quad \left(2E_0^2 - 3\right) B^2_{0,1} b^{(0)}_{n-2,-2} - 6 E_0 B_{0,1} b^{(0)}_{n-1,-3}, \end{aligned}$$

$$64 b^{(0)}_{n,-3} + 96 i b^{(0)}_{n-2,-3} - 52 b^{(0)}_{n-4,-3} - 12 i b^{(0)}_{n-6,-3} + b^{(0)}_{n-8,-3} \sim -6 E_0 B_{0,1} b^{(0)}_{n-1,-2} - 64 b^{(0)}_{n,-3},$$

$$9 b^{(0)}_{n,-2} - 24 i b^{(0)}_{n-2,-2} - 22 b^{(0)}_{n-4,-2} - 8 i b^{(0)}_{n-6,-2} + b^{(0)}_{n-8,-2} \sim 0,$$

$$-4 b^{(0)}_{n-4,-1} - 4 i b^{(0)}_{n-6,-1} + b^{(0)}_{n-8,-1} \sim -6 E_0 B_{0,1} \left(b^{(0)}_{n-1,-2} + b^{(0)}_{n-1,0} \right),$$

$$b^{(0)}_{n,0} + 2 b^{(0)}_{n-4,0} + b^{(0)}_{n-8,0} \sim 0,$$

$$-4 b^{(0)}_{n-4,1} + 4 i b^{(0)}_{n-6,1} + b^{(0)}_{n-8,1} \sim -6 E_0 B_{0,1} \left(b^{(0)}_{n-1,0} + b^{(0)}_{n-1,2} \right),$$

$$9 b^{(0)}_{n,2} - 24 i b^{(0)}_{n-2,2} - 22 b^{(0)}_{n-4,2} + 8 i b^{(0)}_{n-6,2} + b^{(0)}_{n-8,2} \sim 0,$$

$$64 b^{(0)}_{n,3} - 96 i b^{(0)}_{n-2,3} - 52 b^{(0)}_{n-4,3} + 12 i b^{(0)}_{n-6,3} + b^{(0)}_{n-8,3} \sim -6 E_0 B_{0,1} b^{(0)}_{n-1,2} - 64 b^{(0)}_{n,3},$$

$$\begin{aligned} 225 b^{(0)}_{n,4} - 240 i b^{(0)}_{n-2,4} - 94 b^{(0)}_{n-4,4} & \\ +16 i b^{(0)}_{n-6,4} + b^{(0)}_{n-8,4} \quad &\sim \quad \left(2E_0^2 - 3\right) B^2_{0,1} b^{(0)}_{n-2,2} - 6 E_0 B_{0,1} b^{(0)}_{n-1,3}, \end{aligned}$$

$$\vdots$$

Note that the equations for $b^{(0)}_{n,-2}$, $b^{(0)}_{n,0}$ and $b^{(0)}_{n,2}$ decouple from the rest. Seeking a solution of the form

$$b^{(0)}_{n,k} = \kappa^n b^{(0)}_k \tag{84}$$

gives

$$\begin{aligned}
\left(-1+4i\kappa^2+3\kappa^4\right)^2 b^{(0)}_{-2} &= 0, &(85)\\
\left(1+\kappa^4\right)^2 b^{(0)}_{0} &= 0, &(86)\\
\left(1+4i\kappa^2-3\kappa^4\right)^2 b^{(0)}_{2} &= 0. &(87)
\end{aligned}$$

and

$$\vdots$$

$$\begin{aligned}
-\left(-1+8i\kappa^2+15\kappa^4\right)^2 b^{(0)}_{-4} - 6B_{0,1}\kappa^7 E_0 b^{(0)}_{-3} + B^2_{0,1}\kappa^6\left(2E_0^2-3\right) b^{(0)}_{-2} &= 0,\\
-\left(-1+6i\kappa^2+8\kappa^4\right)^2 b^{(0)}_{-3} - 6B_{0,1}\kappa^7 E_0 b^{(0)}_{-2} &= 0,\\
\left(i+2\kappa^2\right)^2 b^{(0)}_{-1} - 6B_{0,1}\kappa^7 E_0\left(b^{(0)}_{-2}+b^{(0)}_{0}\right) &= 0,\\
\left(i-2\kappa^2\right)^2 b^{(0)}_{1} - 6B_{0,1}\kappa^7 E_0\left(b^{(0)}_{0}+b^{(0)}_{2}\right) &= 0,\\
-\left(1+6i\kappa^2-8\kappa^4\right)^2 b^{(0)}_{3} - 6B_{0,1}\kappa^7 E_0 b^{(0)}_{2} &= 0,\\
-\left(1+8i\kappa^2-15\kappa^4\right)^2 b^{(0)}_{4} - 6B_{0,1}\kappa^7 E_0 b^{(0)}_{3} + B^2_{0,1}\kappa^6\left(2E_0^2-3\right) b^{(0)}_{2} &= 0,
\end{aligned}$$

$$\vdots$$

As before the eigenmodes with $\kappa^2 = \pm i$ dominate those with $\kappa^2 = \pm i/3$.

From (85)-(87), we find that $\kappa^2 = i$ implies $b^{(0)}_0, b^{(0)}_2 \neq 0$ and $b^{(0)}_{-2} = 0$. Conversely, if $\kappa^2 = -i$ then $b^{(0)}_2 = 0$ and $b^{(0)}_{-2}, b^{(0)}_0 \neq 0$.

3.4.1 First eigenvalue: $\kappa_1 = e^{i\pi/4}$

If $\kappa = e^{i\pi/4}$ then

$$b^{(0)}_{-2} = b^{(0)}_{-3} = b^{(0)}_{-4} = b^{(0)}_{-5} = \ldots = 0,$$

while

$$\begin{aligned}
b^{(0)}_{-1} &= \frac{2}{3}\, e^{3i\pi/4} E_0 B_{0,1} b^{(0)}_0 &(88)\\
b^{(0)}_{1} &= 6e^{3i\pi/4} E_0 B_{0,1}\left(b^{(0)}_0 + b^{(0)}_2\right), &(89)\\
b^{(0)}_{3} &= \frac{2}{3}\, e^{3i\pi/4} E_0 B_{0,1} b^{(0)}_2, &(90)\\
b^{(0)}_{4} &= -\frac{3i}{64}\left(2E_0^2-1\right) B^2_{0,1} b^{(0)}_2, &(91)
\end{aligned}$$

$$\vdots$$

and the components $b_0^{(0)}$ and $b_2^{(0)}$ of the eigenvector are still unknown. Considering the equations for $k = 0, 2$ at order $1/n$, we obtain

$$\begin{aligned} -2iB_{0,1}^2\left(38E_0^2-3\right)\left(2b_0^{(0)}+b_2^{(0)}\right) &= 0, \\ -2iB_{0,1}^2\left(38E_0^2-3\right)\left(b_0^{(0)}+2b_2^{(0)}\right) &= 0, \end{aligned}$$

and we recover the solvability condition $38E_0^2 = 3$ of the weakly nonlinear analysis since, otherwise, $b_0^{(0)} = b_2^{(0)} = 0$. Solving the equations arising at $O\left(1/n\right)$ for $b_k^{(1)}$, $k = -2, \ldots, 3$, we find

$$b_{-2}^{(1)} = \frac{3i}{38}B_{0,1}^2 b_0^{(0)}, \tag{92}$$

$$b_{-1}^{(1)} = \frac{2i^{5/2}}{114^{3/2}}B_{0,1}\left(\left(2181B_{0,1}^2+304\left(\beta-2i(\alpha-1)\right)\right)b_0^{(0)}+727B_{0,1}^2 b_2^{(0)}-114ib_0^{(1)}\right), \tag{93}$$

$$b_1^{(1)} = \frac{6^{1/2}i^{5/2}}{19^{3/2}}B_{0,1}\left(1118B_{0,1}^2\left(b_0^{(0)}+b_2^{(0)}\right)-57i\left(b_0^{(1)}+b_2^{(1)}\right)\right), \tag{94}$$

$$b_3^{(1)} = \frac{2i^{5/2}}{114^{3/2}}B_{0,1}\left(727B_{0,1}^2 b_0^{(0)}+\left(2181B_{0,1}^2+304\left(3\beta+2i(\alpha-1)\right)\right)b_2^{(0)}-114ib_2^{(1)}\right) \tag{95}$$

Then, at $O\left(1/n^2\right)$, we finally obtain

$$\begin{aligned} &\left(76+\frac{61392B_{0,1}^4}{19}-304(\alpha-1)^2\right)b_0^{(0)}+\frac{2}{19}B_{0,1}^2\left(14429B_{0,1}^2+304\left(i+\beta\right)\right)b_2^{(0)} \\ &\qquad +108iB_{0,1}^2\left(b_{-2}^{(1)}+b_2^{(1)}\right)-6\left(1-i\right)\sqrt{57}B_{0,1}\left(b_{-1}^{(1)}+b_1^{(1)}\right)+120iB_{0,1}^2 b_0^{(1)} = 0, \\ &\frac{2}{19}B_{0,1}^2\left(14429B_{0,1}^2+304\left(\beta-i\right)\right)b_0^{(0)}+\left(\frac{61392B_{0,1}^4}{19}+76\left(1-4\left(\alpha-1-i\beta\right)^2\right)\right)b_2^{(0)} \\ &\qquad +108iB_{0,1}^2 b_0^{(1)}-6\left(1-i\right)\sqrt{57}B_{0,1}\left(b_1^{(1)}+b_3^{(1)}\right)+120iB_{0,1}^2 b_2^{(1)} = 0. \end{aligned}$$

Substituting the values of $b_k^{(1)}$ from (92)-(95), and remembering that $B_{0,1} = i\sqrt{19\beta/2}$, this yields

$$\begin{aligned} \left(\frac{7345}{734}+\frac{8i(\alpha-1)}{\sqrt{734}}-4(\alpha-1)^2\right)b_0^{(0)}+\frac{1}{367}\left(2203-2i\sqrt{734}\right)b_2^{(0)} &= 0, \\ \frac{1}{367}\left(2203+2i\sqrt{734}\right)b_0^{(0)}+\left(\frac{7341}{734}-4(\alpha-1)^2\right)b_2^{(0)} &= 0. \end{aligned}$$

For a non-zero solution, the determinant

$$(\alpha-1)^4-i\sqrt{\frac{2}{367}}(\alpha-1)^3-\frac{7343}{1468}(\alpha-1)^2+\frac{7341i(\alpha-1)}{1468\sqrt{734}}+\frac{34495065}{8620096}=0,$$

which is analogous to (31) from §2. Although this equation looks nastier than (31), the roots turn out to be simply

$$\alpha = -1 + \frac{i\beta}{2}, \quad \alpha = \frac{i\beta}{2}, \quad \alpha = 2 + \frac{i\beta}{2}, \quad \alpha = 3 + \frac{i\beta}{2}, \tag{96}$$

remembering that $\beta = 1/\sqrt{734}$. Each of these values of α produces an eigenvector associated to $\kappa = \sqrt{i}$. However, due to the factorial factor, the eigenvector with $\alpha = 3 + i\beta/2$ dominates for large n, so we restrict our attention to this one. In this case

$$b_2^{(0)} = e^{-i\psi} b_0^{(0)},$$

where

$$\tan\psi = \frac{6\beta}{9 - \beta^2} = \frac{6\sqrt{734}}{6605}, \qquad \text{so that} \qquad e^{-i\psi} = \frac{3i + \beta}{3i - \beta}. \tag{97}$$

Second eigenvalue: $\kappa_2 = e^{-3i\pi/4}$ The procedure is the same as before and yields the same possible values of α. For $\alpha = 3 + i\beta/2$, we have again

$$b_{-2}^{(0)} = 0 \qquad \text{and} \qquad b_2^{(0)} = e^{-i\psi} b_0^{(0)},$$

with ψ given by (97).

Third eigenvalue $\kappa_3 = e^{-i\pi/4}$ This time, we obtain $b_2^{(0)} = 0$ and the possible values for α are now $-1 - i\beta/2$, $-i\beta/2$, $2 - i\beta/2$, and $3 - i\beta/2$. The last one is the dominant one, and leads to

$$b_{-2}^{(0)} = e^{i\psi} b_0^{(0)},$$

with ψ as before.

Fourth eigenvalue: $\kappa_4 = e^{3i\pi/4}$ Finally, we find

$$b_2^{(0)} = 0 \qquad \text{and} \qquad b_{-2}^{(0)} = e^{i\psi} b_0^{(0)}.$$

3.4.2 Combining the eigenvectors

Let us fix henceforth $\alpha = 3 + i\beta/2$. Combining the four eigenvectors, with coefficients λ_1, λ_2, λ_3, λ_4, we see that

$$\begin{aligned}
f_n(x,X) &= \sum_{k=-n-1}^{n+1} A_{n,k} e^{ik\tilde{x}} \sim \sum_{k=-n-1}^{n+1} \frac{B_{n,k}\, e^{ik\tilde{x}}}{(i\pi - X)^{\frac{n+1}{2}+\frac{ik\beta}{2}}} \\
&\sim \frac{\Gamma(n/2+\alpha)}{(i\pi-X)^{\frac{n+1}{2}}} \left(\lambda_1 e^{in\pi/4} \left(1 + \frac{e^{-i\psi} e^{2i\tilde{x}}}{(i\pi - X)^{i\beta}} \right) + \lambda_2 e^{-3in\pi/4} \left(1 + \frac{e^{-i\psi} e^{2i\tilde{x}}}{(i\pi - X)^{i\beta}} \right) \right) \\
&\quad + \frac{\Gamma(n/2+\bar{\alpha})}{(i\pi-X)^{\frac{n+1}{2}}} \left(\lambda_3 e^{-in\pi/4} \left(1 + \frac{e^{i\psi} e^{-2i\tilde{x}}}{(i\pi - X)^{-i\beta}} \right) + \lambda_4 e^{3in\pi/4} \left(1 + \frac{e^{i\psi} e^{-2i\tilde{x}}}{(i\pi - X)^{-i\beta}} \right) \right) \\
&\sim \frac{e^{in\pi/4}\Gamma(n/2+\alpha)}{(i\pi-X)^{\frac{n+1}{2}}} \left(\lambda_1 + (-1)^n \lambda_2 \right) \left(1 + \frac{e^{-i\psi} e^{2i\tilde{x}}}{(i\pi - X)^{i\beta}} \right) \\
&\quad + \frac{e^{-in\pi/4}\Gamma(n/2+\bar{\alpha})}{(i\pi-X)^{\frac{n+1}{2}}} \left(\lambda_3 + (-1)^n \lambda_4 \right) \left(1 + \frac{e^{i\psi} e^{-2i\tilde{x}}}{(i\pi - X)^{-i\beta}} \right)
\end{aligned}$$

From the form of equation (81) and inspection of the first few orders of the weakly nonlinear analysis, we find that

$$A_{2n+1,2k+1} = A_{2n,2k} = 0,$$

that is, odd harmonics vanish for odd values of n, while even harmonics vanish for even n. Thus $\lambda_1 = -\lambda_2$, $\lambda_3 = -\lambda_4$, and

$$\begin{aligned}
f_n(x,X) &\sim \lambda_1 \frac{e^{in\pi/4}\Gamma(n/2+\alpha)}{(i\pi-X)^{\frac{n+1}{2}}} \left(1 - (-1)^n \right) \left(1 + \frac{e^{-i\psi} e^{2i\tilde{x}}}{(i\pi - X)^{i\beta}} \right) \\
&\quad + \lambda_3 \frac{e^{-in\pi/4}\Gamma(n/2+\bar{\alpha})}{(i\pi-X)^{\frac{n+1}{2}}} \left(1 - (-1)^n \right) \left(1 + \frac{e^{i\psi} e^{-2i\tilde{x}}}{(i\pi - X)^{-i\beta}} \right)
\end{aligned} \tag{98}$$

as $n \to \infty$ and $X \to i\pi$.

3.5 Outer expansion away from $X = i\pi$

We now determine the behaviour of f_n away from the singularities at $X = \pm i\pi$. We will show in this section that

$$\begin{aligned}
f_n(x,X) &\sim \frac{e^{in\pi/4}\Gamma(n/2+\alpha)}{(i\pi-X)^{\frac{n}{2}+\alpha}} \left(1 - (-1)^n \right) \left(F_0^{(0)}(X) + F_2^{(0)}(X) e^{2i\tilde{x}} \right) \\
&\quad + \frac{e^{-in\pi/4}\Gamma(n/2+\bar{\alpha})}{(i\pi-X)^{\frac{n}{2}+\bar{\alpha}}} \left(1 - (-1)^n \right) \left(H_0^{(0)}(X) + H_{-2}^{(0)}(X) e^{-2i\tilde{x}} \right) + \text{c.c.}
\end{aligned}$$

where $F_0^{(0)}$, $F_2^{(0)}$, $H_{-2}^{(0)}$ and $H_0^{(0)}$ are given by (110), (111), (114) and (115) respectively.

Away from $X = i\pi$, motivated by (82), we use the ansatz

$$A_{n,k}(X) \sim \kappa^n \frac{\Gamma(n/2+\alpha_k)}{(i\pi - X)^{n/2+\alpha_k}} \left(F_k^{(0)}(X) + \frac{1}{n} F_k^{(1)}(X) + \ldots \right) \tag{99}$$

as $n \to \infty$. Substituting into (81), we soon find, at $O(\Gamma(n/2+\alpha))$, that

$$\left(-1 + 4i\kappa^2 + 3\kappa^4\right)^2 F_{-2}^{(0)}(X) = \left(1+\kappa^4\right)^2 F_0^{(0)}(X) = \left(1 + 4i\kappa^2 - 3\kappa^4\right)^2 F_2^{(0)}(X) = 0. \tag{100}$$

Hence, the possible values for κ are again $\pm\sqrt{\pm i}$. Let us consider first the eigenvalue $\kappa = e^{i\pi/4}$.

3.5.1 First eigenvalue: $\kappa_1 = e^{i\pi/4}$

As before, this choice of κ yields

$$64 F_{-2}^{(0)}(X) = 0,$$

so that $F_{-2}^{(0)}(X) = F_{-3}^{(0)}(X) = F_{-4}^{(0)}(X) = \ldots = 0$. Meanwhile, equations (88)-(91) become

$$\begin{aligned}
F_{-1}^{(0)} &= \frac{2}{3} e^{3i\pi/4} E_0 \bar{A}_0 F_0^{(0)}, \\
F_1^{(0)} &= 6\, e^{3i\pi/4} E_0 \left(A_0 F_0^{(0)} + \bar{A}_0 F_2^{(0)} \right), \\
F_3^{(0)} &= \frac{2}{3} e^{3i\pi/4} E_0 A_0 F_2^{(0)}, \\
F_4^{(0)} &= -\frac{3i}{64} \left(2E_0^2 - 1\right) A_0^2 F_2^{(0)}, \\
&\vdots
\end{aligned}$$

At $O(1/n)$, the equations for $k = 0, 2$ yield, respectively,

$$\begin{aligned}
2\bar{A}_0 \left(38E_0^2 - 3\right) \left(2A_0 F_0^{(0)} + \bar{A}_0 F_2^{(0)} \right) &= 0, \\
2A_0 \left(38E_0^2 - 3\right) \left(A_0 F_0^{(0)} + 2\bar{A}_0 F_2^{(0)} \right) &= 0,
\end{aligned}$$

which again are automatically satisfied by (66). Finally, at $O(1/n^2)$, we obtain the following pair of equations for $F_0^{(0)}$ and $F_2^{(0)}$:

$$\begin{aligned}
0 &= 4F_0^{(0)\prime\prime} - \frac{16i}{19} |A_0|^2 F_0^{(0)\prime} - F_0^{(0)} \left(1 + \frac{26460}{361} |A_0|^4 - 4\sqrt{114} E_2 |A_0|^2 + \frac{16i}{19} A_0 \bar{A}_0' \right) \\
&\quad - F_2^{(0)} \left(\frac{17640}{361} |A_0|^2 \bar{A}_0^2 - 2\sqrt{114} E_2 \bar{A}_0^2 + \frac{16i}{19} \bar{A}_0 \bar{A}_0' \right),
\end{aligned} \tag{101}$$

$$\begin{aligned}
0 &= 4F_2^{(0)\prime\prime} + \frac{16i}{19} |A_0|^2 F_2^{(0)\prime} - F_2^{(0)} \left(1 + \frac{26460}{361} |A_0|^4 - 4\sqrt{114} E_2 |A_0|^2 - \frac{16i}{19} \bar{A}_0 A_0' \right) \\
&\quad - F_0^{(0)} \left(\frac{17640}{361} |A_0|^2 A_0^2 - 2\sqrt{114} E_2 A_0^2 - \frac{16i}{19} A_0 A_0' \right).
\end{aligned} \tag{102}$$

As in the analysis away from the Maxwell point, these equations are a linearised version of the amplitude equation (70). Let us use the amplitude/phase decomposition

$$F_0^{(0)} = (\mathcal{R}_1 - i\mathcal{R}_0\phi_1)\, e^{-i\phi_0}, \qquad F_2^{(0)} = (\mathcal{R}_1 + i\mathcal{R}_0\phi_1)\, e^{i\phi_0}, \tag{103}$$

where R_0 and ϕ_0 are given by (75) and (77). After substituting (103) into (101), (102) the resulting equation for ϕ_1 can readily be integrated once to give

$$\phi_1' = -\frac{2\mathcal{R}_0\mathcal{R}_1}{19} + \frac{19K_3}{\mathcal{R}_0^2}, \tag{104}$$

where K_3 is constant, while the equation for $\mathcal{R}_1$ is

$$4\mathcal{R}_1'' - \left(1 - 6\sqrt{114}\mathcal{R}_0^2 E_2 + \frac{44040}{361}\mathcal{R}_0^4\right)\mathcal{R}_1 = 8K_3\mathcal{R}_0. \tag{105}$$

We seek four independent solutions of (101)-(102) by finding four independent solutions of (104)-(105).

We start with the case $K_3 = 0$. In this case (105) is the linearisation of the amplitude equation (70). With $K_3 = 0$ one solution of (104)-(105) is simply $\mathcal{R}_1 = 0$, $\phi_1 = K_4$, where K_4 is constant. This gives

$$F_0^{(0)} = -iK_4A_0, \qquad F_2^{(0)} = iK_4A_0,$$

and corresponds to translational invariance with respect to x.

With $K_3 = 0$ a non-trivial solution to (105) is given by $\mathcal{R}_1 = K_1\mathcal{R}_0'$. This gives

$$F_0^{(0)} = K_1A_0', \qquad F_2^{(0)} = K_1A_0',$$

and corresponds to translational invariance with respect to X. Still with $K_3 = 0$, a second non-trivial solution to (105) can be found using variation of parameters to be

$$\begin{aligned}
\mathcal{R}_1(X) &= \mathcal{R}_0'(X)\int_{i\pi}^{X}\frac{ds}{\mathcal{R}_0'(s)^2} \\
&= \sqrt{\frac{2}{19\beta}}\left(\frac{1}{1+e^{-X}}\right)^{3/2}\left[6 - 2e^{-2X} + e^X + 6e^{-X}\left(\frac{1}{2} + X - i\pi\right)\right], \\
\phi_1 &= -\frac{2}{19}\int_{i\pi}^{X}\mathcal{R}_0(s)\mathcal{R}_1(s)\,ds = \frac{2}{19}\left(5 - e^X + 4i\pi - 4X + 6\frac{X - i\pi}{1+e^X}\right).
\end{aligned}$$

The choice for the lower integration bound comes in anticipation with matching with the inner solution at $X = i\pi$. The resulting solution for $F_0^{(0)}$, $F_2^{(0)}$ is

$$\begin{aligned}
F_0^{(0)} &= \frac{\sqrt{2}K_2e^{3X/2}}{\sqrt{19\beta}\,(1+e^X)^{3/2-i\beta/2}}\left\{6 - 2e^{-2X} + e^X + 6e^{-X}\left(\frac{1}{2} + X - i\pi\right)\right. \\
&\quad \left. - i\beta\left[4 - 4X + 4i\pi - e^X + 2e^{-X}\left(\frac{5}{2} + X - i\pi\right)\right]\right\}
\end{aligned} \tag{106}$$

$$F_2^{(0)} = \frac{\sqrt{2}K_2 e^{3X/2}}{\sqrt{19\beta}\,(1+e^X)^{3/2+i\beta/2}}\left\{6-2e^{-2X}+e^X+6e^{-X}\left(\frac{1}{2}+X-i\pi\right)\right.$$
$$\left.+\,i\beta\left[4-4X+4i\pi-e^X+2e^{-X}\left(\frac{5}{2}+X-i\pi\right)\right]\right\} \quad (107)$$

Finally, we take K_3 nonzero. Then (105) is an inhomogeneous equation. Since we have just determined two independent solutions of the homogeneous equation we can again use the method of variation of parameters. After some manipulation, we obtain

$$\begin{aligned}\mathcal{R}_1 &= K_3\mathcal{R}_0'(X)\int_{i\pi}^{X}\frac{\mathcal{R}_0(s)^2}{\mathcal{R}_0'(s)^2}\,ds\\ &= K_3\sqrt{\frac{19\beta}{2}}\left(\frac{1}{1+e^{-X}}\right)^{3/2}\left[4+e^X+2e^{-X}\left(\frac{3}{2}+X-i\pi\right)\right],\\ \phi_1 &= -\frac{2}{19}\int_{i\pi}^{X}\mathcal{R}_0(s)\mathcal{R}_1(s)\,ds+19K_3\int_{i\pi}^{X}\frac{ds}{\mathcal{R}_0(s)^2}.\end{aligned}$$

3.5.2 Summary

To summarise, $F_0^{(0)}$, $F_2^{(0)}$ can be written as

$$F_0^{(0)}(X) = \left[\mathcal{R}_0'\int_{i\pi}^{X}\frac{K_2+K_3\mathcal{R}_0^2}{\mathcal{R}_0'^2}ds+\frac{2i\mathcal{R}_0}{19}\int_{i\pi}^{X}\mathcal{R}_0\mathcal{R}_0'\left(\int_{i\pi}^{s}\frac{K_2+K_3\mathcal{R}_0^2}{\mathcal{R}_0'^2}dt\right)ds\right.$$
$$\left.-i\mathcal{R}_0\int_{i\pi}^{X}\frac{19K_3}{\mathcal{R}_0^2}ds\right]e^{-i\phi_0}+K_1A_0'-iK_4A_0, \quad (108)$$

$$F_2^{(0)}(X) = \left[\mathcal{R}_0'\int_{i\pi}^{X}\frac{K_2+K_3\mathcal{R}_0^2}{\mathcal{R}_0'^2}ds-\frac{2i\mathcal{R}_0}{19}\int_{i\pi}^{X}\mathcal{R}_0\mathcal{R}_0'\left(\int_{i\pi}^{s}\frac{K_2+K_3\mathcal{R}_0^2}{\mathcal{R}_0'^2}dt\right)ds\right.$$
$$\left.+\,i\mathcal{R}_0\int_{i\pi}^{X}\frac{19K_3}{\mathcal{R}_0^2}ds\right]e^{i\phi_0}+K_1A_0'+iK_4A_0. \quad (109)$$

3.5.3 Second eigenvalue: $\kappa_2 = e^{5i\pi/4}$

We label the amplitudes associated with this eigenvalue G. As happened near $X = i\pi$, the solutions for $G_0^{(0)}$ and $G_2^{(0)}$ turn out to be the same as those for $F_0^{(0)}$ and $F_2^{(0)}$.

3.5.4 Third and fourth eigenvalues: $\kappa_3 = e^{-i\pi/4}$, $\kappa_4 = e^{3i\pi/4}$

We label these H and J respectively.

For these eigenvalues we find that $H_{-2}^{(0)}$ and $J_{-2}^{(0)}$ satisfy the same equations as $F_0^{(0)}$ and $H_0^{(0)}$ and $J_0^{(0)}$ satisfy the same equations as $F_2^{(0)}$.

3.5.5 Matching with the inner region $X = i\pi$

In order to match with the inner solution we need that, as $X \to i\pi$,

$$\frac{F_k^{(0)}(X)}{(i\pi - X)^{n/2+\alpha_k}} \sim \frac{\text{const.}}{(i\pi - X)^{\frac{n+1}{2}+\frac{ik\beta}{2}}},$$

i.e.

$$F_{-2}^{(0)}(X) \sim \frac{\text{const.}}{(i\pi - X)^{\frac{1}{2}-\alpha-i\beta}}, \quad F_0^{(0)}(X) \sim \frac{\text{const.}}{(i\pi - X)^{\frac{1}{2}-\alpha}}, \quad F_2^{(0)}(X) \sim \frac{\text{const.}}{(i\pi - X)^{\frac{1}{2}-\alpha+i\beta}},$$

as $X \to i\pi$. From (109) we find

$$\begin{aligned} F_2^{(0)} \sim\ & K_1 \left(\frac{i\sqrt{19\beta/8}}{(i\pi - X)^{3/2+i\beta/2}} + \dots \right) + K_2 \left(-\frac{(3i+\beta)}{3\sqrt{38\beta}} (i\pi - X)^{5/2-i\beta/2} + \dots \right) \\ & + K_3 \left(-\sqrt{\frac{19}{2\beta}} \left(1 + 2i\beta + \beta^2\right) (i\pi - X)^{3/2-i\beta/2} + \dots \right) \\ & + K_4 \left(\frac{\sqrt{19\beta/2}}{(i\pi - X)^{1/2+i\beta/2}} + \dots \right). \end{aligned}$$

We see that matching is possible providing α takes one of the values in (96). The dominant value of $\alpha = 3 + i\beta/2$ corresponds to the solution multiplying K_2. Focusing just on this solution, we have, away from $X = i\pi$, for $\kappa = e^{i\pi/4}$,

$$F_0^{(0)}(X) \sim K_2^1 \left[\mathcal{R}_0' \int_{i\pi}^X \frac{ds}{\mathcal{R}_0'^2} + \frac{2i\mathcal{R}_0}{19} \int_{i\pi}^X \mathcal{R}_0 \mathcal{R}_0' \left(\int_{i\pi}^s \frac{dt}{\mathcal{R}_0'^2} \right) ds \right] e^{-i\phi_0} \tag{110}$$

$$F_2^{(0)}(X) \sim K_2^1 \left[\mathcal{R}_0' \int_{i\pi}^X \frac{ds}{\mathcal{R}_0'^2} - \frac{2i\mathcal{R}_0}{19} \int_{i\pi}^X \mathcal{R}_0 \mathcal{R}_0' \left(\int_{i\pi}^s \frac{dt}{\mathcal{R}_0'^2} \right) ds \right] e^{i\phi_0}, \tag{111}$$

for $\kappa = e^{5i\pi/4}$,

$$G_0^{(0)}(X) \sim K_2^2 \left[\mathcal{R}_0' \int_{i\pi}^X \frac{ds}{\mathcal{R}_0'^2} + \frac{2i\mathcal{R}_0}{19} \int_{i\pi}^X \mathcal{R}_0 \mathcal{R}_0' \left(\int_{i\pi}^s \frac{dt}{\mathcal{R}_0'^2} \right) ds \right] e^{-i\phi_0} \tag{112}$$

$$G_2^{(0)}(X) \sim K_2^2 \left[\mathcal{R}_0' \int_{i\pi}^X \frac{ds}{\mathcal{R}_0'^2} - \frac{2i\mathcal{R}_0}{19} \int_{i\pi}^X \mathcal{R}_0 \mathcal{R}_0' \left(\int_{i\pi}^s \frac{dt}{\mathcal{R}_0'^2} \right) ds \right] e^{i\phi_0}, \tag{113}$$

for $\kappa = e^{-i\pi/4}$,

$$H_{-2}^{(0)}(X) \sim K_2^3 \left[\mathcal{R}_0' \int_{i\pi}^X \frac{ds}{\mathcal{R}_0'^2} + \frac{2i\mathcal{R}_0}{19} \int_{i\pi}^X \mathcal{R}_0 \mathcal{R}_0' \left(\int_{i\pi}^s \frac{dt}{\mathcal{R}_0'^2} \right) ds \right] e^{-i\phi_0} \tag{114}$$

$$H_0^{(0)}(X) \sim K_2^3 \left[\mathcal{R}_0' \int_{i\pi}^X \frac{ds}{\mathcal{R}_0'^2} - \frac{2i\mathcal{R}_0}{19} \int_{i\pi}^X \mathcal{R}_0 \mathcal{R}_0' \left(\int_{i\pi}^s \frac{dt}{\mathcal{R}_0'^2} \right) ds \right] e^{i\phi_0}, \tag{115}$$

for $\kappa = e^{3i\pi/4}$,

$$J_{-2}^{(0)}(X) \sim K_2^4 \left[\mathcal{R}_0' \int_{i\pi}^{X} \frac{ds}{\mathcal{R}_0'^2} + \frac{2i\mathcal{R}_0}{19} \int_{i\pi}^{X} \mathcal{R}_0 \mathcal{R}_0' \left(\int_{i\pi}^{s} \frac{dt}{\mathcal{R}_0'^2} \right) ds \right] e^{-i\phi_0} \tag{116}$$

$$J_{0}^{(0)}(X) \sim K_2^4 \left[\mathcal{R}_0' \int_{i\pi}^{X} \frac{ds}{\mathcal{R}_0'^2} - \frac{2i\mathcal{R}_0}{19} \int_{i\pi}^{X} \mathcal{R}_0 \mathcal{R}_0' \left(\int_{i\pi}^{s} \frac{dt}{\mathcal{R}_0'^2} \right) ds \right] e^{i\phi_0}. \tag{117}$$

Matching in the vicinity of $X = i\pi$ with (98) gives

$$\begin{aligned} K_2^1 = -K_2^2 &= -\frac{3\sqrt{38\beta}}{3i+\beta} e^{-i\psi} \lambda_1 = \frac{3\sqrt{38\beta}}{\beta - 3i} \lambda_1, \\ K_2^3 = -K_2^4 &= -\frac{3\sqrt{38\beta}}{3i+\beta} \lambda_3 = \frac{3\sqrt{38\beta}}{\beta - 3i} e^{i\psi} \lambda_3, \end{aligned}$$

which are self-consistent by (97).

Hence, the singularity at $X = i\pi$ generates the late terms

$$\begin{aligned} f_n(x, X) \sim & \frac{e^{in\pi/4}\Gamma(n/2+\alpha)}{(i\pi - X)^{\frac{n}{2}+\alpha}} \left(1 - (-1)^n\right) \left(F_0^{(0)}(X) + F_2^{(0)}(X) e^{2i\tilde{x}} \right) \\ & + \frac{e^{-in\pi/4}\Gamma(n/2+\bar{\alpha})}{(i\pi - X)^{\frac{n}{2}+\bar{\alpha}}} \left(1 - (-1)^n\right) \left(H_0^{(0)}(X) + H_{-2}^{(0)}(X) e^{-2i\tilde{x}} \right) \end{aligned} \tag{118}$$

in the rest of the complex plane, where $\alpha = 3 + i\beta/2$ and $F_0^{(0)}$, $F_2^{(0)}$, $H_{-2}^{(0)}$ and $H_0^{(0)}$ are given by (110), (111), (114) and (115) respectively.

As before, we can determine the contribution from $X = -i\pi$ by symmetry to be

$$\begin{aligned} f_n(x, X) \sim & \frac{e^{-in\pi/4}\Gamma(n/2+\bar{\alpha})}{(-i\pi - X)^{\frac{n}{2}+\bar{\alpha}}} \left(1 - (-1)^n\right) \left(\bar{F}_0^{(0)}(X) + \bar{F}_2^{(0)}(X) e^{-2i\tilde{x}} \right) \\ & + \frac{e^{in\pi/4}\Gamma(n/2+\alpha)}{(-i\pi - X)^{\frac{n}{2}+\alpha}} \left(1 - (-1)^n\right) \left(\bar{H}_0^{(0)}(X) + \bar{H}_{-2}^{(0)}(X) e^{2i\tilde{x}} \right) \end{aligned} \tag{119}$$

Note that, as in the inner region, the dominant terms in the series vanish for n even. This is related to the fact that the derivative terms in equation (79) couple every second term in the expansion. The result is that when we truncate optimally and study the remainder, we need only consider the odd terms in the series.

3.6 Crossing the Stokes line

As in §2.6 we truncate the series after N terms and write

$$f(\tilde{x}, X) = \sum_{n=0}^{N-1} \epsilon^n f_n(\tilde{x}, X) + R_N(x, X).$$

The equation for the remainder R_N is then

$$\begin{aligned}
&R_{N_{\tilde{x}\tilde{x}\tilde{x}\tilde{x}}} + 2R_{N_{\tilde{x}\tilde{x}}} + R_N \\
&\quad + 4\epsilon^2 R_{N_{\tilde{x}\tilde{x}\tilde{x}X}} + 6\epsilon^4 R_{N_{\tilde{x}\tilde{x}XX}} + 4\epsilon^6 R_{N_{\tilde{x}XXX}} + \epsilon^8 R_{N_{XXXX}} + 4\epsilon^2 R_{N_{\tilde{x}X}} + 2\epsilon^4 R_{N_{XX}} \\
&\quad + \epsilon^2(3f_0^2 R_N + \cdots) + \epsilon^4 R_N + 6\epsilon(E_0 + \epsilon E_1 + \cdots)(f_0 + \epsilon f_1 + \cdots)R_N \\
&\sim \quad - 3\epsilon\,\delta E(f_0^2 + 2\epsilon f_0 f_1 + \cdots) \\
&\quad + \epsilon^N\,(f_{N_{\tilde{x}\tilde{x}\tilde{x}\tilde{x}}} + 2f_{N_{\tilde{x}\tilde{x}}} + f_N) \\
&\quad + \epsilon^{N+2}\,(-6f_{N-2_{\tilde{x}\tilde{x}XX}} - 4f_{N-4_{\tilde{x}XXX}} - f_{N-6_{XXXX}} - 2f_{N-2_{XX}}) \\
&\quad + \epsilon^{N+4}\,(-4f_{N-2_{\tilde{x}XXX}} - f_{N-4_{XXXX}}) \\
&\quad + \epsilon^{N+6}\,(-f_{N-2_{XXXX}}) + \cdots\,,
\end{aligned} \tag{120}$$

where we have used the equation for f_N to simplify the right-hand side, and we are assuming that N is odd. We must comment in particular on the first term on the right-hand side, proportional to δE. This term arises due to the deviation of E from the Maxwell point, and is the crucial term which will allow us to join up-fronts and down-fronts. The size of δE is unknown at present, but we will see that it turns out to be exponentially small. The omitted terms in (120), represented by $\cdots$, are all lower order as $N \to \infty$, $\epsilon \to 0$. As before, when we approximate the terms on the right-hand side of (120) as $N \to \infty$ and $\epsilon \to 0$ we will obtain terms from the singularity at $X = i\pi$ through (118) and terms from the singularity at $X = -i\pi$ through (119); we denote the former by rhs^+ and the latter by rhs^- (with the corresponding contributions to R_N denoted by R_N^+ and R_N^- as before). Each of these will be composed of two parts—one for the eigenvalues κ_1, κ_2 (which we denote by the subscript F), and one for the eigenvalues κ_3, κ_4 (which we denote by the subscript H). In addition to these contributions, this time we will also have a contribution due to the term proportional to δE; we denote this term on the right-hand side by $\mathrm{rhs}^{\delta E}$ (with the corresponding contribution to R_N denoted by $R_N^{\delta E}$). We compute first rhs^+. Now, as $\epsilon \to 0$, $N \to \infty$,

$$\mathrm{rhs}_F^+ \sim \epsilon^N e^{iN\pi/4} e^{i\tilde{x}} \frac{\Gamma(N/2+\alpha)}{(i\pi - X)^{N/2+\alpha}} \sum_{k=0,2} e^{i(k-1)\tilde{x}} C_k \tag{121}$$

where

$$\begin{aligned}
C_k \;=\; & F_k^{(0)} \left((k^2-1)^2 - i\epsilon^2(6k^2 - 4k - 1)\frac{(N/2+\alpha)}{(i\pi - X)} \right. \\
& + \epsilon^4(-4k+1)\frac{(N/2+\alpha)(N/2+\alpha+1)}{(i\pi - X)^2} \\
& \left. + \epsilon^6 i \frac{(N/2+\alpha)(N/2+\alpha+1)(N/2+\alpha+2)}{(i\pi - X)^3} \right)
\end{aligned}$$

We can see from (118) that the ratio of successive terms (remembering that n is odd so successive terms correspond to n and $n+2$) is approximately $in\epsilon^2/2(i\pi - X)$. Thus the optimal truncation point, corresponding to the smallest term, is approximately $N = 2|X - i\pi|/\epsilon^2$.

Since N depends on $|X-i\pi|$ only we write $X-i\pi = re^{i\theta}$ giving $N = 2r/\epsilon^2 + 2\nu$, where ν is required to ensure that N is an (odd) integer, but is bounded as $\epsilon \to 0$. We first approximate the premultiplier of the sum in (121) at optimal truncation, following [21]. Writing

$$e^{i\tilde{x}} = e^{ix}e^{-i\varphi} = e^{i(X-i\pi)/\epsilon^2}e^{-\pi/\epsilon^2}e^{-i\varphi}, \tag{122}$$

we find

$$\begin{aligned}
& e^{i(X-i\pi)/\epsilon^2}\epsilon^{N+2\alpha}e^{i(N+2\alpha)\pi/4}\frac{\Gamma(N/2+\alpha)}{(i\pi-X)^{N/2+\alpha}} \\
&\sim \frac{\sqrt{2\pi}\,e^{ire^{i\theta}/\epsilon^2}\epsilon^{2r/\epsilon^2+2\nu+2\alpha}e^{i\pi/2(r/\epsilon^2+\nu+\alpha)}(r/\epsilon^2+\alpha+\nu)^{r/\epsilon^2+\alpha+\nu-1/2}e^{-r/\epsilon^2-\alpha-\nu}}{r^{r/\epsilon^2+\nu+\alpha}e^{i(\theta+\pi)(r/\epsilon^2+\nu+\alpha)}} \\
&\sim \frac{\sqrt{2\pi}\,\epsilon e^{-i\pi/2(r/\epsilon^2+\nu+\alpha)}(1+\epsilon^2(\alpha+\nu)/r)^{r/\epsilon^2+\alpha+\nu-1/2}e^{-r/\epsilon^2-\alpha-\nu}e^{ire^{i\theta}/\epsilon^2}}{r^{1/2}e^{i\theta(r/\epsilon^2+\nu+\alpha)}} \\
&\sim \frac{\sqrt{2\pi}\,\epsilon e^{-i\pi/2(r/\epsilon^2+\nu+\alpha)}e^{\alpha+\nu}e^{-r/\epsilon^2-\alpha-\nu}e^{ire^{i\theta}/\epsilon^2}}{r^{1/2}e^{i\theta(r/\epsilon^2+\nu+\alpha)}} \\
&\sim \frac{\sqrt{2\pi}\,\epsilon e^{-i\pi/2(r/\epsilon^2+\nu+\alpha)}e^{-r/\epsilon^2}e^{ire^{i\theta}/\epsilon^2}}{r^{1/2}e^{i\theta(r/\epsilon^2+\nu+\alpha)}}.
\end{aligned}$$

This expression is exponentially small except in the vicinity of the Stokes line $\theta = -\pi/2$. Writing $\theta = -\pi/2 + \epsilon\bar{\theta}$ gives

$$e^{i(X-i\pi)/\epsilon^2}\epsilon^{N+2\alpha}e^{i(N+2\alpha)\pi/4}\frac{\Gamma(N/2+\alpha)}{(i\pi-X)^{N/2+\alpha}} \sim \frac{\sqrt{2\pi}\,\epsilon e^{-r\bar{\theta}^2/2}}{r^{1/2}}. \tag{123}$$

We also need to approximate C_k near the Stokes line. We find

$$\begin{aligned}
C_k &\sim F_k^{(0)}\left((k^2-1)^2 - (6k^2-4k-1)e^{-i\epsilon\bar{\theta}} - (-4k+1)e^{-2i\epsilon\bar{\theta}} - e^{-3i\epsilon\bar{\theta}}\right) + O(\epsilon^2) \\
&\sim F_k^{(0)}\left(k(k^3-8k+8) + 2i(3k^2-6k+2)\epsilon\bar{\theta} + \cdots\right).
\end{aligned}$$

Thus

$$C_0 \sim 4i\epsilon\bar{\theta}F_0^{(0)} + \cdots, \qquad C_2 \sim 4i\epsilon\bar{\theta}F_2^{(0)} + \cdots. \tag{124}$$

Combining (123) and (124) we find that in the vicinity of the Stokes line (121) gives

$$\mathrm{rhs}_F^+ \sim \epsilon^{-2\alpha}e^{-i\alpha\pi/2}e^{-\pi/\epsilon^2}e^{-i\varphi}\frac{\sqrt{2\pi}\,\epsilon e^{-r\bar{\theta}^2/2}}{r^{1/2}}\left(e^{-i\tilde{x}}4i\epsilon\bar{\theta}F_0^{(0)} + e^{i\tilde{x}}4i\epsilon\bar{\theta}F_2^{(0)}\right). \tag{125}$$

3.7 Solution of the remainder equation

With $X = i\pi + re^{i\theta}$ we have

$$\frac{\partial}{\partial X} = -\frac{ie^{-i\theta}}{r}\frac{\partial}{\partial\theta},$$

so that in the vicinity of the Stokes line, with $\theta = -\pi/2 + \epsilon\bar{\theta}$, we have

$$\frac{\partial}{\partial X} = \frac{e^{-i\epsilon\bar{\theta}}}{r\epsilon}\frac{\partial}{\partial\bar{\theta}}.$$

Thus equation (120) for the remainder due to the right-hand side rhs_F^+ (which arises from the eigenvalues $\kappa = \pm e^{i\pi/4}$ and the singularity at $i\pi$, and which we write as R_F^+) becomes

$$\begin{aligned}
&R^+_{F_{\tilde{x}\tilde{x}\tilde{x}\tilde{x}}} + 2R^+_{F_{\tilde{x}\tilde{x}}} + R^+_F \\
&\quad + 4\epsilon\frac{(1-i\epsilon\bar{\theta})}{r}R^+_{F_{\tilde{x}\tilde{x}\tilde{x}\bar{\theta}}} + \frac{6\epsilon^2}{r^2}R^+_{F_{\tilde{x}\tilde{x}\bar{\theta}\bar{\theta}}} + 4\epsilon\frac{(1-i\epsilon\bar{\theta})}{r}R^+_{F_{\tilde{x}\bar{\theta}}} + \frac{2\epsilon^2}{r^2}R^+_{F_{\bar{\theta}\bar{\theta}}} \\
&\quad + 3\epsilon^2 f_0^2 R_F^+ + 6E_0\epsilon f_0 R_F^+ + 6E_0\epsilon^2 f_1 R_F^+ + 6E_1\epsilon^2 f_0 R_F^+ + o(\epsilon^2 R_F^+) \\
&\sim\ 4i\sqrt{2\pi}\,\epsilon^{2-2\alpha}e^{-i\alpha\pi/2}e^{-\pi/\epsilon^2}e^{-i\varphi}\frac{e^{-r\bar{\theta}^2/2}}{r^{1/2}}\left(e^{-i\tilde{x}}\bar{\theta}F_0^{(0)} + e^{i\tilde{x}}\bar{\theta}F_2^{(0)}\right). \qquad (126)
\end{aligned}$$

As before, equation (126) must be solved via a multiple scales expansion, since the rescaled X coordinate $\bar{\theta}$ is still much longer than the fast scale x. The forcing terms in (126) are resonant terms, so that the solution will be an order of magnitude larger: $R_F^+ = O(\epsilon^{-2\alpha}e^{-\pi/\epsilon^2})$. We seek an expansion of the form

$$R_F^+ \sim \epsilon^{-2\alpha}e^{-\pi/\epsilon^2}\left(R_0^+ + \epsilon R_1^+ + \epsilon^2 R_2^+ + \cdots\right).$$

Then, at leading order,

$$R^+_{0_{\tilde{x}\tilde{x}\tilde{x}\tilde{x}}} + 2R^+_{0_{\tilde{x}\tilde{x}}} + R_0^+ = 0,$$

so that

$$R_0^+ = S_{-1}(\bar{\theta})e^{-i\tilde{x}} + S_1(\bar{\theta})e^{i\tilde{x}}.$$

Equating coefficients at $O(e^{-\pi/\epsilon^2}\epsilon^{1-2\alpha})$ gives

$$\begin{aligned}
R^+_{1_{\tilde{x}\tilde{x}\tilde{x}\tilde{x}}} + 2R^+_{1_{\tilde{x}\tilde{x}}} + R_1^+ &= -\frac{4}{r}\left(R^+_{0_{\tilde{x}\tilde{x}\tilde{x}\bar{\theta}}} + R^+_{0_{\tilde{x}\bar{\theta}}}\right) - 6E_0 f_0 R_0^+ \\
&= -6E_0\left(A_0e^{i\tilde{x}} + \bar{A}_0e^{-i\tilde{x}}\right)\left(S_{-1}(\bar{\theta})e^{-i\tilde{x}} + S_1(\bar{\theta})e^{i\tilde{x}}\right),
\end{aligned}$$

with solution

$$R_1^+ = -6E_0\left(\frac{\bar{A}_0S_{-1}}{9}e^{-2i\tilde{x}} + A_0S_{-1} + \bar{A}_0S_1 + \frac{A_0S_1}{9}e^{2i\tilde{x}}\right).$$

Finally, equating coefficients at $O(e^{-\pi/\epsilon^2}\epsilon^{2-2\alpha})$ gives

$$\begin{aligned}
R^+_{2_{\tilde{x}\tilde{x}\tilde{x}\tilde{x}}} + 2R^+_{2_{\tilde{x}\tilde{x}}} + R_2^+ &= \frac{4}{r^2}\left(S''_{-1}(\bar{\theta})e^{-i\tilde{x}} + S''_1(\bar{\theta})e^{i\tilde{x}}\right) \\
&\quad - 3\left(A_0e^{i\tilde{x}} + \bar{A}_0e^{-i\tilde{x}}\right)^2\left(S_{-1}(\bar{\theta})e^{-i\tilde{x}} + S_1(\bar{\theta})e^{i\tilde{x}}\right) \\
&\quad + E_0^2\left(A_0e^{i\tilde{x}} + \bar{A}_0e^{-i\tilde{x}}\right)\left(4\bar{A}_0S_{-1}e^{-2i\tilde{x}} + 36A_0S_{-1} + 36\bar{A}_0S_1 + 4A_0S_1e^{2i\tilde{x}}\right) \\
&\quad + E_0^2\left(2A_0^2e^{2i\tilde{x}} + 2\bar{A}_0^2e^{-2i\tilde{x}} + 36|A_0|^2\right)\left(S_{-1}(\bar{\theta})e^{-i\tilde{x}} + S_1(\bar{\theta})e^{i\tilde{x}}\right) \\
&\quad + 4i\sqrt{2\pi}\,e^{-i\alpha\pi/2}e^{-i\varphi}\frac{e^{-r\bar{\theta}^2/2}}{r^{1/2}}\bar{\theta}\left(e^{-i\tilde{x}}F_0^{(0)} + e^{i\tilde{x}}F_2^{(0)}\right).
\end{aligned}$$

Above, we have omitted terms resulting from the expansion of $A_0(X)$ in terms of $\bar{\theta}$ but these are non resonant.

The solvability condition that there are no inhomogeneous terms of the form $e^{\pm i\tilde{x}}$ then gives

$$\begin{aligned}
-\frac{4}{r^2}S''_{-1}(\bar{\theta}) + \left(3 - 38E_0^2\right)\left(\bar{A}_0^2 S_1 + 2|A_0|^2 S_{-1}\right) &= 4i\sqrt{2\pi}\, e^{-i\alpha\pi/2}e^{-i\varphi}\frac{e^{-r\bar{\theta}^2/2}}{r^{1/2}}\bar{\theta}F_0^{(0)}, \\
-\frac{4}{r^2}S''_{1}(\bar{\theta}) + \left(3 - 38E_0^2\right)\left(A_0^2 S_{-1} + 2|A_0|^2 S_{1}\right) &= 4i\sqrt{2\pi}\, e^{-i\alpha\pi/2}e^{-i\varphi}\frac{e^{-r\bar{\theta}^2/2}}{r^{1/2}}\bar{\theta}F_2^{(0)},
\end{aligned}$$

Since $3 - 38E_0^2 = 0$ we find

$$\begin{aligned}
S_{-1} &\sim 2i\sqrt{\pi}\, e^{-i\alpha\pi/2}e^{-i\varphi}F_0^{(0)}\int_{-\infty}^{\frac{\sqrt{r}\bar{\theta}}{\sqrt{2}}} e^{-v^2}\, dv, \\
S_{1} &\sim 2i\sqrt{\pi}\, e^{-i\alpha\pi/2}e^{-i\varphi}F_2^{(0)}\int_{-\infty}^{\frac{\sqrt{r}\bar{\theta}}{\sqrt{2}}} e^{-v^2}\, dv,
\end{aligned}$$

where we have imposed the matching condition that S_{-1} and $S_1 \to 0$, as $\bar{\theta} \to -\infty$. Thus, across the Stokes line as $\bar{\theta}$ goes from $-\infty$ to ∞,

$$2i\pi\, e^{-i\alpha\pi/2}e^{-i\varphi}\epsilon^{-2\alpha}e^{-\pi/\epsilon^2}\left(F_0^{(0)}e^{-i\tilde{x}} + F_2^{(0)}e^{i\tilde{x}}\right) \tag{127}$$

is switched on by rhs_F^+.

By symmetry as we cross the Stokes line along the positive imaginary axis from $-i\pi$

$$-2i\pi\, e^{i\bar{\alpha}\pi/2}e^{i\varphi}\epsilon^{-2\bar{\alpha}}e^{-\pi/\epsilon^2}\left(\bar{F}_0^{(0)}e^{i\tilde{x}} + \bar{F}_2^{(0)}e^{-i\tilde{x}}\right) \tag{128}$$

is switched on by rhs_F^-.

3.7.1 rhs_H^+ and rhs_H^- and $\text{rhs}^{\delta E}$

The Stokes line associated with rhs_H^+ lies on

$$\text{Re}\left(\frac{-i}{i\pi - X}\right) > 0,$$

corresponding to $\theta = \pi/2$ and so does not intersect the real axis. Similarly the Stokes line associated with rhs_H^- lies on

$$\text{Re}\left(\frac{i}{-i\pi - X}\right) > 0,$$

corresponding to $X = -i\pi + re^{i\theta}$ with $\theta = -\pi/2$ and so does not intersect the real axis.

On the other hand, the term $\text{rhs}^{\delta E}$ is not large in the vicinity of the Stokes line, and so does not generate such a boundary layer solution. It's importance is felt away from the Stokes line, as we now establish.

3.8 Solution away from the Stokes line

Away from the Stokes line we expand

$$R_N = \epsilon^{-2}\,\delta E\left(R_0\left(x,X\right)+\epsilon R_1\left(x,X\right)+\epsilon^2 R_2\left(x,X\right)+\cdots\right).$$

As usual, at $O(\epsilon^0)$ we have

$$\mathcal{L}R_0 \equiv \frac{\partial^4 R_0}{\partial x^4}+2\frac{\partial^2 R_0}{\partial x^2}+R_0=0$$

so that

$$R_0 = S_0(X)e^{i\tilde{x}}+\bar{S}_0(X)e^{-i\tilde{x}}. \tag{129}$$

At $O(\epsilon)$

$$\mathcal{L}R_1 = -6E_0 f_0 R_0,$$

so that

$$R_1 = -\frac{2E_0A_0S_0e^{2i\tilde{x}}}{3}-\frac{2E_0\bar{A}_0\bar{S}_0e^{-2i\tilde{x}}}{3}-6E_0A_0\bar{S}_0-6\bar{A}_0S_0. \tag{130}$$

At $O(\epsilon^2)$

$$\begin{aligned}\mathcal{L}R_2 &= -3f_0^2R_0-6E_0f_0R_1-6E_0R_0f_1\\ &= (2E_0^2-1)3A_0^2S_0e^{3i\tilde{x}}+\text{c.c.}\end{aligned}$$

Thus

$$R_2 = S_2e^{i\tilde{x}}-\frac{3A_0^2S_0e^{3i\tilde{x}}}{76}+\text{c.c.} \tag{131}$$

At $O(\epsilon^3)$

$$\begin{aligned}\mathcal{L}R_3 &= -4\frac{\partial^2R_1}{\partial X\partial x}-4\frac{\partial^4R_1}{\partial X\partial x^3}-6f_0R_0f_1-3f_0^2R_1-6E_0R_0f_2-6E_0f_0R_2\\ &\quad -6E_0f_1R_1-6E_2f_0R_0-3f_0^2\\ &= -6E_2\bar{A}_0S_0-6E_0\bar{A}_0S_2+\frac{1118E_0}{19}A_0\bar{A}_0^2S_0\\ &\quad -\left(6E_2A_0S_0+6E_0A_0S_2+16iE_0\left(S_0A_0'+A_0S_0'\right)-\frac{727E_0}{38}\left(A_0^3\bar{S}_0+3A_0^2\bar{A}_0S_0\right)\right)e^{2i\tilde{x}}\\ &\quad +\frac{80E_0}{19}A_0^3S_0e^{4i\tilde{x}}+c.c.\end{aligned}$$

The solution at this order is

$$\begin{aligned}R_3 &= -6E_2\bar{A}_0S_0-6E_0\bar{A}_0S_2+\frac{1118E_0}{19}A_0\bar{A}_0^2S_0\\ &\quad -\left(\frac{2}{3}E_2A_0S_0+\frac{2}{3}E_0A_0S_2+\frac{16i}{9}iE_0\left(S_0A_0'+A_0S_0'\right)-\frac{727E_0}{342}\left(A_0^3\bar{S}_0+3A_0^2\bar{A}_0S_0\right)\right)e^{2i\tilde{x}}\\ &\quad +\frac{16E_0}{855}A_0^3S_0e^{4i\tilde{x}}+c.c.\end{aligned} \tag{132}$$

Finally, at $O(\epsilon^4)$ we must again eliminate secular terms on the right-hand side of the equation, which gives the solvability conditions

$$\begin{aligned} 0 &= 4S_0'' + \frac{16i}{19}|A_0|^2 S_0' - S_0\left(1 + \frac{26460}{361}|A_0|^4 - 4\sqrt{114}E_2|A_0|^2 - \frac{16i}{19}\bar{A}_0A_0'\right) \\ &\quad -\bar{S}_0\left(\frac{17640}{361}|A_0|^2 A_0^2 - 2\sqrt{114}E_2A_0^2 - \frac{16i}{19}A_0A_0'\right) + 2\sqrt{114}\,A_0|A_0|^2, \end{aligned} \tag{133}$$

$$\begin{aligned} 0 &= 4\bar{S}_0'' - \frac{16i}{19}|A_0|^2 \bar{S}_0' - \bar{S}_0\left(1 + \frac{26460}{361}|A_0|^4 - 4\sqrt{114}E_2|A_0|^2 + \frac{16i}{19}A_0\bar{A}_0'\right) \\ &\quad -S_0\left(\frac{17640}{361}|A_0|^2 \bar{A}_0^2 - 2\sqrt{114}E_2\bar{A}_0^2 + \frac{16i}{19}\bar{A}_0\bar{A}_0'\right) + 2\sqrt{114}\,\bar{A}_0|A_0|^2, \end{aligned}$$

Equation (133) is an inhomogeneous version of the linearised amplitude equation (70), which was already encountered in equations (101), (102) in §3.5, where the homogeneous solutions were calculated. To these we must add a particular integral due to the inhomogeneous term, which we now calculate. Let us use again the decomposition

$$S_0 = (\mathcal{R}_1 + i\mathcal{R}_0\phi_1)\,e^{i\phi_0},$$

which leads to the particular solution

$$\phi_1 = -\frac{2}{19}\int^X \mathcal{R}_0(s)\mathcal{R}_1(s)\,ds,$$

$$4\mathcal{R}_1'' - \mathcal{R}_1\left(1 - 6\sqrt{114}E_2\mathcal{R}_0^2 + \frac{44040\mathcal{R}_0^4}{361}\right) + 2\sqrt{114}\mathcal{R}_0^3 = 0.$$

Since we know the two homogeneous versions of the equation we can calculate a particular integral by variation of parameters. However, since the perturbation arises as a small change in E, we can spot the solution as being $\partial\mathcal{R}_0/\partial E_2$ evaluated at $E_2 = \frac{4}{19}\sqrt{\frac{367}{57}}$, giving

$$\phi_1 = \frac{19}{8}\sqrt{\frac{57}{2}}\beta^2\left(e^X + \frac{1}{1+e^X}\right)$$

and

$$\mathcal{R}_1 + i\mathcal{R}_0\phi_1 = \frac{361\sqrt{3}}{16}i\beta^{3/2}\left(\frac{e^X}{1+e^X}\right)^{3/2}\left(\beta e^{-X} + e^X(i+\beta) + 2i + \beta\right). \tag{134}$$

Thus, combining all the terms we have calculated, away from the Stokes line,

$$R_N \sim S_0(X)e^{i\tilde{x}} + \bar{S}_0(X)e^{-i\tilde{x}},$$

with

$$\begin{aligned} S_0 &= \left[\mathcal{R}_0' \int_{i\pi}^{X} \frac{B_2 + B_3\mathcal{R}_0^2}{\mathcal{R}_0'^2}\, ds - \frac{2i\mathcal{R}_0}{19} \int_{i\pi}^{X} \mathcal{R}_0\mathcal{R}_0' \left(\int_{i\pi}^{s} \frac{B_2 + B_3\mathcal{R}_0^2}{\mathcal{R}_0'^2} dt \right) \right. \\ &\quad \left. + i\mathcal{R}_0 \int_{i\pi}^{X} \frac{19K_3}{\mathcal{R}_0^2} ds \right] e^{i\phi_0} + B_1 A_0' + iB_4 A_0 + \frac{\delta E}{\epsilon^2} \frac{\partial A_0}{\partial E_2}, \end{aligned}$$

for some constants $B_1, \ldots, B_4$. Now B_1 corresponds to translating the solution f_0 in X and is therefore not important. Similarly B_4 corresponds to translating the solution f_0 in x. The important coefficient is B_2, since this is the solution which is switched on across the Stokes line, and it is the one which grows as $X \to \infty$. Focusing for a moment on this contribution let us match across the Stokes line to determine B_2. Let us write

$$\begin{aligned} S_0 &= B_2^+ \left[\mathcal{R}_0' \int_{i\pi}^{X} \frac{ds}{\mathcal{R}_0'^2} - \frac{2i\mathcal{R}_0}{19} \int_{i\pi}^{X} \mathcal{R}_0\mathcal{R}_0' \left(\int_{i\pi}^{s} \frac{dt}{\mathcal{R}_0'^2} \right) ds \right] e^{i\phi_0} \\ &\quad + B_2^- \left[\mathcal{R}_0' \int_{-i\pi}^{X} \frac{ds}{\mathcal{R}_0'^2} - \frac{2i\mathcal{R}_0}{19} \int_{-i\pi}^{X} \mathcal{R}_0\mathcal{R}_0' \left(\int_{-i\pi}^{s} \frac{dt}{\mathcal{R}_0'^2} \right) ds \right] e^{i\phi_0} \\ &= \frac{B_2^+}{K_2^1} F_2^{(0)} + \frac{B_2^-}{\bar{K}_2^1} \bar{F}_0^{(0)}, \end{aligned}$$

Then, by matching with (127) and (128) as we pass through the Stokes line we find

$$\begin{aligned} B_2^+ &= 2i\pi\, K_2^1 e^{-i\alpha\pi/2} e^{-i\varphi} \epsilon^{-2\alpha} e^{-\pi/\epsilon^2}, \\ B_2^- &= -2i\pi\, \bar{K}_2^1 e^{i\bar{\alpha}\pi/2} e^{i\varphi} \epsilon^{-2\bar{\alpha}} e^{-\pi/\epsilon^2}. \end{aligned}$$

Thus, for $X > 0$,

$$\begin{aligned} S_0 &= B_2^+ \left[\mathcal{R}_0' \int_{i\pi}^{X} \frac{ds}{\mathcal{R}_0'^2} - \frac{2i\mathcal{R}_0}{19} \int_{i\pi}^{X} \mathcal{R}_0\mathcal{R}_0' \left(\int_{i\pi}^{s} \frac{dt}{\mathcal{R}_0'^2} \right) ds \right] e^{i\phi_0} \\ &\quad + B_2^- \left[\mathcal{R}_0' \int_{-i\pi}^{X} \frac{ds}{\mathcal{R}_0'^2} - \frac{2i\mathcal{R}_0}{19} \int_{-i\pi}^{X} \mathcal{R}_0\mathcal{R}_0' \left(\int_{-i\pi}^{s} \frac{dt}{\mathcal{R}_0'^2} \right) ds \right] e^{i\phi_0} \\ &\quad + \frac{\delta E}{\epsilon^2} \frac{\partial A_0}{\partial E_2}, \end{aligned}$$

Now, as $X \to \infty$,

$$\mathcal{R}_0 \sim \sqrt{\frac{19\beta}{2}} \left(1 - \frac{e^{-X}}{2} + \cdots \right)$$

and

$$\begin{aligned} S_0 &\sim \left(B_2^+ \sqrt{\frac{2}{19\beta}} + B_2^- \sqrt{\frac{2}{19\beta}} - \frac{\delta E}{\epsilon^2} \frac{361\sqrt{3}}{16} \beta^{3/2} \right) e^X (1 - i\beta)\, e^{i\phi_0} \\ &= \left(-\frac{4\sqrt{2}\,\pi\Lambda e^{\beta\pi/4} e^{-\pi/\epsilon^2}}{\sqrt{19\beta}\,\epsilon^6} \cos(\chi - \varphi - \beta \log\epsilon) - \frac{\delta E}{\epsilon^2} \frac{361\sqrt{3}}{16} \beta^{3/2} \right) e^X (1 - i\beta)\, e^{i\phi_0}, \end{aligned} \tag{135}$$

where

$$K_2^1 = \Lambda e^{i\chi},$$

with Λ and χ real.

3.9 The existence of stationary fronts

We see that the far-field behaviour (135) is similar to that found in §2 away from the Maxwell point (61), but there is an extra exponentially growing term due to the perturbation from the Maxwell point δE. Now, in order to have a genuine front solution, we need the coefficient of e^X in the far-field behaviour to vanish. For δE in the range

$$|\,\delta E| < \delta E_c = \frac{64\sqrt{2}\,\pi\Lambda e^{\beta\pi/4}e^{-\pi/\epsilon^2}}{\beta^2 361\sqrt{57}\,\epsilon^4} \tag{136}$$

there are two possible values of φ, and a stationary front is possible. As δE approaches the endpoints of this range there is a bifurcation as the two solutions coalesce and disappear.

Thus we have been able to demonstrate the "pinning" of the front, allowing it to remain stationary over an (exponentially small) range of values of δE. This pinning is similar to that found in [42] for front solutions in differential-difference equations. However, in [42] the fast scale arose from the discrete nature of the underlying problem; here it arises from the multiscale nature of the solution itself.

With the far-field behaviour of a single front (135) we can do much more than study single front solutions; we can now generate the full bifurcation diagram by considering solutions with multiple fronts.

4 Joining fronts

Knowing the exponentially small correction (135) to the up-front, we are finally in a position to construct a localised pattern enclosed between two fronts. While exponentially small, the term S_0 in (135) is exponentially growing in the slow scale X and becomes of order one when $X = O(1/\epsilon^2)$. A localised pattern solution can thus be constructed as a composite expansion that combines an up-front at $X = 0$ and a down-front located at a distance $X = L/\epsilon^2$. Matching the two fronts inside the periodic domain is the last step required to complete our analysis.

The up-front solution is

$$f \sim f_0 + \cdots + \epsilon^{N-1} f_{N-1} + R_N,$$

where

$$f_0 = A_0(X)\, e^{i(x+\varphi)} + \bar{A}_0(X)\, e^{-i(x+\varphi)}, \qquad R_N \sim S_0(X)\, e^{i(x+\varphi)} + \bar{S}_0(X)\, e^{-i(x+\varphi)}.$$

Focusing just on the fundamental harmonic $e^{i(x+\varphi)}$, we use (135) and the first two terms $A_0+\epsilon^2 A_2$ computed in Appendix A, Eq. (168), to obtain, for $1 \ll X \ll 1/\epsilon^2$,

$$\begin{aligned} f \;\sim\; & e^{-i\beta X/2} e^{i(x+\varphi)} \left\{ \sqrt{\frac{19\beta}{2}} \left[1 - \epsilon^2 \Delta - \frac{1+i\beta}{2} \left(1 + 2541 \beta^3 \epsilon^2 X \right) e^{-X} \right] \right. \\ & \left. - \left[\frac{4\,\pi \Lambda e^{\beta\pi/4} e^{-\pi/\epsilon^2}}{\sqrt{19\beta/2}\,\epsilon^6} \cos\left(\chi - \varphi - \beta \log \epsilon \right) + \frac{\delta E}{\epsilon^2} \frac{361\sqrt{3}}{16} \beta^{3/2} \right] e^{X} \left(1 - i\beta \right) \right\} + c.c. \end{aligned} \tag{137}$$

where $\Delta = \beta^4 \left(\frac{80629}{114\beta} + i\, \frac{172666595}{456} \right)$.

By symmetry, the far field of the down-front as $X - L/\epsilon^2 \to -\infty$ is given by (137) with $X \to L/\epsilon^2 - X$ and $x \to L/\epsilon^4 - x$. Note though that the phase shift φ can be different for the two fronts; indeed this is one of the key variables which allows the oscillations from the two solutions to match. Thus, for $1 \ll L/\epsilon^2 - X \ll 1/\epsilon^2$,

$$\begin{aligned} f \;\sim\; & e^{-i\beta(L/\epsilon^2 - X)/2} e^{i(L/\epsilon^4 - x + \hat{\varphi})} \left\{ \sqrt{\frac{19\beta}{2}} \left[1 - \epsilon^2 \Delta - \frac{1+i\beta}{2} \left(1 + 2541 \beta^3 \left(L - \epsilon^2 X \right) \right) e^{X - L/\epsilon^2} \right] \right. \\ & \left. - \left[\frac{4\,\pi \Lambda e^{\beta\pi/4} e^{-\pi/\epsilon^2}}{\sqrt{19\beta/2}\,\epsilon^6} \cos\left(\chi - \hat{\varphi} - \beta \log \epsilon \right) + \frac{\delta E}{\epsilon^2} \frac{361\sqrt{3}}{16} \beta^{3/2} \right] e^{L/\epsilon^2 - X} \left(1 - i\beta \right) \right\} + c.c. \end{aligned} \tag{138}$$

We now need to make sure (137) and (138) match for $X = O(1/\epsilon^2)$ and $L/\epsilon^2 - X = O(1/\epsilon^2)$. However, the expansions above are not uniformly valid in these limits, owing to the $\epsilon^2 X e^{-X}$ term. Hence, we must construct an outer expansion that is valid inside the extended periodic domain and match it with (137) and (138).

4.1 Outer expansion inside the periodic domain

In order to generate an approximation which is valid for $X = O(1/\epsilon^2)$ we need to introduce a third super-slow scale $\xi = \epsilon^4 x = \epsilon^2 X$. On this new length scale, the fronts (137) and (138) appear as boundary layers. Examining (137), we can anticipate that the amplitude associated with e^{ix} will be a constant plus an exponentially-small X-dependent solution.

Let us develop the multiple-scales solution

$$f \sim f_0\left(x, X, \xi\right) + \epsilon f_1\left(x, X, \xi\right) + \ldots,$$

with the usual expansion for E_{hg}

$$E_{hg} \sim E_0 + \epsilon^2 E_2 + \epsilon^4 E_4 + \ldots + \delta E.$$

In Appendix A, E_4 is found to be $\frac{63711\sqrt{3/38}}{264974}$. The first four orders of the analysis proceed in exactly the same way as in §3.2, except that, this time,

$$f_0 = A_0(X,\xi) e^{i\tilde{x}} + \bar{A}_0(X,\xi) e^{-i\tilde{x}}.$$

At $O(\epsilon^4)$, we thus get the solvability condition

$$4A_{0_{XX}} + \frac{16iA_{0_X}|A_0|^2}{19} - \frac{8820|A_0|^4A_0}{361} + 2\sqrt{114}E_2|A_0|^2A_0 - A_0 = 0, \tag{139}$$

and, in view of (137), we assume the solution

$$A_0(X,\xi) = \sqrt{\frac{19\beta}{2}}\, e^{i\phi_0}, \tag{140}$$

where $\phi_0(X,\xi) = -\beta X/2 + \Phi(\xi)$. The super-slow function $\Phi(\xi)$ is determined in Appendix A and is given by $\Phi = \frac{43163}{4310048}\,\xi$. Similarly, we have

$$A_2(X,\xi) = -\sqrt{\frac{19\beta}{2}}\beta^4 \left(\frac{80629}{114\beta} + i\frac{172666595}{456}\right) e^{i\phi_0}\,. \tag{141}$$

The equation for f_4 is then

$$\mathcal{L}f_4 = \left(4E_0E_2A_0^3 - \frac{48}{19}A_0^2A_2 - \frac{3504}{1805}\,|A_0|^2\,A_0^3 - \frac{56i}{19}A_0^2A_{0_X}\right) e^{3i\tilde{x}} + \frac{16}{1805}A_0^5\, e^{5i\tilde{x}} + \text{c.c.},$$

giving

$$f_4 = \left(4E_0E_2A_0^3 - \frac{48}{19}A_0^2A_2 - \frac{3504}{1805}\,|A_0|^2\,A_0^3 - \frac{56i}{19}A_0^2A_{0_X}\right) \frac{e^{3i\tilde{x}}}{64} + \frac{16}{1805}A_0^5\,\frac{e^{5i\tilde{x}}}{576} + \text{c.c.}.$$

To save space, we omit to write the expression for f_5, although it is necessary for the following steps.

The terms proportional to $e^{\pm X}$ are exponentially-small corrections to the solution above and therefore satisfy to good approximation the linearised equation

$$\left(1+\partial_x^2\right)^2\, R_N + 6\epsilon E_{hg}(f_0 + \epsilon f_1 + \ldots)R_N + 3\epsilon^2(f_0+\epsilon f_1+\ldots)^2R_N + \epsilon^4 R_N = 0. \tag{142}$$

Expanding

$$R_N \sim R_0\,(x,X,\xi) + \epsilon R_1\,(x,X,\xi) + \ldots,$$

we get formally the same problem as in §3.8. We thus have

$$\begin{aligned}
R_0 &= S_0(X,\xi)\, e^{i\tilde{x}} + \text{c.c.},\\
R_1 &= -6\bar{A}_0(X,\xi)S_0(X,\xi) - \frac{2E_0A_0(X,\xi)S_0(X,\xi)e^{2i\tilde{x}}}{3} + \text{c.c.},\\
R_2 &= S_2(X,\xi)e^{i\tilde{x}} - \frac{3A_0(X,\xi)^2S_0(X,\xi)e^{3i\tilde{x}}}{76} + \text{c.c.},\\
&\vdots
\end{aligned}$$

The amplitude equation for S_0 is

$$\begin{aligned} 0 &= 4S_{0_{XX}} + \frac{16i}{19}\left|A_0\right|^2 S_{0_X} - S_0\left(1 + \frac{26460}{361}\left|A_0\right|^4 - 4\sqrt{114}E_2\left|A_0\right|^2 - \frac{16i}{19}\bar{A}_0 A_{0_X}\right) \\ &\quad -\bar{S}_0\left(\frac{17640}{361}\left|A_0\right|^2 A_0^2 - 2\sqrt{114}E_2 A_0^2 - \frac{16i}{19}A_0 A_{0_X}\right). \end{aligned}$$

Writing $S_0 = (u_0(X,\xi) + iv_0(X,\xi))\, e^{i\phi_0}$ and using (140), we obtain

$$4u_{0_{XX}} - 4\beta v_{0_X} - 2940\beta^2 u_0 = 0, \tag{143}$$

$$4v_{0_{XX}} + 4\beta u_{0_X} = 0. \tag{144}$$

Integrating the second equation, we find[2] $v_{0_X} = -\beta u_0$ and the first equation simplifies as

$$4u_{0_{XX}} - 4u_0 = 0.$$

Hence, we have $u_0 = a(\xi)\, e^X + b(\xi)\, e^{-X}$, and

$$S_0 = a(\xi)\,(1 - i\beta)\; e^X + b(\xi)\,(1 + i\beta)\; e^{-X}. \tag{145}$$

Pursuing the calculation up to $O(\epsilon^6)$, a new solvability condition is eventually obtained for S_2. Setting $S_2 = (u_2(X,\xi) + iv_2(X,\xi))\, e^{i\phi_0}$, it reads

$$\begin{aligned} 4u_{2_{XX}} - 4\beta v_{2_X} - 2940\beta^2 u_2 &= -\left(\frac{2938}{367}\, a_\xi + \frac{1333981247995\beta}{45080947056}\, a\right) e^X \\ &\quad + \left(\frac{2938}{367}\, b_\xi - \frac{1587801142645}{45080947056}\, b\right) e^{-X}, \end{aligned} \tag{146}$$

$$\begin{aligned} 4v_{2_{XX}} + 4\beta u_{2_X} &= \left(4\beta\, a_\xi + \frac{8572403643}{45080947056}\, a\right) e^X \\ &\quad + \left(4\beta\, b_\xi - \frac{339292298293}{45080947056}\, b\right) e^{-X}. \end{aligned} \tag{147}$$

Integrating the second of these equation and substituting the result into the first, we get

$$4u_{2_{XX}} - 4u_2 = -8\, e^X\, \left(a_\xi + 2541\beta^3 a\right) + 8\, e^{-X}\, \left(b_\xi - 2541\beta^3 b\right). \tag{148}$$

Since $e^{\pm X}$ is solution of the homogeneous equation, u_2 will diverge secularly in X unless

$$a(\xi) = a_0\, e^{-\gamma\,\xi}, \qquad b(\xi) = b_0\, e^{\gamma\,\xi}, \qquad \gamma \equiv 2541\beta^3. \tag{149}$$

The far-field solution inside the localised pattern is therefore

$$f \sim e^{-i\beta X/2} e^{i(x+\check{\varphi})} e^{i\Phi_\xi \xi}\left[\sqrt{\frac{19\beta}{2}}\left(1 - \epsilon^2\Delta\right) + a_0\,(1 - i\beta)\; e^{X-\gamma\,\xi} + b_0\,(1 + i\beta)\; e^{-X+\gamma\,\xi}\right] + c.c., \tag{150}$$

[2] In fact, we should be writing $v_{0_X} = -\beta u_0 + c(\xi)$ for some unknown function $c(\xi)$. We have also omitted the term $-3\epsilon\,\delta E\left(f_0^2 + 2\epsilon f_0 f_1 + \ldots\right)$ in the right hand side of (142). These would be necessary for a comprehensive matching, but do not change the final result and we discard them here for simplicity.

where we have introduced a new constant phase $\check{\varphi}$ for the fast oscillations.

We need to match (137), (138), and (150) by requiring that

$$\lim_{X\to\infty} f\left(x, X, 0^-\right) \sim \lim_{\xi\to 0^+} f\left(x, X, \xi\right), \qquad \lim_{\xi\to L^-} f\left(x, X, \xi\right) \sim \lim_{X-L/\epsilon^2\to-\infty} f\left(x, X, L^+\right).$$

Equating the constant amplitude oscillations in (137) and (150), we find

$$e^{-i\beta X/2}e^{i(x+\varphi)}\sqrt{\frac{19\beta}{2}}\left(1-\epsilon^2\Delta\right) = e^{-i\beta X/2}e^{i(x+\check{\varphi})}\sqrt{\frac{19\beta}{2}}\left(1-\epsilon^2\Delta\right).$$

Hence

$$\check{\varphi} = \varphi.$$

Matching the $e^{\pm X}$ terms we find

$$a_0 = \frac{-4\,\pi\Lambda e^{\beta\pi/4}e^{-\pi/\epsilon^2}}{\sqrt{19\beta/2}\,\epsilon^6}\cos\left(\chi-\varphi-\beta\log\epsilon\right) - \frac{\delta E}{\epsilon^2}\frac{361\sqrt{3}}{16}\beta^{3/2}, \tag{151}$$

$$b_0 = \frac{-1}{2}\sqrt{\frac{19\beta}{2}}. \tag{152}$$

Next, considering (138) and (150), matching the constant amplitudes yields

$$\varphi+\hat{\varphi} = \frac{-L}{\epsilon^4} + \frac{\beta L}{2\epsilon^2} - \Phi_\xi L + 2m\pi, \tag{153}$$

while the $e^{\pm X}$ terms yield

$$a_0\, e^{-\gamma L} = \frac{-1}{2}\sqrt{\frac{19\beta}{2}}\, e^{-L/\epsilon^2}, \tag{154}$$

$$b_0\, e^{\gamma L} = \left(\frac{-4\,\pi\Lambda e^{\beta\pi/4}e^{-\pi/\epsilon^2}}{\sqrt{19\beta/2}\,\epsilon^6}\cos\left(\chi-\hat{\varphi}-\beta\log\epsilon\right) - \frac{\delta E}{\epsilon^2}\frac{361\sqrt{3}}{16}\beta^{3/2}\right) e^{L/\epsilon^2}. \tag{155}$$

Eliminating a_0 and b_0 from (151), (152), (154), and (155), these matching conditions become

$$\frac{1}{2}\sqrt{\frac{19\beta}{2}}\, e^{-L/\epsilon^2+\gamma L} = \frac{\delta E}{\epsilon^2}\frac{361\sqrt{3}}{16}\beta^{3/2} + \frac{4\,\pi\Lambda e^{\beta\pi/4}e^{-\pi/\epsilon^2}}{\sqrt{19\beta/2}\,\epsilon^6}\cos\left(\chi-\varphi-\beta\log\epsilon\right), \tag{156}$$

$$\frac{1}{2}\sqrt{\frac{19\beta}{2}}\, e^{-L/\epsilon^2+\gamma L} = \frac{\delta E}{\epsilon^2}\frac{361\sqrt{3}}{16}\beta^{3/2} + \frac{4\,\pi\Lambda e^{\beta\pi/4}e^{-\pi/\epsilon^2}}{\sqrt{19\beta/2}\,\epsilon^6}\cos\left(\chi-\hat{\varphi}-\beta\log\epsilon\right). \tag{157}$$

Equations (153), (156) and (157) are, finally, the three equations which determine the remaining unknowns L, ϕ and $\hat{\phi}$, in terms of the bifurcation parameter δE. Note that, by (156) and (157), we must have

$$\cos\left(\chi-\varphi-\beta\log\epsilon\right) = \cos\left(\chi-\hat{\varphi}-\beta\log\epsilon\right). \tag{158}$$

5 The bifurcation diagram

There are two different types of solution of equation (158). One set of solutions is given by

$$\hat{\varphi} = \varphi + 2n\pi, \tag{159}$$

for $n \in \mathbb{Z}$. A second set of solutions is given by

$$\hat{\varphi} = -\varphi + 2\chi - 2\beta \log \epsilon + 2n\pi, \tag{160}$$

for $n \in \mathbb{Z}$. These two solutions give very different behaviours, as we now demonstrate.

5.1 The snakes

Suppose first that (159) holds. Then (153) gives

$$\varphi = -\frac{L}{2\epsilon^4} + \frac{\beta L}{4\epsilon^2} - \frac{\Phi_\xi}{2} L + k\pi, \tag{161}$$

which, on substituting into (156) gives

$$\frac{8\sqrt{19}}{361\sqrt{6}\beta}\,\epsilon^2 e^{-L/\epsilon^2+\gamma L} = \delta E + \frac{64\sqrt{2}\,\pi\Lambda e^{\beta\pi/4}e^{-\pi/\epsilon^2}}{\beta^2 361\sqrt{57}\,\epsilon^4} \cos\left(\frac{L}{2\epsilon^4} - \frac{\beta L}{4\epsilon^2} + \frac{\Phi_\xi}{2} L + \chi - \beta\log\epsilon - k\pi\right). \tag{162}$$

This is the equation which describes the snaking bifurcation diagram. The separation between fronts, L/ϵ^4, acts as a measure of the norm of the solution, and (162) describes how this varies with δE, the bifurcation parameter. We make a few remarks.

(i) The left-hand side rapidly becomes exponentially small, even by comparison to $e^{-\pi/\epsilon^2}$, so that the width of the snake rapidly approaches $2\,\delta E_c$, where

$$\delta E_c = \frac{64\sqrt{2}\,\pi\Lambda e^{\beta\pi/4}e^{-\pi/\epsilon^2}}{\beta^2 361\sqrt{57}\,\epsilon^4}.$$

This width is exponentially small in ϵ and is, of course, the same as the range of values of δE for which stationary fronts are possible (136).

(ii) Equation (162) describes two interleaving curves, one for $k = 0$ and one for $k = 1$, corresponding to the centre of the bump being a local minimum and a local maximum.

(iii) Each cycle around the snake corresponds to a full cycle of the cosine, which corresponds to L increasing by approximately $4\pi\epsilon^4$. Since this corresponds to x increasing by 4π, it means that two peaks are added to the solution during each cycle.

There are still two constants in formula (162) which we need to determine, namely Λ and χ. In principle these can be calculated by iterating the recurrence relations (83) to suitably large values of n. However, even using acceleration techniques such as Richardson extrapolation it is computationally difficult to generate enough terms in the expansion.

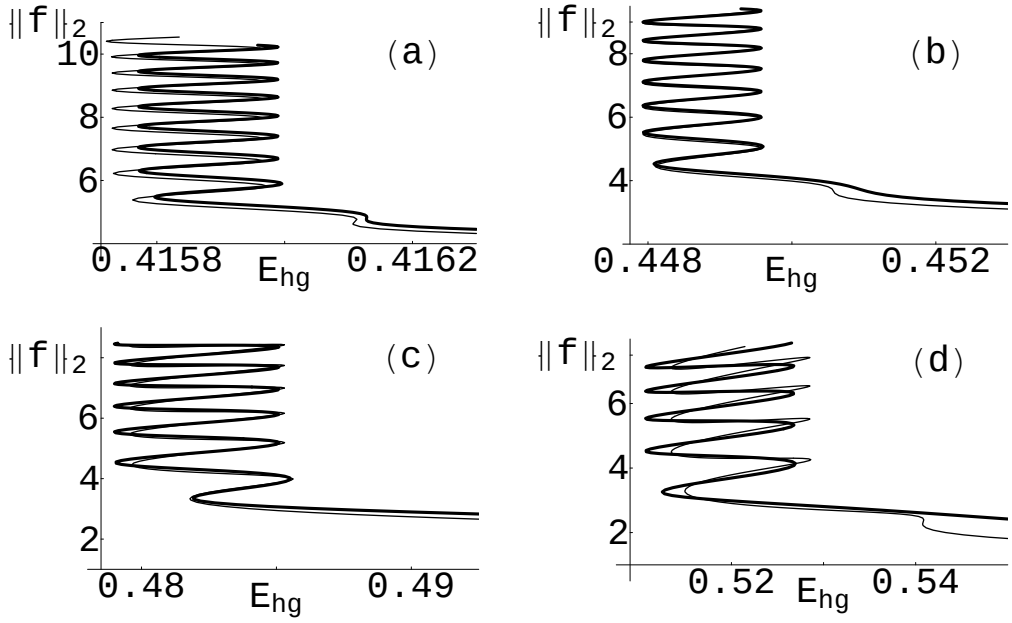

Figure 4: Bifurcation diagram for various values of ϵ: (a) $\epsilon = 0.495$, (b) $\epsilon = 0.55$, (c) $\epsilon = 0.6$, (d) $\epsilon = 0.65$. Thick line: analytical formula. Thin line: numerical simulation.

In Figure 4 we show a comparison numerical computations of the snakes using Auto [3] and the asymptotic formula (162), with several values of ϵ. Here Λ and χ chosen to give the best fit, which was obtained for

$$\frac{64\sqrt{2}\,\pi\Lambda e^{\beta\pi/4}}{\beta^2 361\sqrt{57}} \approx 2.439, \qquad \chi \approx -0.5. \tag{163}$$

Even though ϵ is not very small, the agreement is remarkable. Note that for the largest values of ϵ, the oscillations of the snakes become tilted. This is due to the remainder R_N in the solution, whose size is proportional to δE. More details on the composite solution effectively used to draw the bifurcation diagrams are given in Appendix B.

Fixing Λ and χ at these values, in Figure 5 we show the width of the snaking oscillation, which is the pinning range (136), as a function of ϵ. The fitting of Λ forces the curve to pass through the numerically determined value at $\epsilon = 0.55$; the remainder of the asymptotic curve is completely determined. Also in Figure 5 we examine the validity of the scaling (136) by plotting $\epsilon^4 \exp(\pi/\epsilon^2)\ \delta E_c$ as a function of ϵ. If our scaling is correct then the points should lie on a straight line. We see that the agreement is very good, and is convincing evidence that the ϵ^{-4} prefactor is correct. We should mention here that Paul Matthews performed an independent check of this scaling with a different numerical code and confirmed to us this result.

We remark that for the smallest values of ϵ, the agreement between analytics and numerics slightly degrades. This is due to the fact that the separation between slow and fast space

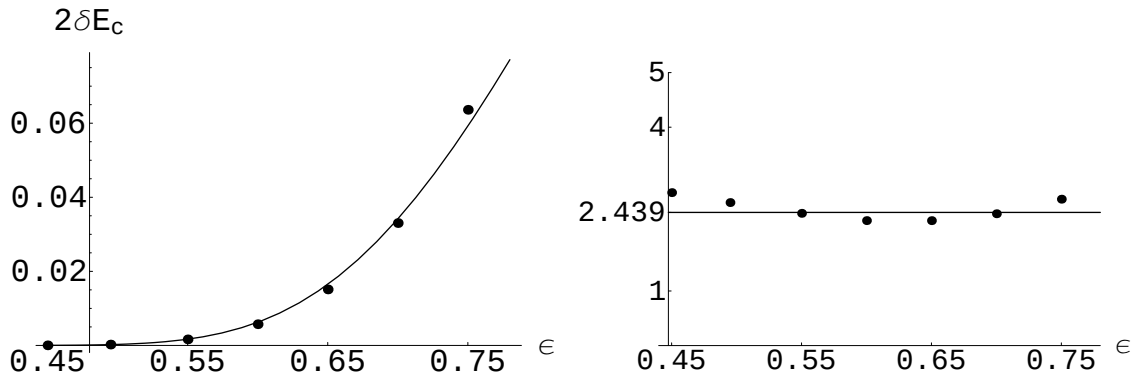

Figure 5: Left: Amplitude of the snaking oscillations (pinning range) in Fig. 4 as a function of ϵ. Right: $\epsilon^4 \exp(\pi/\epsilon^2)\ \delta E_c$ as a function of ϵ. Dots: numerical; line: analytical.

scales become more and more pronounced and difficult to cope with using Auto. In particular, the scale of the front becomes so slow that localised patterns rapidly become of comparable size to the finite domain of numerical integration. When the oscillations completely invade the domain of integration, snaking stops. This, we observe, is accompanied by a slight shift in the Maxwell point [already noticeable in Fig. 4 (a)]. The amplitude of snaking oscillation, on the other hand, remains very much the same as if the domain was infinite.

5.2 The ladders

Now suppose that (160) holds. Then (153) gives

$$2\chi - 2\beta \log \epsilon = \frac{\beta L}{2\epsilon^2} - \frac{L}{\epsilon^4} + 2k\pi. \tag{164}$$

This equation determines L, so that in this case the length of the pattern is independent of δE. Equation (156) gives

$$\frac{8\sqrt{19}}{361\sqrt{6}\beta}\,\epsilon^2 e^{-L/\epsilon^2+\gamma L} = \delta E + \frac{64\sqrt{2}\,\pi\Lambda e^{\beta\pi/4}e^{-\pi/\epsilon^2}}{\beta^2 361\sqrt{57}\,\epsilon^4}\cos\left(\chi - \varphi - \beta\log\epsilon\right). \tag{165}$$

With L given by (164) there are solutions to (165) for δE in a finite range given by the maximum and minimum values of the cosine. At the ends of this range there is one possible solution for φ in $[0, 2\pi)$, while inside the range there are two possible values of φ for each value of δE. Thus (165) describes two solution branches each parameterised by φ, which form links between the two snaking solution branches found above.

The bifurcation diagram thus calculated is shown in Figure 6, in which the bifurcation points between the snakes and the ladders are shown as filled circles. Note that these bifurcation points are not the same as the saddle-node bifurcations at the folds, although the two bifurcations are exponentially close, since the left-hand side of (165) decays exponentially to zero as L increases.

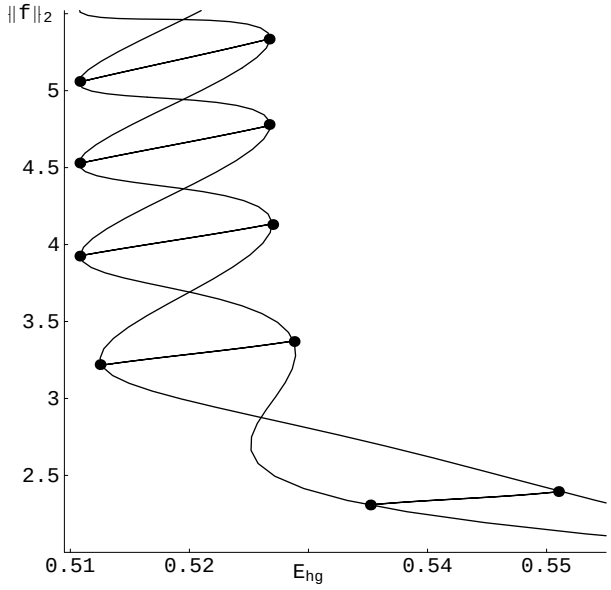

Figure 6: The full analytical bifurcation diagram for $\epsilon = 0.65$, showing the ladder structure joining the interweaving snakes. Each line represents two solutions, which bifurcate from the snakes at the dots. Note that these are not at the folds of the snakes, but do approach them exponentially as L increases.

6 Discussion

We have performed a beyond-all-orders multiples-scales analysis of the Swift-Hohenberg equation (1) in the vicinity of a modulation instability (§2) and in the vicinity of the Maxwell point (§3).

In §2 we found multiple-scales solutions comprising a fast oscillation modulated by a slowly varying amplitude which took the form of a localised "bump" [of the usual sech form; see equation (9)]. The translational invariance of equation (1) leads to each solution representing a one-parameter family of solutions. However, when the multiple-scales ansatz is used one spatial variable becomes two spatial variables, and there are therefore two degrees of freedom associated with translational invariance. This extra degree of freedom arises as a "phase difference" between the fast and slow scales. This phase difference is not determined at any order of ϵ: it is selected by exponentially-small terms beyond all orders. Such a situation is common in singular perturbation problems, and has been studied in a number of systems in the last few years [19, 20, 21, 42].

Here the leading order amplitude has a pair of singularities in the complex plane, and these singularities result in a divergent asymptotic expansion for the amplitude with associated Stokes lines. By truncating the multiple-scales expansion at its smallest term (optimal truncation) we were able to explicitly see the switching on of exponentially-subdominant terms as the Stokes line was crossed via an extension of the usual Stokes line smoothing calculation [12, 28]. The width of the Stokes line is small by comparison to the slow scale but large by comparison to the fast scale, so that the smoothing is accomplished via a multiple scales expansion, as in [1].

The exponentially-small term switched on across the Stokes line is exponentially growing in the slow scale. Thus, eventually, it would become order one, so that the single bump solution will not in general satisfy the condition of decay at infinity. In order for the solution to be valid at infinity the coefficient of the growing exponential must be zero. This is the condition which determines the phase shift between the fast and slow scales; it selects two values for this phase shift from the continuum, corresponding to the two possible symmetries in the solution (the centre of the amplitude bump can correspond to a peak or a trough in the fast oscillation). Thus we have demonstrated the two solutions which bifurcate at the modulation instability. For these two solutions the amplitude is monotonic in the bifurcation parameter E_{hg}, tending to infinity as the Maxwell point is approached.

In §3 we examined the Maxwell point in more detail by considering a multiple-scales analysis of a front solution. The multiple-scales analysis, and the corresponding beyond-all-orders calculation, is more complicated in this case, with solvability conditions occurring at fifth order in the expansions rather than at third order. We found that, as in §2, the leading order amplitude for the front has a singularity in the complex plane of the slow scale, which generates a divergent asymptotic expansion and a Stokes line across which an exponentially-subdominant but exponentially-growing term is switched on. Now, however, we have the possibility of generating another exponentially-growing term by perturbing the bifurcation parameter E_{hg} away from the Maxwell point (if such a perturbation is applied at any other point the resulting solution decays at infinity). As in §2, to obtain a valid approximation

the coefficient of the exponentially-growing term must be zero. This time this results in an equation relating the phase shift between the fast and slow scales and the perturbation of the bifurcation parameter from the Maxwell point, δE. This equation describes a closed loop of solutions: there are two solutions for any $|\,\delta E| < \delta E_c$ which disappear via a fold at the endpoints of the interval. Thus we have shown that there is a range of values of δE for which a steady front solution is possible. The width of this range is given by (136), and is exponentially small in ϵ.

Armed with the far-field behaviour of a single front from §3, we considered in §4 solutions comprising two fronts separated by a period of sustained oscillation. The exponentially-small but exponentially-growing term in the far-field of the first front eventually grows to be order one and matches into the second down-switching front. By matching the far-fields of the two fronts together we were able to generate the bifurcation diagram for the solutions found in §2 near the Maxwell point. The matching was made slightly more complicated by the fact that the fronts must be well-separated to give the exponential enough time to grow, which introduces a third scale requiring a three-scale multiple-scales analysis in the region between fronts. On this super-slow scale, fronts appear as boundary layers.

The bifurcation diagram is effectively described by equations (153), (156) and (158). The solutions to these equations are of two types. The first type comprises two interleaving snaking bifurcation curves which are the extension of the bifurcation curves of §2 into the region close to the Maxwell point. The width of the snakes rapidly approaches the pinning region $|\,\delta E| < \delta E_c$ as the length of the sustained oscillation increases.

The second type of solution comprises a "ladder" in the diagram, in which two solutions form a closed loop which meets each snake at a bifurcation point. These loops are the two-front analogues of the loop of single-front solutions found in §3. The existence of such steady asymmetric solutions relies on the fact that the Swift-Hohenberg equation is variational. These solutions generally become travelling waves in the presence of non-variational terms. However, this is probably yet a smaller effect than the exponentially-small terms we have computed. Indeed, had we studied a subcritical bifurcation in another, non-variational equation, we would still have obtained a variational problem at each finite order of the multiple scale (Ginzburg-Landau amplitude equation and linearised versions). This is true for any subcritical bifurcation problem. Non-variational effects on localised patterns must be quite subtle to study but are certainly worth the while, as equation (1) often appears decorated with the non-variational terms $|\partial E/\partial x|^2$ and $E\,\partial^2 E/\partial x^2$ as an asymptotic limit of chemical, optical or biological systems [47]; see also [64].

A by-product of our analysis, which can be useful for future reference, are the fourth-order formulae $E_0 + \epsilon^2 E_2 + \epsilon^4 E_4$ and $1 - \epsilon^2\beta/2 + \epsilon^4\Phi_\xi$ for the Maxwell point and the wave number of the localised pattern, respectively. The latter point was investigated numerically in some detail in [16, 18]. Given that in practice, ϵ is not so small, the fourth order terms above give a significant improvement in the comparison between numerically and analytically computed bifurcation curves.

Clearly the present analysis can be extended to multiple bump solutions, both far and near the Maxwell point. In the latter case, the growing exponentials from each front need

to be tracked through the solution until the far-field of the last front, at which point the condition of no further exponential growth needs to be applied [1]. Numerical bifurcation diagrams of two-bump solutions have been computed in [73].

Dynamical fronts could also be described by letting f depend exponentially-slowly on time. In this case $-\partial f/\partial t$ would appear in the right-hand-side of (120) and would be treated in the same fashion as $-3\epsilon\,\delta E\,(f_0^2 + 2\epsilon f_0 f_1 + \ldots)$, as in [42].

Snaking bifurcation diagrams have been observed in many other problems, notably difference or differential-difference equations [76]. This is related to the fact that in these problems too there is a finite pinning range for the bifurcation parameter in which a front solution will remain stationary. In the (singular) limit of small separation, in which the difference equations become differential equations, the pinning range is exponentially small in that separation [42], and a beyond-all-orders analysis will be necessary to elucidate the snaking behaviour. On the other hand delay-differential equations with Hopf bifurcations also give rise to snaking bifurcation diagrams [5]. Such systems can display well-separated time-scales [35, 57], so that a beyond-all-order multiple-timescale analysis can be envisaged there too.

Acknowledgments Gregory Kozyreff is a research associate at the Fonds de la Recherche Scientifique-FNRS (Belgium). We also thank Paul Matthews for his independent numerical check of the scaling for δE_c.

A Multiple-scales analysis up to 6$^{\text{th}}$ order

In §4, we use the far-field expressions for the up- and down-front in order to find matching conditions between them. However, matching occurs at $X = O(1/\epsilon^2)$ and we therefore have to derive an expression for the front in this limit. One may expect, in particular, a slow drift in frequency to set in on this super-slow scale. To determine this, we therefore resume the multiple scale analysis in the beginning of §3. Specifically, we seek for a solution of the form

$$f \sim f_0\,(x, X, \xi) + \epsilon\, f_1\,(x, X, \xi) + \ldots,$$

where $\xi = \epsilon^4 x = \epsilon^2 X$, and we let

$$E = E_0 + \epsilon^2\, E_2 + \epsilon^4\, E_4 + \ldots + \delta E$$

in (62). The first few orders of the calculation are the same as before, except that, this time,

$$f_0 = A_0(X, \xi)\, e^{i\tilde{x}} + \bar{A}_0(X, \xi)\, e^{-i\tilde{x}}.$$

A_0 satisfies the same solvability condition as before, but integration of (71) now yields

$$\phi_0 = -\int^X \frac{\mathcal{R}_0^2(s)}{19} ds + \Phi\,(\xi)\,,$$

so that

$$A_0(X, \xi) = \sqrt{\frac{19\beta}{2}} \frac{e^{X/2 + i\Phi(\xi)}}{(1 + e^X)^{1/2 + i\beta/2}}.$$

Solving further the $O(\epsilon^4)$ and $O(\epsilon^5)$ problem, we eventually get, at $O(\epsilon^6)$ the following solvability condition for A_2:

$$\begin{aligned}
0 &= 4A_{2_{XX}} + \frac{16i}{19}\left|A_0\right|^2 A_{2_X} - A_2\left(1 + \frac{26460}{361}\left|A_0\right|^4 - 4\sqrt{114}E_2\left|A_0\right|^2 - \frac{16i}{19}\bar{A}_0 A_{0_X}\right) \\
&\quad -\bar{A}_2\left(\frac{17640}{361}\left|A_0\right|^2 A_0^2 - 2\sqrt{114}E_2 A_0^2 - \frac{16i}{19}A_0 A_{0_X}\right) \\
&\quad +\frac{16i}{19}\left|A_0\right|^2 A_{0_\xi} - \left(1 - \frac{1040\sqrt{734}}{1083}\left|A_0\right|^2 + \frac{31614}{361}\left|A_0\right|^4\right) iA_{0_X} - \frac{44}{19}\bar{A}_0 A_{0_X}^2 \\
&\quad +\left(2\sqrt{114}E_2 - \frac{18072}{361}\left|A_0\right|^2\right) iA_0^2\bar{A}_{0_X} + 8A_{0_{X\xi}} \\
&\quad +A_0\left|A_0\right|^2\left(\frac{4942}{1083} + 2\sqrt{114}E_4 - \frac{9724\sqrt{734}}{6859}\left|A_0\right|^2 + \frac{1186412}{20577}\left|A_0\right|^4\right). \qquad (166)
\end{aligned}$$

Equation (166) is a linearised version of (70) with a forcing term. Setting $A_2 = (\mathcal{R}_2 + i\mathcal{R}_1\phi_2)\, e^{i\phi_0}$, and making use of (72) to eliminate highest derivatives of $\mathcal{R}_0$, we find

$$\phi_{2_X} = \frac{1}{8} - \frac{2}{19}\mathcal{R}_0\mathcal{R}_2 - \frac{187\sqrt{734}}{2166}\mathcal{R}_0^2 + \frac{24799}{4332}\mathcal{R}_0^4 - \Phi_\xi + \frac{19B_3}{\mathcal{R}_0^2}, \qquad (167)$$

where B_3 is constant. The equation for $\mathcal{R}_2$ is then

$$4\mathcal{R}_{2_{XX}} - \mathcal{R}_2\left(1 - 6\sqrt{114}E_2\mathcal{R}_0^2 + \frac{44040\mathcal{R}_0^4}{361}\right) = 4\frac{\partial g}{\partial \mathcal{R}_0} + 8B_3\mathcal{R}_0,$$

where

$$4\frac{\partial g}{\partial \mathcal{R}_0} = -\left(\frac{4828}{1083} + 2\sqrt{114}E_4\right)\mathcal{R}_0^3 + \frac{9280\sqrt{734}}{6859}\mathcal{R}_0^5 - \frac{365208}{6859}\mathcal{R}_0^7.$$

Using the method of variation of parameters, a particular solution associated to $g(\mathcal{R}_0)$ is

$$\mathcal{R}_{0_X}\int^X \mathcal{R}_{0_X}^{-2}\left(\int^s \mathcal{R}_{0_X}\frac{\partial g}{\partial \mathcal{R}_0}\, dt\right) ds = \mathcal{R}_{0_X}\int^X \frac{g\left(\mathcal{R}_0\right)}{\mathcal{R}_{0_X}^2}\, ds$$

The general solution of (166) is thus

$$\begin{aligned}
A_2 &= \left[\mathcal{R}_{0_X}\int^X \frac{B_2 + B_3\mathcal{R}_0^2 + g\left(\mathcal{R}_0\right)}{\mathcal{R}_{0_X}^2}\, ds - \frac{2i\mathcal{R}_0}{19}\int^X \mathcal{R}_0\mathcal{R}_{0_X}\left(\int^s \frac{B_2 + B_3\mathcal{R}_0^2 + g\left(\mathcal{R}_0\right)}{\mathcal{R}_{0_X}^2}\, dt\right) ds\right. \\
&\quad \left. +i\mathcal{R}_0\int^X\left(\frac{19B_3}{\mathcal{R}_0^2} - \frac{187\sqrt{734}\mathcal{R}_0^2}{2166} + \frac{24799\mathcal{R}_0^4}{4332}\right) ds + i\mathcal{R}_0\left(\frac{1}{8} - \Phi_\xi\right) X\right] e^{i\phi_0} \\
&\quad +B_1 A_{0_X} + iB_4 A_0.
\end{aligned}$$

Letting $X \to -\infty$, we find that

$$A_2 \sim \sqrt{\frac{38}{\beta}}\, e^{-X/2}\, e^{i\,\phi_0}\, \left(\beta^2 \frac{437 - 93952\, B_2}{1216} - iB_3\right).$$

Hence, A_2 would diverge exponentially unless

$$B_2 = \frac{437}{93952}, \qquad B_3 = 0.$$

Considering next the limit $X \to \infty$, we find that

$$A_2 \sim \sqrt{\frac{19\beta}{2}} \left[\frac{19\sqrt{114}\,\beta}{16}\,(1 - i\beta)\left(\frac{63711\sqrt{3/38}}{264974} - E_4\right) e^X + i\left(\frac{43163}{4310048} - \Phi_\xi\right) X\right] e^{i\phi_0}$$

Hence, exponential growth and secular divergence in X are avoided if

$$E_4 = \frac{63711\sqrt{3/38}}{264974}, \qquad \Phi_\xi = \frac{43163}{4310048}\,.$$

This provides a correction to the Maxwell point and a frequency correction to the oscillations over very long distances. Assuming these values, the full large-X behaviour of A_2 becomes

$$A_2 \sim -\sqrt{\frac{19\beta}{2}}\beta^3 \left(\frac{80629}{114} + i\,\frac{172666595\beta}{456} + 2541\frac{1 + i\beta}{2} X\, e^{-X}\right) e^{i\,\phi_0} + O\left(e^{-X}\right).$$

Moreover, for large values of X, we have

$$\begin{aligned} \mathcal{R}_0 &= \sqrt{\frac{19\beta}{2}} \frac{1}{(1 + e^{-X})^{1/2}} \sim \sqrt{\frac{19\beta}{2}} \left(1 - \frac{e^{-X}}{2} + \ldots\right), \\ e^{i\,\phi_0} &= \frac{e^{i\,\Phi_\xi \xi}}{(1 + e^X)^{i\beta/2}} \sim e^{-i\,\beta X/2 + i\,\Phi_\xi \xi} \left(1 - \frac{i\beta e^{-X}}{2} + \ldots\right). \end{aligned}$$

Hence a two-term expression for the front is

$$\begin{aligned} A_0 + \epsilon^2 A_2 \sim \quad & \sqrt{\frac{19\beta}{2}} \left[1 - \epsilon^2\beta^4 \left(\frac{80629}{114\beta} + i\,\frac{172666595}{456}\right)\right. \\ & \left. - \frac{1 + i\beta}{2}\left(1 + 2541\beta^3\epsilon^2 X\right) e^{-X}\right] e^{-i\,\beta/2 + i\,\Phi_\xi \xi} + O\left(e^{-2X}, \epsilon^2 e^{-X}\right). \quad (168) \end{aligned}$$

We see that although A_2 now remains bounded for large values of X, the term $X\, e^{-X}$ in A_2 means that the expansion is not uniform for $X = O(1/\epsilon^2)$. In order to join fronts separated by distances of $O(1/\epsilon^2)$ we need to match the front solutions with a three-scale solution in the oscillating region, as is done in §4.

B Composite expansions used to plot Figures 4 and 6

In order to draw the bifurcation diagram, we found it sufficient to use the left and right front solutions to construct a composite solution. In addition, we removed directly all the "dangerous" exponentially-growing terms, as well as the terms proportional to $X \pm i\pi$; these are taken care of by the matching procedure of §4. Indeed, numerical errors can leave residual factors of, say, 10^{-17} in front of exponentially-growing terms and these eventually blow up, making L^2 norm evaluation inaccurate. In practice, we used

$$f(x,\varphi,\epsilon) + f(\frac{L}{\epsilon^4} - x, \hat{\varphi}, \epsilon) - f_{\rm mid}(x,\epsilon),$$

where f is the approximate left-front solution and $f_{\rm mid}$ represents the common terms between the left- and right-front solutions inside the periodic domain to avoid double counting. The approximate left solution is

$$f \sim \left[A_0 e^{i\tilde{x}+i\Phi_\xi \xi} - \epsilon \left(\frac{E_0 A_0^2}{3}\, e^{2i\left(\tilde{x}+\Phi_\xi\xi\right)} - 3E_0|A_0|^2 \right) + c.c. \right] + R_N,$$

where A_0 is given by (78), $\tilde{x} = x + \varphi$ and [see (106), (107), and (134)]

$$\begin{aligned} R_N &= \frac{e^{3X/2} e^{i\tilde{x}+i\Phi_\xi\xi}}{\left(1+e^X\right)^{3/2+i\beta/2}} \left[\frac{\delta E}{\epsilon^2} \frac{361\beta^{3/2}\sqrt{3}}{16} \left(-2 + i\beta + i\beta e^{-X}\right) - \frac{4\pi\Lambda e^{\beta\pi/4} e^{-\pi/\epsilon^2}}{\sqrt{19\beta/2}\,\epsilon^6} \right. \\ &\left. \times \cos\left(\chi - \varphi - \beta\log\epsilon\right) \mathcal{H}(X) \left(6 - 2e^{-2X} + \frac{3}{2}\, e^{-X} + i\beta\left(4 + 5e^{-X}\right) \right) \right] + c.c.\,. \end{aligned}$$

The function $\mathcal{H}$ above is the Heaviside function, being one for $X > 0$ and zero otherwise. Note that the inclusion of R_N in the approximate solution is necessary to reproduce the tilted snaking observed when ϵ becomes appreciable. Finally,

$$\begin{aligned} f_{\rm mid} &= e^{i\tilde{x} - i\beta X/2 + i\Phi_\xi\xi} \left(\sqrt{\frac{19\beta}{2}} + \frac{\delta E}{\epsilon^2} \frac{361\beta^{3/2}\sqrt{3}}{16} \left(-2 + i\beta\right) - \frac{4\pi\Lambda e^{\beta\pi/4} e^{-\pi/\epsilon^2}}{\sqrt{19\beta/2}\,\epsilon^6} \right. \\ &\left. \times \cos\left(\chi - \varphi - \beta\log\epsilon\right) \left(6 + 4i\beta\right) \right) - \frac{19\epsilon\beta E_0}{6} e^{2i\left(\tilde{x} - \beta X/2 + \Phi_\xi\xi\right)} - 57\epsilon\beta E_0 + c.c.\,. \end{aligned}$$

References

[1] K. L. Adams, J. R. King, and R. H. Tew. Beyond-all-order effects in multiple-scales asymptotics: travelling-wave solutions to the Kuramoto-Sivashinsky equation. *J. Eng. Math.*, 45:197, 2003.

[2] I. S. Aranson, B.A. Malomed, L.M. Pismen, and L.S. Tsimring. Crystallization kinetics and self-induced pinning in cellular patterns. *Phys. Rev. E*, 62(1):R5–R8, Jul 2000.

[3] AUTO 97. available at http://cmvl.cs.concordia.ca/auto/. Concordia University, Montreal.

[4] S. Barbay, Y. Ménesguen, X. Hachair, L. Leroy, I. Sagnes, and R. Kuszelewicz. Incoherent and coherent writing and erasure of cavity solitons in an optically pumped semiconductor amplifier. *Opt. Lett.*, 31:1504, 2006.

[5] D. A. W. Barton, B. Krauskopf, and R. E. Wilson. Homoclinic bifurcations in a neutral delay model of a transmission line oscillator. *Nonlinearity*, 20:809–829, 2007.

[6] O. Batiste and E. Knobloch. Simulation of localized states of stationary convection in ^{3}he-^{4}he mixtures. *Phys. Rev. Lett.*, 95:244501, 2005.

[7] O. Batiste, E. Knobloch, A. Alonso, and I. Mercader. Spatially localized binary-fluid convection. *J. Fluid Mech.*, 560:149, 2006.

[8] M Beck, J. Knobloch, D. J. B. Lloyd, B. Sandstede, and T. Wagenknecht. Snakes, ladders, and isolas of localized patterns. *Preprint*, 2008.

[9] D. Bensimon, B. I. Shraiman, and V. Croquette. Nonadiabatic effects in convection. *Phys. Rev. A*, 38:5461, 1988.

[10] A. Bergeon and E. Knobloch. Spatially localized states in natural doubly diffusive convection. *Physics of Fluids*, 20(3):034102, 2008.

[11] M. Le Berre, E. Ressayre, and A. Tallet. Why does a Ginzburg-Landau diffraction equation become a diffusion equation in the passive ring cavity? *Quantum Semiclass. Opt.*, 7:1, 1995.

[12] M. V. Berry. Uniform asymptotic smoothing of Stokes discontinuities. *Proc. Roy. Soc. Lond. A*, A422:7–21, 1989.

[13] D. Boyer and J. Vi nals. Grain boundary pinning and glassy dynamics in stripe phases. *Phys. Rev. E*, 65:046119, 2002.

[14] D. Boyer and J. Vi nals. Weakly nonlinear theory of grain boundary motion in patterns with crystalline symmetry. *Phys. Rev. Lett.*, 89:055501, 2002.

[15] C.J. Budd and R. Kuske. Localized periodic patterns for the non-symmetric generalized Swift-Hohenberg equation. *Physica D*, 208:73, 2005.

[16] J. Burke and E. Knobloch. Localized states in the generalized Swift-Hohenberg equation. *Phys. Rev. E*, 73, 2006.

[17] J. Burke and E. Knobloch. Snakes and ladders: Localized states in the Swift-Hohenberg equation. *Phys. Lett. A*, 360, 2007.

[18] John Burke and Edgar Knobloch. Homoclinic snaking: Structure and stability. *Chaos: An Interdisciplinary Journal of Nonlinear Science*, 17(3):037102, 2007.

[19] S. J. Chapman. On the rôle of Stokes lines in the selection of Saffman-Taylor fingers with small surface tension. *Europ. J. Appl. Math.*, 10:513–534, 1999.

[20] S. J. Chapman and J. R. King. The selection of Saffman-Taylor fingers by kinetic undercooling. *J. Eng. Math.*, 46(1):1–32, 2003.

[21] S J Chapman, J R King, and K L Adams. Exponential asymptotics and Stokes lines in nonlinear ordinary differential equations. *Proc. Roy. Soc. Lond. A*, 454:2733–2755, 1998.

[22] M. G. Clerc, C. Falcon, and Tirapegui. Comment on "Asymptotics of large bound states of localized structures". *Phys. Rev. Lett.*, 100(5):049401, 2008.

[23] S. Coombes, G.J. Lord, and M.R. Owen. Waves and bumps in neuronal networks with axo-dendritic synaptic interactions. *Physica D*, 178:219, 2003.

[24] P. Coullet, C. Riera, and C. Tresser. Stable static localized structures in one dimension. *Phys. Rev. Lett*, 84:3069, 2000.

[25] C. Crawford and H. Riecke. Oscillon-type structures and their interaction in a Swift-Hohenberg model. *Physica D*, 129:83, 1999.

[26] M. C. Cross and P. C. Hohenberg. Pattern formation outside of equilibrium. *Rev. Mod. Phys.*, 65:852, 1993.

[27] A B Olde Daalhuis, S J Chapman, J R King, J R Ockendon, and R H Tew. Stokes phenomenon and matched asymptotic expansions. *SIAM J. Appl. Math.*, 55(6):1469–1483, 1995.

[28] A. B. Olde Daalhuis, S. J. Chapman, J. R. King, J. R. Ockendon, and R. H. Tew. Stokes phenomenon and matched asymptotic expansions. *SIAM J. Appl. Math.*, 55(6):1469–1483, 1995.

[29] J. H. P. Dawes. Localised pattern formation with a large-scale mode: slanted snaking. *SIAM J. Appl. Dyn. Syst.*, 7(1):186–206, 2008.

[30] R. B. Dingle. *Asymptotic Expansions: their Derivation and Interpretation.* Academic Press, 1973.

[31] R. Edmunds, G. W. Hunt, and M. A. Wadee. Parallel folding in multilayered structures. *J. Mech. Phys. Solids*, 54:384–400, 2006.

[32] F. Fernández-Sánchez, E. Freire, and A. J. Rodríguez-Luis. Analysis of the T-point-Hopf bifurcation. *Physica D*, 237:292–305, 2008.

[33] W. J. Firth, L. Columbo, and T. Maggipinto. On homoclinic snaking in optical systems. *Chaos: An Interdisciplinary Journal of Nonlinear Science*, 17(3):037115, 2007.

[34] W. J. Firth, L. Columbo, and A. J. Scroggie. Proposed resolution of theory-experiment discrepancy in homoclinic snaking. *Physical Review Letters*, 99(10):104503, 2007.

[35] G. Giacomelli and A. Politi. Relationship between delayed and spatially extended dynamical systems. *Phys. Rev. Lett.*, 76(15):2686–2689, Apr 1996.

[36] D. Gomila, A.J. Scroggie, and W.J. Firth. Bifurcation structure of dissipative solitons. *Physica D*, 227:70–77, 2007.

[37] A. Hagberg, A. Yochelis, H. Yizhaq, C. Elphick, L. Pismen, and E. Meron. Linear and nonlinear front instabilities in bistable systems. *Physica D*, 217:186, 2006.

[38] M' F. Hilali, S. Métens, P. Borckmans, and G. Dewel. Pattern selection in the generalized Swift-Hohenberg model. *Phys. Rev. E*, 51(3):2046–2052, Mar 1995.

[39] G. W. Hunt, G. J. Lord, and A. R. Champneys. Homoclinic and heteroclinic orbits underlying the post-buckling of axially-compressed cylindrical shells. *Comput. Methods Appl. Mech. Engrg.*, 170:239, 1999.

[40] G. W. Hunt, M. A. Peletier, A. R. Champneys, P. D. Woods, M. A. Wadee, C. J. Budd, and G. J. Lord. Cellular buckling in long structures. *Nonlinear Dynamics*, 21:3, 2000.

[41] O. Jensen, V.O. Pannbacker, G. Dewel, and P. Borkmans. Subcritical transition to turing structures. *Phys. Lett. A*, 179:91, 1993.

[42] J. R. King and S. J. Chapman. Asymptotics beyond all orders and stokes lines in nonlinear differential-difference equations. *Europ. J. Appl. Math.*, 12:433–463, 2001.

[43] E. Knobloch. Spatially localized structures in dissipative systems: open problems. *Nonlinearity*, 21:T45–T60, 2008.

[44] J. Knobloch and T. Wagenknecht. Homoclinic snaking near a heterolinic cycle in reversible systems. *Physica D*, 206:82, 2005.

[45] G. Kozyreff and S. J. Chapman. Asymptotics of large bound states of localized structures. *Phys. Rev. Lett.*, 97(4):044502, 2006.

[46] G. Kozyreff and S. J. Chapman. Reply on the comment by M.G. Clerc et al. *Phys. Rev. Lett.*, 100(5):049402, 2008.

[47] G. Kozyreff and M. Tlidi. Nonvariational real Swift-Hohenberg equation for biological, chemical, and optical systems. *Chaos: An Interdisciplinary Journal of Nonlinear Science*, 17(3):037103, 2007.

[48] B. Krauskopf and B. E. Oldeman. Bifurcations of global reinjection orbits near a saddle-node Hopf bifurcation. *Nonlinearity*, 19:2149–2167, 2006.

[49] Bernd Krauskopf and Thorsten Rieß. A Lin's method approach to finding and continuing heteroclinic connections involving periodic orbits. *Nonlinearity*, 21(8):1655–1690, 2008.

[50] O. Lejeune, M. Tlidi, and P. Couteron. Localized vegetation patches: A self-organized response to resource scarcity. *Phys. Rev. E*, 66:10901(R), 2002.

[51] O. Lioubashevski, Y. Hamiel, A. Agnon, Z. Reches, and J. Fineberg. Oscillons and propagating solitary waves in a vertically vibrated colloidal suspension. *Phys. Rev. Lett.*, 83(16):3190–3193, Oct 1999.

[52] D. J. B. Lloyd and B. Sandstede. Localized radial solutions of the Swift-Hohenberg equation. *Preprint*, 2008.

[53] D. J. B. Lloyd, B. Sandstede, D. Avitabile, and A. R. Champneys. Localized hexagons patterns of the planar Swift-Hohenberg equation. *SIAM J. Appl. Dyn. Syst.*, 7(3):1049–1100, 2008.

[54] Boris A. Malomed, Alexander A. Nepomnyashchy, and Michael I. Tribelsky. Domain boundaries in convection patterns. *Phys. Rev. A*, 42(12):7244–7263, Dec 1990.

[55] P. Mandel. *Theoretical problems in cavity nonlinear optics.* Cambridge University Press, Cambridge, 1997.

[56] J. M. McSloy, W. J. Firth, G. K. Harkness, and G. L. Oppo. Computationally determined existence and stability of transverse structures. ii. Multipeaked cavity solitons. *Phys. Rev. E*, 66:46606, 2002.

[57] M. Nizette. Front dynamics in a delayed-feedback system with external forcing. *Physica D*, 183:220–244, 2003.

[58] P. V. Paulau, A. J. Scroggie, A. Naumenko, T. Ackemann, N. A. Loiko, and W. J. Firth. Localized traveling waves in vertical-cavity surface-emitting lasers with frequency-selective optical feedback. *Physical Review E (Statistical, Nonlinear, and Soft Matter Physics)*, 75(5):056208, 2007.

[59] J.-J. Perraud, A. De Wit, E. Dulos, P. De Kepper, G. Dewel, and P. Borckmans. One-dimensional ''spirals'': Novel asynchronous chemical wave sources. *Phys. Rev. Lett.*, 71(8):1272–1275, Aug 1993.

[60] U. Peschel, E. Egorov, and F. Lederer. Discrete cavity solitons. *Opt. Lett.*, 29(16):1909–1911, Aug 2004.

[61] Y. Pomeau. Front motion, metastability and subcritical bifurcations in hydrodynamics. *Physica D*, 23:3, 1986.

[62] R. Richter and I. V. Barashenkov. Two-dimensional solitons on the surface of magnetic fluids. *Physical Review Letters*, 94(18):184503, 2005.

[63] H. Riecke. Localized structures in pattern-forming systems. In *Pattern Formation in Continuous and Coupled Systems*, volume 115, page 215. IMA, 1999.

[64] V. Rottschafer and A. Doelman. On the transition from the Ginzburg-Landau equation to the extended Fisher-Kolmogorov equation. *Physica D*, 118:261–292, 1998.

[65] H. Sakaguchi and H.R. Brand. Stable localized solutions of arbitrary length for the quintic Swift-Hohenberg equation. *Physica D*, 97:274, 1996.

[66] J.M. Soto-Crespo, N. Akhmediev, and G. Town. Interrelation between various branches of stable solitons in dissipative systems -conjecture for stability criterion. *Opt. Commun.*, 199:282, 2001.

[67] Y. Tanguy, T. Ackemann, W. J. Firth, and R. Jäger. Realization of a semiconductor-based cavity soliton laser. *Physical Review Letters*, 100(1):013907, 2008.

[68] V. B. Taranenko, I. Ganne, R. J. Kuszelewicz, and C. O. Weiss. Patterns and localized structures in bistable semiconductor resonators. *Phys. Rev. A*, 61:63818, 2000.

[69] M. Tlidi, P. Mandel, and R. Lefever. Localized structures and localized patterns in optical bistability. *Phys. Rev. Lett*, 73:640, 1994.

[70] P.B. Umbanhowar, F. Melo, and H.L. Swinney. Localized excitations in a vertically vibrated granular layer. *Nature*, 382:793, 1996.

[71] A. G. Vladimirov, J. M. McSloy, D. V. Skryabin, and W. J. Firth. Two-dimensional clusters of solitary structures in driven optical cavities. *Phys. Rev. E*, 65(4):046606, Mar 2002.

[72] M. K. Wadee and A. P. Bassom. Effects of exponentially small terms in the perturbation approach to localized buckling. *Proc. R. Soc. Lond. A*, 455:2351, 1999.

[73] M. K. Wadee, C. D. Coman, and A. P. Bassom. Solitary wave interaction phenomena in a strut buckling model incorporating restabilisation. *Physica D*, 163:26, 2002.

[74] T. S. Yang. On traveling-wave solutions of the kuramoto-sivashinski equation. *Physica D*, 110:25, 1997.

[75] T. S. Yang and T. R. Akylas. On asymmetric gravity-capillary solitary waves. *J. Fluid Mech.*, 330:215, 1997.

[76] A. V. Yulin, A. R. Champneys, and D. V. Skryabin. Discrete cavity solitons due to saturable nonlinearity. *Phys. Rev. A*, 78(1):011804, 2008.